



Universiteit  
Leiden  
The Netherlands

## **The search for new treatment strategies for malignant pleural mesothelioma**

Schunselaar, L.M.

### **Citation**

Schunselaar, L. M. (2019, January 15). *The search for new treatment strategies for malignant pleural mesothelioma*. Retrieved from <https://hdl.handle.net/1887/67915>

Version: Not Applicable (or Unknown)

License: [Licence agreement concerning inclusion of doctoral thesis in the Institutional Repository of the University of Leiden](#)

Downloaded from: <https://hdl.handle.net/1887/67915>

**Note:** To cite this publication please use the final published version (if applicable).

Cover Page



Universiteit Leiden



The following handle holds various files of this Leiden University dissertation:

<http://hdl.handle.net/1887/67915>

**Author:** Schunselaar, L.M.

**Title:** The search for new treatment strategies for malignant pleural mesothelioma

**Issue Date:** 2019-01-15

# **The search for new treatment strategies for malignant pleural mesothelioma**

Laurel Marloes Schunselaar

ISBN: 978-94-6323-448-1

Copyright: Laurel Marloes Schunselaar, 2019

Cover: the cover depicts lungs covering an asbestomine in Asbestos, Quebec, Canada. Mesothelioma cells are depicted as background in the sky and water

Layout: Laurel Schunselaar & Rutger Schunselaar

The work described in this thesis was performed at the division of Cell Biology II, the division of Molecular Pathology and the division of Oncogenomics in combination with the Thoracic Oncology department at the Netherlands Cancer Institute, Amsterdam, The Netherlands. The work was supported by grants from the Institute of Chemical Immunology (ICI) and the KWF Dutch Cancer Society.

Financial support for printing this thesis was provided by the Netherlands Cancer Institute.

Printed by: Gildeprint, Enschede

# The search for new treatment strategies for malignant pleural mesothelioma

Proefschrift

Ter verkrijging van  
de graad van Doctor aan de Universiteit Leiden,  
op gezag van Rector Magnificus prof. mr. C.J.J.M. Stolker,  
volgens besluit van het College voor Promoties  
te verdedigen op dinsdag 15 januari 2019  
klokke 11.15 uur

Door

Laurel Marloes Schunselaar

Geboren te Enschede

op 17 augustus 1987

**Promotor**

Prof. dr. J.J.C. Neefjes

**Mede-promotor**

Prof. dr. P. Baas

**Co-promotor**

Prof. dr. W. Zwart

*Eindhoven University, Nederlands Kanker Instituut*

**Promotiecommissie**

Prof. dr. R.C. Hoeben

Prof. dr. H. Ovaa

Prof. dr. M. van der Stelt

Prof. dr. B. van der Water

Prof. dr. P. E. Postmus

Prof. dr. F. Baas

Prof. dr. D. Fennell *University of Leicester*

Prof. dr. M.J. Goumans

Dr. I. Berlin

Dr. J.A. Burgers *Nederlands Kanker Instituut*

nie ergern nür wundern



## Table of Contents

<b>Thesis Outline</b>		9
<b>Chapter 1</b>	A Catalogue of Treatments and Technologies for Malignant Pleural Mesothelioma.	13
<b>Chapter 2</b>	Chemical Profiling of Primary Mesothelioma Cultures Defines Subtypes with Different Expression Profiles and Clinical Responses.	33
<b>Chapter 3</b>	Comprehensive Pharmacogenomic Profiling of Malignant Pleural Mesothelioma Identifies a Subgroup Sensitive to FGFR Inhibition.	61
<b>Chapter 4</b>	Throphoblast Glycoprotein is Associated With a Favorable Outcome for Mesothelioma and a Target for Antibody Drug Conjugates.	101
<b>Chapter 5</b>	Targeting BAP1: a New Paradigm for Mesothelioma	121
<b>Chapter 6</b>	General Discussion	129
<b>Addendum</b>	English Summary	145
	Nederlandse Samenvatting	149
	Curriculum Vitae	152
	List of Publications	153
	Dankwoord	155



# Thesis Outline



My research has focused on a relative unknown tumor type: malignant pleural mesothelioma (MPM). Mesothelioma is an aggressive tumor of the mesothelial cells lining the pleura, peritoneum, pericardium and tunica vaginalis. Accounting for 70% of all cases, the most common form is MPM.

MPM is strongly associated with exposure to asbestos. Although the use of asbestos is banned in most developed countries, Russia, China, Brazil, and Kazakhstan continue to produce asbestos for the use in developing countries. Due to the latency period between exposure and presentation of the tumor, ranging from 20 to 50 years, the incidence of MPM has slightly increased over the last years. In 2015, the incidence in Europa was 3 cases per 100.000 persons.

Histologically, MPM is classified in three subtypes; epithelioid type (60% of the cases), sarcomatoid type (20% of the cases), and biphasic type (20% of the cases), the latter containing both epithelioid and sarcomatoid cells. Survival is associated with histological subtype, with epithelioid MPM having the best prognosis and sarcomatoid MPM the worst. The overall median survival is 12-15 months, when patients receive first-line chemotherapy. This first-line chemotherapy consists of a platinum-based combination with an anti-folate. Since the last 15 years, no further improvement in second-line therapy has been realized.

The poor prognosis of patients with MPM indicates the importance to find more effective treatments for this patient population. Therefore, this thesis focused on finding new treatment strategies for patients with MPM.

**Chapter 1** gives an overview of the efforts made in testing new treatments in MPM (till 2016), both on the clinical as well as on the translational level.

**Chapter 2** presents a method in which primary MPM cultures were chemically profiled to determine second-line treatment for patients. With this personalized treatment strategy we were able to predict individual patient responses to selected drugs. Based on chemical profiling, MPM could be subdivided in three groups, so called; responders, intermediate responders and non-responders.

This model together with cell line and mouse models, also identified a novel targetable pathway in MPM. In **Chapter 3**, an FGFR inhibitor-sensitive subgroup is identified by combining high-throughput drug screens, comprehensive molecular characterization and functional assays. BAP1 protein could serve as a potential biomarker to select patients for FGFR inhibitor treatment.

---

In **Chapter 4**, a different treatment strategy is tested. We show that the 5T4 antigen is expressed in MPM cells and internalized upon binding by specific antibodies. By targeting 5T4, with antibody-drug conjugates (ADC), high 5T4 expressing MPM cells were effectively killed, showing a promising novel strategy in the treatment of this tumor type.

Although the mutational load in MPM is intermediate, BAP1 is identified as one of the molecular targets in the treatment of MPM. **Chapter 5** describes the multiple interaction partners of BAP1 as well as proteins under influence of BAP1. The phenotypic effect of BAP1 is diverse, but pre-clinical data on inhibitors reversing these phenotypic effects is promising.

Finally, **Chapter 6** discusses how the different treatment strategies described in this thesis may ultimately contribute to improve survival outcome for patients with MPM. Furthermore, it discusses which other treatments are tested in patients with MPM and what would be necessary to improve survival outcome in this patient population.



# Chapter 1

## A Catalogue of Treatment and Technologies for Malignant Pleural Mesothelioma

Laurel M. Schunselaar\*, Josine M.M.F. Quispel-Janssen\*, Jacques Neefjes and Paul Baas

\*equal contribution

Expert Rev Anticancer Ther, 2016; 16(4):455-63



## **Abstract**

Malignant pleural mesothelioma is an aggressive fatal malignancy with a prognosis that has not significantly improved in the last decades. This review summarizes the current state of treatment and the various attempts that are made to improve overall survival for patient with malignant pleural mesothelioma. It also discusses technologies and protocols to test new and hopefully more effective compounds in a more individualized manner. These developments are expected to improve the prognosis for this group of patients.

## **Keywords**

chemotherapy, immunotherapy, mesothelioma, mouse models, pre-clinical models, primary tumor culture, targeted agent, treatment.

## **Introduction**

Malignant pleural mesothelioma (MPM) is an aggressive tumor that arises by neoplastic transformation of the mesothelial cells lining the pleural cavity [1-4]. In the United States, the incidence is approximately 1.05 cases per 100,000 persons [5]. In Europe, the incidence in males is higher, around 3 cases per 100,000 persons [6]. The occurrence of MPM is associated with asbestos exposure. There is a latency period of around 30-50 years between asbestos exposure and development of MPM. Even though all handling of asbestos is strictly regulated in Europe since 2005, the incidence is not expected to decrease before 2020 [4-9]. In addition, outside Europe, some other developed countries have only controlled the import or still produce asbestos and less-developed countries still use or even expand the use of asbestos [5-7]. This results in an estimated 125 million asbestos-exposed people and 43,000 annual deaths due to asbestos-related diseases worldwide [4, 9].

The prognosis for patients with MPM is poor. If untreated, most patients die in the first year after diagnosis [4, 8]. First-line chemotherapy treatment consists of a platinum-based combination with pemetrexed [3, 6, 10]. This combination provides a 3-month survival benefit over cisplatin alone and a 6-month survival benefit over nontreated patients [11, 12]. Around 40% of the patients with MPM respond to the combination [8, 11, 13, 14]. For patients that do not respond to first-line chemotherapy or become progressive after treatment, there is no standard second-line regimen [6, 14]. European Society for Medical Oncology Clinical Guidelines recommend enrolling eligible patients in clinical trials [6, 7].

## **First-line treatment in mesothelioma**

Almost every chemotherapy regimen has been tested in mesothelioma [15-17]. The most effective anticancer drugs are cisplatin, antimetabolites (methotrexate and pemetrexed), and anthracyclines (doxorubicin and daunorubicin). Anticancer drugs with no or minor activity in MPM are the taxanes, topoisomerase inhibitors, alkylating agents and the vinca-alkaloids with the exception of vinorelbine. The most studied anthracycline is doxorubicin. This drug showed some activity in a number of clinical trials with varying response rates [15-17].

Until 2000, nearly all studies tested single agents. In 2002, a meta-analysis suggested that combination therapy gave better response rates than single-agent therapy [18]. The first clinical trial that compared single-agent therapy to a combination was performed by Vogelzang et al. [11]. This resulted in the standard first-line treatment combination of cisplatin and pemetrexed.

This combination therapy combines two drugs with different activities. Cisplatin is a platinum ion with two chloride atoms and two amine groups. One chloride is first removed for a hydroxyl group yielding  $\text{PtCl}(\text{H}_2\text{O})(\text{NH}_3)_2^+$ . This form binds strongly to the G basis in deoxyribonucleic acid (DNA). Here, the second chloride atom can be removed yielding a cross-linking molecule between two G bases on different DNA strands. While the majority of interactions are between two G-G bases, other interaction, such as G-A, can also be detected. DNA strand crosslinking obviously induces substantial problems with DNA strand separation during mitosis and is supposed to be the major mechanism of cell death [19]. Pemetrexed is an antifolate that inhibits the biosynthesis of purine and pyrimidine nucleotides by inhibiting the enzymes dihydrofolate reductase, thymidylate synthase (TS) and glycinamide ribonucleotide formyltransferase (RNF). Pemetrexed enters the cell by the reduced folate carrier. Folylpolylglutamate synthetase polyglutamates pemetrexed to a form that has a 100-fold greater affinity for the enzymes TS and RNF. As a result, cell growth is attenuated due to a reduced amount of DNA bases available for DNA replication. Both drugs have serious side effects; cisplatin can cause serious nephrotoxicity that is controlled by expanding the kidney fluid volume before treatment. Antifolates induce elevated levels of homocysteine. Homocysteine accumulation causes severe toxicities such as , neutropenia, thrombocytopenia and diarrhea. With supplementation of vitamin B12 and folic acid homocysteine can be recycled into methionine or converted into cysteine [11, 20, 21].

## **The search for new treatment options for MPM**

A phase III trial by Vogelzang et al. showed patients receiving cisplatin with pemetrexed had an overall survival (OS) of 12.1 months versus 9.3 months for patients receiving cisplatin. Also time to progression (TTP) was higher in the cisplatin with pemetrexed group (5.7 months) compared to the cisplatin group (3.9 months). Approximately 40 % of the patients had a partial response (PR). A retrospective analysis of the follow-up data showed that patients receiving two or more lines of treatment had a significant longer survival. Sixty-two percent of the patients received single-agent therapy and 38% combination therapy. For patients with two or more lines of chemotherapy, the median survival time (MST) from start of first-line treatment was 15.3 months for those receiving first-line pemetrexed and cisplatin versus 12.2 months for patients that previously received first-line cisplatin. For patients that did not receive second-line chemotherapy, MST was 9.8 months in the cisplatin/pemetrexed group and 6.8 months in the cisplatin group. This analysis suggests that a selected group of eligible patients could benefit from a second-line treatment, but the most effective second-line treatment for this patient population has not yet been identified [22]. Since then, various other second-line phase II trials have been conducted as will be discussed below.

### *Inhibitors of growth factors*

Growth factors and their receptors play an important role in the development of mesothelioma. The epidermal growth factor receptor (EGFR) plays a role in cell proliferation, differentiation, migration, adhesion and survival. EGFR is highly overexpressed in mesothelioma. However, EGFR tyrosine kinase inhibitors erlotinib and gefitinib as well as the EGFR antibody cetuximab did not show any response. EGFR is not a tumor driver as suggested from the absence of sensitizing mutations in the EGFR tyrosine kinase domain, which may explain the lack of response to EGFR inhibitors [4, 20, 23].

Another transmembrane tyrosine kinase is activated by platelet-derived growth factor (PDGF) and plays a role in cell proliferation. Imatinib and dasatinib are anticancer drugs that inhibit the kinase activity of the PDGF receptor, but phase II studies with these drugs in patients with MPM were disappointing [4, 8, 20, 23].

### *Inhibitors of angiogenesis*

A third growth factor activating kinase receptor is the vascular endothelial growth factor (VEGF), which plays a role in angiogenesis. VEGF expression levels are high in a large portion of MPM tumors and they may activate the VEGF receptor to induce angiogenesis in tumors. Therefore, different VEGF-receptor inhibitors were consequently tested in phase II studies. These include small kinase inhibitors sorafenib, sunitinib, vatalanib and cediranib, which did not improve response rates or OS for patients with MPM [4, 8, 10, 20, 23]. Thalidomide was the most promising agent; however, no benefit in TTP or OS was observed in a large randomized phase III study [24]. Bevacizumab, an antibody binding VEGF, has recently been tested in a phase III trial in combination with cisplatin and pemetrexed. In patient who were able to receive bevacizumab, the OS was significantly extended in the pemetrexed/cisplatin/bevacizumab (PCB) group (18.8 months) versus the pemetrexed/cisplatin (PC) group (16.1 months). Second-line treatment with pemetrexed or with a platinum containing treatment was allowed in this study protocol and may have affected the OS. An improvement in progression-free survival (PFS) for the PCB group (9.2 months) versus the PC group (7.3 months) was also observed. Even though more patients stopped treatment in the PCB group due to toxicity, the quality of life in this group was considerably better than in the control group. However, absence of masking could have influenced the quality-of-life results, so these results should be interpreted with caution [25].

### *Other targeted agents*

Other targeted agents investigated as second-line treatment are bortezomib, vorinostat, everolimus, defactinib, asparagine-glycine-arginine-human tumor necrosis factor alpha (NGR-hTNF $\alpha$ ) and amatuximab.

Bortezomib, an inhibitor of the 20S proteasome, was tested in two phase II studies. As a

single agent in second-line treatment, it was not active. Also, in combination with cisplatin, bortezomib failed to meet the primary objectives [26, 27].

Vorinostat is a histone deacetylase (HDAC) inhibitor. HDACs are regulatory enzymes that manipulate histone modifications resulting in changes in the cell epigenetics. Inhibiting HDACs results in expression of genes associated with cell cycle arrest, apoptosis, and tumor suppression [20, 23]. Preclinical and phase I data showed promising results, which could not be confirmed in a randomized double-blind phase III study with single agent vorinostat [28].

A percentage of 35-40% of the patients with MPM have mutations in the neurofibromatosis type 2 (NF2) gene that encodes the protein merlin. Merlin downregulates the activity of the kinase mammalian target of rapamycin (mTOR) and blocks focal adhesion kinase (FAK) activation. Mutations in NF2 then results in activated mTOR and FAK [4, 10]. Everolimus is an inhibitor of mTOR that was tested in patients with MPM, yet the phase II study did not meet its primary endpoint [29]. Another compound targeting the NF2-pathway is defactinib, a FAK-inhibitor. While preclinical data again were promising, the placebo-controlled phase II study was early terminated due to reasons of futility [30]. Possibly the inhibition of the NF2/mTOR/FAK pathway was not sufficient to control MPM.

Tumor necrosis factor alpha (TNF- $\alpha$ ) is a secreted protein that induces apoptosis in endothelial-tumor cells via caspase activation. To target the protein to the tumor tissue and at the same time limit general side effects of TNF- $\alpha$ , TNF- $\alpha$  was fused to the tumor homing peptide sequence NGR [8, 10, 23]. A single agent phase II trial in 57 patients with MPM showed promising results [31]. In the following randomized phase III trial, patients who progressed on first-line treatment received weekly NGR-hTNF $\alpha$  or placebo in combination with gemcitabine, vinorelbine, doxorubicin, or best supportive care. In the intention to treat analysis the OS was not significant different between the NGR-hTNF $\alpha$  group and placebo group [32]. Currently, a maintenance phase II trial with NGR-hTNF $\alpha$  is ongoing, the primary objective is TTP (NCT01358084) (Table 1).

Amatuximab (MORab-009) is a chimeric monoclonal antibody that binds with high affinity to mesothelin [8, 10, 20, 33]. Mesothelin is a tumor-differentiating antigen, present at mesothelial cells lining the pleura, peritoneum and pericardium. Its biological function is unknown [4, 20, 33]. Mesothelin is highly expressed in epithelial MPM, but not in sarcomatoid MPM. The limited expression in normal mesothelial cells and high expression in tumor cells makes it an attractive target [23, 33-35]. Preclinical studies showed that amatuximab has activity against mesothelin expressing tumor cells [20, 36]. In a single-arm phase II study, cisplatin and pemetrexed were combined with amatuximab for six cycles, which was followed by amatuximab-maintenance therapy in case of response or stable disease (SD).

The primary endpoint, 3-month improvement in PFS compared to historical controls, was not met. However, with a PR in 39% of the patients and SD in 51% of the patients, the study concluded that amatuximab has activity in MPM [33]. Finding biomarkers to select patients for whom this drug would be effective is important. A randomized placebo-controlled study to investigate survival benefit is planned.

### *Oncolytic viral therapy*

A different approach in cancer therapy employs oncolytic viruses that are emerged to selectively eliminate cells with particular driver mutations. Different viruses including adenovirus, measles virus, vesicular stomatis virus, replication competent retrovirus, and the genetic engineered Newcastle disease virus have been tested in preclinical studies with good results [37-44]. To date one phase I/IIa study is testing the safety, tolerability and biological effect of the selectively replication-competent herpes simplex virus HSV1716 (NCT01721018) (Table 1).

### *Immunotherapy in MPM*

There are reported cases of spontaneous regression of MPM, which were associated with lymphocyte infiltration in the tumor. Lymphocyte infiltration in MPM is also associated with improved survival [45-47]. This data suggest that MPM could be an immunogenic tumor, which makes immunotherapy an interesting therapeutic option [45, 48, 49].

There have been several different immunotherapy approaches tested. One of those is an antibody-drug conjugate. SS1P is a recombinant pseudomonas toxin coupled to the variable fragment of an anti-mesothelin antibody [35, 50]. In phase I clinical trials, the vast majority of patients developed antibody responses to SS1P after one cycle of treatment, preventing further treatment unless this response is eliminated. Pentostatin and cyclophosphamide are drugs that deplete lymphocytes, preventing the formation of antitoxin antibodies. A phase II trial showed that pretreatment with these agents allowed patients to receive more cycles of treatment with SS1P, resulting in improved clinical responses [50].

While we discussed reagents directly targeting MPM, specific activation of immune responses in patients would be an alternative way of immunotherapy. A new wave of antibodies controlling checkpoints in immune cell control has shown strong responses in other tumors including non-small-cell lung cancer and melanoma [51-57]. These antibodies block the activities of programmed cell death protein 1 (PD-1), programmed death ligand 1 (PD-L1), and cytotoxic T-lymphocyte antigen 4 (CTLA-4)

PD-L1 is expressed in many tumor cells, including MPM [48, 49, 58-61]. Binding of PD-L1 to its receptor PD-1 on T cells inhibits proliferation and activation of T cells and quenches

immune responses against the tumor. As a result, tumors that express PD-L1 evade cytotoxic T-cell control. Consequently, blocking PD-1 with antibodies allows activation of cytotoxic T cells. Mansfield et al. showed positive PD-L1 expression in 40% of MPM tissues by immunohistochemistry (IHC) staining. Cedres et al. reported that 20.8% of the cases are positive for PD-L1 expression. Both articles report a higher incidence of PD-L1 expression in sarcomatoid MPM than in epitheloid MPM and describe that PD-L1 expression is associated with a poor prognosis [48, 49].

In a phase I study pembrolizumab, a PD-1 receptor antibody, was not only safe and tolerable for patients, also a disease control rate (DCR) of 76% was observed. Twenty-five patients with MPM received pembrolizumab after first line of treatment. Seven patients had a PR and 12 experienced SD [62]. Recently, a phase II study with second-line pembrolizumab treatment in MPM has opened for patient accrual (NCT 02399371). The first primary objective is determining the overall response rate in an unselected patient population and in a patient population with PD-L1 positive MPM. The second primary objective is to determine the threshold for PD-L1 expression using 22C3 antibody based IHC in correlation to tumor response (Table 1).

Nivolumab, another PD-1 receptor antibody, is currently evaluated in a single-arm phase II study in patients with recurrent MPM (NCT02497508). The primary objective of this study is the DCR at 12 weeks, which is expected to increase from 20% to 40% (Table 1).

Tremelimumab is a monoclonal antibody against CTLA-4. Blocking CTLA-4 will activate cytotoxic T cells directly. Two single-arm phase II studies have been conducted, both showing encouraging clinical activity [63, 64]. Therefore, a randomized double-blind placebo-controlled phase II study is now evaluating the efficacy of tremelimumab. The primary objective is demonstrating a 50% improvement in OS from 7 to 10.5 months (NCT01843374). Tremelimumab is also tested in combination with the anti-PD-L1 checkpoint inhibitor durvalumab. The primary outcome of this phase II study is immune-related objective response rate (NCT02588131) (Table 1).

While these checkpoint inhibitors, allow an OS improvement of 20% in melanoma patients, the current studies should show whether these could be reproduced for patients with mesothelioma or whether it predominantly induces PRs with only limited survival benefit.

### *Vaccines*

Vaccines against mesothelioma cells may increase the immune responses against the tumor. In 2005, Hegmans et al. reported that vaccination with antigen-pulsed dendritic cells (DCs) prevented tumor outgrowth in mice [65]. In the following phase I study, ten patients received

mature DCs, pulsed with the patient's own tumor lysate, after chemotherapy. The treatment was feasible and safe and in some patients antitumor immune responses were detected. Whether this has any effects on survival of patients with mesothelioma should be further tested [66]. The DCs in this study were pulsed with tumor extracts in which only a minor portion of the antigens are tumor specific and relevant for the immune system. Pulsing DCs with only one tumor-associated antigen should provide more specific responses. The MESODEC study is a phase I/II trial in which patients are treated with DCs that are loaded with Wilms tumor 1 (WT-1). WT-1 is a transcription factor, which is highly overexpressed in mesothelioma cells. The general objective of the MESODEC study is to show the feasibility and safety of WT-1-targeted DC vaccination in combination with chemotherapy. Whether this treatment enables the induction of a systemic and immune response is also evaluated (NCT02649829) (Table 1). Another strategy focusing on WT-1 is vaccination of patients with synthetic peptides derived from the WT-1 protein sequence. WT-1 could be targeted with a T-cell-based immunotherapeutic approach because it is processed and presented at the cell surface in the context of major histocompatibility complex class I molecules. A pilot study showed the vaccine gave minimal toxicity and induced immune responses against WT-1 in a high proportion of patients [67]. Currently, two phase II studies with WT-1 vaccination are ongoing. In both studies, WT-1 vaccination in combination with granulocyte macrophage colony stimulating factor with or without the vaccine adjuvant (montanide), is given after combined modality therapy. Primary outcome is 1-year PFS (NCT01890980 and NCT01265433) (Table 1).

Immunotherapy against cancer is a fast-developing treatment strategy with antibody-drug conjugates, new reagents to overcome immune checkpoints in order to boost immune responses, and vaccination strategies that are all tested in phase II studies on patients with mesothelioma. The prospects are bright for a subgroup of patients but these have to be selected.

### **Pre-clinical models in translational research for MPM**

If clinical trials reveal one thing, it is that many drugs fail in phase II studies. Most of the drugs described in this review were active in preclinical studies, but lacked antitumor activity in the clinical setting. It is apparently difficult to predict clinical outcome with preclinical models. Selection of compounds for further clinical development is challenging. This is even more urgent in MPM since the disease is heterogeneous, the patient population is small and many new drugs are generated. Preclinical models are essential for a better selection process. Several factors are important in a good preclinical model. First of all, the preclinical model should resemble the patients' tumor, ideally with a representation of the stroma surrounding the tumor cells, the surrounding immune cells and vasculature. With many new

**Table 1** Ongoing phase II and III trials in mesothelioma.

Drug	Clinical trial number	Primary outcome	Description
Growth factor inhibitor			
IMC-A12	NCT01160458	CRR	Evaluate the safety and effectiveness of IMC-A12, an antibody blocking type I insulin like growth factor in patients that previously received chemotherapy
Targeted agents			
cetuximab	NCT00996567	PFS	Multicenter open phase II study testing cetuximab in combination with pemetrexed and cisplatin or carboplatin as first line treatment
Alisertib	NCT02293005	DCR	Evaluate the safety and effectiveness of alisertib an inhibitor of aurora kinase A protein
Defactinib	NCT02004028	Biomark respons	Assess biomarker response from tumor tissue of patients that received defactinib prior to surgery
NGR-hTNF $\alpha$	NCT01358084	PFS	Randomized double blind phase II study to determine efficacy of NGR-hTNF $\alpha$ as maintenance treatment
amatuximab	NCT02357147	OS	Multicenter, double blind randomized phase II study evaluating the safety and efficacy of amatuximab in combination with pemetrexed and cisplatin as first line treatment.
Oncolytic viruses			
HSV1/716	NCT01721018	Safety, tolerability	Phase I/IIa of the safety, tolerability and biological effect of single and repeat administration of the herpes simplex virus
Immunotherapy			
Pembrolizumab	NCT02399371	Ability PD-L1 to predict response, OS	Phase II study to evaluate the effect of pembrolizumab on OS.
Nivolumab	NCT02497508	DCR	Single arm phase II study to determine if nivolumab will improve DCR from 20% to 40% at 12 weeks.
Tremelimumab	NCT01843374	OS	Phase IIb, randomized double blind study to determine the effect of tremelimumab on OS.
Tremelimumab + MEDI4736	NCT02588131	ORR	NIBIT-MESO1 is a phase II, open label, single arm study evaluating the efficacy of tremelimumab in combination with the $\alpha$ PD-L1, MEDI4736
Vaccine			
DC vaccination	NCT02649829	Number patients *	MESODEC is a phase I/II trial to show the feasibility and safety of WT-1 targeted DC vaccination in combination with chemotherapy prior to surgery.
WT-1 vaccination	NCT01890980	One year PFS	Phase II study determining if PFS is extended for patients receiving WT1 vaccine and montanide + GM-CSF after multimodality treatment compared to patients receiving montanide + GM-CSF after multimodality treatment
WT-1 vaccination	NCT01265433	One year PFS	Phase II study determining if PFS is extended for patients receiving WT1 vaccine and montanide + GM-CSF after multimodality treatment compared to patients receiving montanide + GM-CSF after multimodality treatment

NGR-hTNF $\alpha$ : peptide asparagine-glycine-arginine – human tumor necrosis factor alpha, DC: dendritic cell, CRR: clinical response rate, PFS: progression free survival, DCR: disease control rate, OS: overall survival, ORR: objective response rate.\* number of resectable patients with feasible and safe DC vaccine product and the number of patients receiving DC vaccination in combination with chemotherapy within the proposed time frame of surgery.

drugs generated, it is important to be able to test multiple drugs at the same time; therefore, the preclinical model should be easy to handle and reproducible in its readout. Another factor is time; it is important to get results within a short period of time, so a preclinical model should not be time consuming. There are many preclinical models available, each with their own advantages and disadvantages.

### *Cell lines*

Most preclinical models are based on cell-line experiments. Cell lines are typically passaged for many years, making them highly selected clonal subpopulations of the original tumor, with many additional genetic aberrations. They then become a relatively poor representation of the original tumor [68-71]. Cell lines can be cultured in monolayer or in spheroids. Spheroids are tumor cells organized in a three-dimensional (3D) arrangement [70]. Monolayer cultures are easy to handle and suitable for large scale drug testing. Spheroids are more laborious but may better reflect the natural conditions of the tumor. They are not suitable for large-scale drug testing since read out of cell survival and quantification is challenging. MPM is a tumor extremely resistant to chemotherapy, mostly due to resistance to apoptosis [70, 72]. Spheroids acquire multicellular resistance to a variety of treatments, which mimics the chemoresistance in patients [73, 74]. Some drugs exhibit sensitivity in monolayer culture but resistance in spheroids. The proteasome inhibitor bortezomib, for example was found to be very effective in monolayer MPM cell-line cultures [75-77]. However, the phase II studies with this drug were disappointing. Lack of activity was also observed in spheroid cultures [26, 27]. Barbone et al. showed that spheroids treated with bortezomib were resistant due to upregulation of Noxa, a BH3-protein that displaces Bim and thereby mediates apoptosis [73].

Perfused microfluidic systems in combination with spheroids, may better reflect the *in vivo* situation, because regulation of drug exposure and mass transport is possible. Ruppen et al. compared static 3D cultures with perfused 3D cultures. For perfused 3D cultures, a microfluidic chip was used. This chip contained two identical channels, each with eight trapping sections and in each section a spheroid. Spontaneously formed spheroids were trapped in the sections, after which nutrients, oxygen and drugs were delivered by diffusion from the main channel. Interestingly, perfused spheroids were twice as resistant to cisplatin compared to static spheroids [74].

### *Primary tumor cultures*

Primary tumor cultures are cultures of single cells isolated from patients, which are propagated for a short period of time in order to prevent formation of clonal subpopulations. Multiple groups generated primary tumor cultures from cells isolated from pleural effusions of patients with MPM. These cultures resemble the original tumor closely regarding

histological and molecular features [14, 71, 78, 79]. Szulkin et al. used primary tumor cultures for chemosensitivity assays and observed a large patient-to-patient variability in sensitivity to drugs. Many cultures were resistant to drugs as was also observed in the clinical setting [14].

Xiang et al. generated spheroids from primary tumor cells. The spheroid of one primary cell line resembled cell-line spheroids, while the spheroid of another primary cell line formed mostly loose aggregates [79]. It was not reported how long these primary cells were cultured and how often they were passaged, which makes it difficult to conclude that single cell spheroid formation from primary tumor cultures is a reproducible system. Tumor fragment spheroids are small biopsies of the tumor cultured on a collagen layer in order to grow out as spheroids. These tumor fragment spheroids exhibit the same complexity of cell types and extracellular matrix as the tumor. They retain many characteristics of the original tumor. Chemosensitivity assays on these tumor fragment spheroids are possible, but only for a very limited number of conditions [72, 73, 80, 81]. Techniques allowing a simple, individual tumor-based drug screen remain challenging.

### *Mouse models*

Animal models are also very important in preclinical drug development. One advantage of animal models is that they can mimic the 3D structure of a tumor and the vasculature around it. Furthermore, it also considers the pharmacokinetics, pharmacodynamics, and toxicity of a compound and in some models even the contribution of the immune system. There are different types of models reported, most of them mouse-based. In older models, mesothelioma tumors were induced by intrapleural or intrabronchial exposure to carcinogen-like asbestos fiber, other natural and synthetic fibers and metals. Mouse models with mesothelial specific expression of oncogenes like SV40, NF2 or p53 were used to accelerate the induction of MPM in asbestos-exposed mice [82-84]. While these models resembled the human mesothelioma in terms of latency, superficial growth, shedding of tumor cells, and growth as spheroids, these models had no loss of function of genes known to be inactivated in human MPM. This made it difficult to understand the molecular mechanism underlying the tumor [82]. Jongsma et al. developed the first genetic mouse model of MPM. Knockout mice, deficient in the NF2 gene, were crossed with INK4A/ARF or p53 deficient mice. The offspring mice rapidly developed mesothelioma, with a high incidence and without further exposure to carcinogens [82, 84]. The tumors that arise in these mice are not representative of the human tumor, but can be constructed with genetic mutations common to most of the patient with MPM. With increasing knowledge about genetic mutations in mesothelioma, it is important to introduce the most prevalent mutations in these genetic mouse models. This will better resemble the human tumor. In other animal models, cell lines were injected in the pleural cavity of the mice. Most available cell lines however, do not form tumors in

**Table 2.** Overview of the available preclinical models and the features based on resembling the tumor, drug testing, and time

Preclinical Model		Resemble patients cells of tumor	Resemble natural conditions of tumor	Drug testing	Time
Cell line models	Monolayer	No	No	Multiple	Fast
	3D spheroids	No	Only to chemo resistance	View	Slow
Primary tumor models	Monolayer	Yes	No	Multiple	Fast
	3D spheroids	Yes	Only to chemo resistance	View	Slow
	Tumor fragments	Yes	Stroma composition Chemo resistance	View	Slow
Mouse models	Asbestos induced	No	Yes	One	Slow
	Genetic	No	Yes	One	Fast
	Xenograft cell lines	No	Yes, however no immune system	One	Slow
	Patient derived xenograft	Yes	Yes, however no immune system	One	Slow

mice [71]. Those that do, may be selected for survival under mouse conditions and may not reflect human MPM. Patient-derived xenografts (PDX) are tumor biopsies or tumor cells from pleural effusions transplanted in nude mice. Kalra et al. showed that a PDX-mouse model for MPM resembles the primary tumor culture and primary tumor regarding both histological and molecular features [71]. A disadvantage of this type of model is that it can only be generated in immune-deficient mice. The immune system may have a role in tumor clearance and sometimes chemotherapy response, which complicates evaluation of the PDX-mouse models. Although there are drawbacks, PDX-mouse models could be very useful in evaluating efficacy of therapeutic agents.

We summarized various cell-based models and mouse models that are available to improve translational research (table 2). Each model has its own advantages and disadvantages and no model is perfect. Which model should be used depends on the aim of the research. Most important, none of the models have been validated by a strong corresponding chemotherapy response between the model and the corresponding patient.

### Expert commentary and five year view

The prognosis for patients with MPM has not improved over the last decade. The current standard of care, cisplatin in combination pemetrexed, has not been replaced by another treatment regimen in 12-year time. Although many therapies have been tested on patients with MPM, none were effective in phase II trials.

There are various reasons for the limited progress in the treatment of mesothelioma. The

first reason is the relatively small size of the patient population. This limits the interest of the pharmaceutical industry but also complicates the execution of large randomized studies. This may be further complicated when mesothelioma is a more diverse tumor than anticipated. It is very difficult to define personalized treatment options unless obvious biomarkers related to treatment success are defined. These are currently lacking.

Yet there are a number of developments that can be expected to improve the prospects for, at least a subgroup of, patients with MPM. First, the genome of many mesothelioma tumors is sequenced and defines genes that are often mutated, including the gene encoding the breast cancer-associated protein 1 (BAP1) [85-87]. BAP1 loss may affect the activity of the histone-methyltransferase EZH2 resulting in unusually high H3K27me3 modifications [88]. This epigenetic marker is also observed in other tumors and suggests that drugs affecting the epigenetic marker may be more selective and effective against MPM. This is indeed suggested in preclinical models. Second, drug screens can be performed on primary tumor cultures of MPM cells or, possibly, spheroids of these cells [14]. The detected drug responses could be coupled to the patient that donated these tumor cells. This will allow personalized treatment for patients with MPM and *ex vivo* testing of larger series of anticancer drugs to select the best combination for the individual patient. Prediction should be accurate to prevent false-negative predictions and inadequate treatment of patients with MPM. This is critical before personalized screening on basis of patients tumor cells will be introduced in the clinic. Third, the latest addition to the cancer-drug repertoire, is immunotherapy with check-point inhibitors. Proteins like PD-1, PD-L1 and CTLA-4 can dampen the adaptive immune response against tumors. Antibodies blocking these proteins establish the local immune responses against cancer, in fact starting a controlled auto-immune response. This new therapy can be effective for tumors with a high mutational load, which does not include MPM. Yet, the unique and high expression of proteins in tissues or tumors may also unleash an immune response and this will be tested for MPM in the near future.

Although the prospects for MPM treatment have not improved over the last decade, there are various developments that may finally lead to a step forward in the treatment of this tumor. The next decade will show serious progress in the fundamental understanding of MPM which in turn will improve outcome of these patients.

## Key issues

- MPM is an aggressive tumor with a poor prognosis. For patients that do not respond to first-line treatment or become progressive after treatment there is no standard second-line treatment available.
- Many inhibitors of growth factors are tested in MPM, most with negative results.

Bevacizumab is the most promising agent.

- For other targeted agents, large phase II and phase III trials have been conducted.
- Immunotherapy is a new development in MPM, studies testing antibodies against PD-1 and CTLA-4 are ongoing.
- Other ongoing trials are focusing on primed DC-vaccination and WT-1 vaccination.
- Many drugs that were active in preclinical models, fail in phase II studies, indicating it is difficult to predict clinical outcome with preclinical models.
- A good preclinical model resembles the patients' tumor, is able to test multiple drugs at the same time and generate results within a short period of time.
- Each model, cell-based or mouse, has its own advantages and disadvantages, no model is perfect. Which model should be used depends on the aim of the research.
- Genome sequencing, drug screens performed on primary MPM cells, and immunotherapy with checkpoint inhibitors, are developments that can be expected to improve MPM.

---

## References

1. Martini, N., et al., *Pleural mesothelioma*. *Ann Thorac Surg*, 1987. **43**(1): p. 113-20.
2. Suzuki, Y., *Pathology of human malignant mesothelioma--preliminary analysis of 1,517 mesothelioma cases*. *Ind Health*, 2001. **39**(2): p. 183-5.
3. van Zandwijk, N., et al., *Guidelines for the diagnosis and treatment of malignant pleural mesothelioma*. *J Thorac Dis*, 2013. **5**(6): p. E254-307.
4. Buikhuisen, W.A., et al., *Second line therapy in malignant pleural mesothelioma: A systematic review*. *Lung Cancer*, 2015. **89**(3): p. 223-31.
5. Henley, S.J., et al., *Mesothelioma incidence in 50 states and the District of Columbia, United States, 2003-2008*. *Int J Occup Environ Health*, 2013. **19**(1): p. 1-10.
6. Baas, P., et al., *Malignant pleural mesothelioma: ESMO Clinical Practice Guidelines for diagnosis, treatment and follow-up*. *Ann Oncol*, 2015.
7. Scherpereel, A., et al., *Guidelines of the European Respiratory Society and the European Society of Thoracic Surgeons for the management of malignant pleural mesothelioma*. *Eur Respir J*, 2010. **35**(3): p. 479-95.
8. Remon, J., et al., *Malignant mesothelioma: new insights into a rare disease*. *Cancer Treat Rev*, 2013. **39**(6): p. 584-91.
9. Wagner, J.C., C.A. Sleggs, and P. Marchand, *Diffuse pleural mesothelioma and asbestos exposure in the North Western Cape Province*. *Br J Ind Med*, 1960. **17**: p. 260-71.
10. Christoph, D.C. and W.E. Eberhardt, *Systemic treatment of malignant pleural mesothelioma: new agents in clinical trials raise hope of relevant improvements*. *Curr Opin Oncol*, 2014. **26**(2): p. 171-81.
11. Vogelzang, N.J., et al., *Phase III study of pemetrexed in combination with cisplatin versus cisplatin alone in patients with malignant pleural mesothelioma*. *J Clin Oncol*, 2003. **21**(14): p. 2636-44.
12. van Meerbeeck, J.P., et al., *Randomized phase III study of cisplatin with or without raltitrexed in patients with malignant pleural mesothelioma: an intergroup study of the European Organisation for Research and Treatment of Cancer Lung Cancer Group and the National Cancer Institute of Canada*. *J Clin Oncol*, 2005. **23**(28): p. 6881-9.
13. Szulkin, A., et al., *Variation in drug sensitivity of malignant mesothelioma cell lines with substantial effects of selenite and bortezomib, highlights need for individualized therapy*. *PLoS One*, 2013. **8**(6): p. e65903.
14. Szulkin, A., et al., *Characterization and drug sensitivity profiling of primary malignant mesothelioma cells from pleural effusions*. *BMC Cancer*, 2014. **14**: p. 709.
15. Janne, P.A., *Chemotherapy for malignant pleural mesothelioma*. *Clin Lung Cancer*, 2003. **5**(2): p. 98-106.
16. Ryan, C.W., J. Herndon, and N.J. Vogelzang, *A review of chemotherapy trials for malignant mesothelioma*. *Chest*, 1998. **113**(1 Suppl): p. 665-73S.
17. Tomek, S., et al., *Chemotherapy for malignant pleural mesothelioma: past results and recent developments*. *Br J Cancer*, 2003. **88**(2): p. 167-74.
18. Berghmans, T., et al., *Activity of chemotherapy and immunotherapy on malignant mesothelioma: a systematic review of the literature with meta-analysis*. *Lung Cancer*, 2002. **38**(2): p. 111-21.
19. Wang, D. and S.J. Lippard, *Cellular processing of platinum anticancer drugs*. *Nat Rev Drug Discov*, 2005. **4**(4): p. 307-20.
20. Kelly, R.J., E. Sharon, and R. Hassan, *Chemotherapy and targeted therapies for unresectable malignant mesothelioma*. *Lung Cancer*, 2011. **73**(3): p. 256-63.
21. Niyikiza, C., et al., *Homocysteine and methylmalonic acid: markers to predict and avoid toxicity from pemetrexed therapy*. *Mol Cancer Ther*, 2002. **1**(7): p. 545-52.
22. Manegold, C., et al., *Second-line (post-study) chemotherapy received by patients treated in the phase III trial of pemetrexed plus cisplatin versus cisplatin alone in malignant pleural mesothelioma*. *Ann Oncol*, 2005. **16**(6): p. 923-7.
23. Astoul, P., et al., *Malignant pleural mesothelioma: from the bench to the bedside*. *Respiration*, 2012. **83**(6): p. 481-93.
24. Buikhuisen, W.A., et al., *Thalidomide versus active supportive care for maintenance in patients with malignant mesothelioma after first-line chemotherapy (NVALT 5): an open-label, multicentre, randomised phase 3 study*. *Lancet Oncol*, 2013. **14**(6): p. 543-51.
25. Zalcman, G., et al., *Bevacizumab for newly diagnosed pleural mesothelioma in the Mesothelioma Avastin Cisplatin Pemetrexed Study (MAPS): a randomised, controlled, open-label, phase 3 trial*. *Lancet*, 2015.

26. Fennell, D.A., et al., *Phase II clinical trial of first or second-line treatment with bortezomib in patients with malignant pleural mesothelioma*. J Thorac Oncol, 2012. **7**(9): p. 1466-70.
27. O'Brien, M.E., et al., *Phase II study of first-line bortezomib and cisplatin in malignant pleural mesothelioma and prospective validation of progression free survival rate as a primary end-point for mesothelioma clinical trials (European Organisation for Research and Treatment of Cancer 08052)*. Eur J Cancer, 2013. **49**(13): p. 2815-22.
28. Krug, L.M., et al., *Vorinostat in patients with advanced malignant pleural mesothelioma who have progressed on previous chemotherapy (VANTAGE-014): a phase 3, double-blind, randomised, placebo-controlled trial*. Lancet Oncol, 2015. **16**(4): p. 447-56.
29. Ou, S.H., et al., *SWOG S0722: phase II study of mTOR inhibitor everolimus (RAD001) in advanced malignant pleural mesothelioma (MPM)*. J Thorac Oncol, 2015. **10**(2): p. 387-91.
30. Devine, A., *Defactinib Disappoints. Can Other Trials Pick Up the Slack?* October 8, 2015: [www.mesotheliomaguide.com](http://www.mesotheliomaguide.com).
31. Gregorc, V., et al., *Phase II study of asparagine-glycine-arginine-human tumor necrosis factor alpha, a selective vascular targeting agent, in previously treated patients with malignant pleural mesothelioma*. J Clin Oncol, 2010. **28**(15): p. 2604-11.
32. Gaafar, R.M., et al., *Phase III trial (NGR015) with NGR-hTNF plus best investigator choice (BIC) versus placebo plus BIC in previously treated patients with advanced malignant pleural mesothelioma (MPM)*. J Clin Oncol, 2015. **33**(suppl; abstr 7501).
33. Hassan, R., et al., *Phase II clinical trial of amatuximab, a chimeric antimesothelin antibody with pemetrexed and cisplatin in advanced unresectable pleural mesothelioma*. Clin Cancer Res, 2014. **20**(23): p. 5927-36.
34. Hassan, R., T. Bera, and I. Pastan, *Mesothelin: a new target for immunotherapy*. Clin Cancer Res, 2004. **10**(12 Pt 1): p. 3937-42.
35. Chowdhury, P.S., K. Chang, and I. Pastan, *Isolation of anti-mesothelin antibodies from a phage display library*. Mol Immunol, 1997. **34**(1): p. 9-20.
36. Hassan, R., et al., *Preclinical evaluation of MORAb-009, a chimeric antibody targeting tumor-associated mesothelin*. Cancer Immun, 2007. **7**: p. 20.
37. Takagi-Kimura, M., et al., *Enhanced antitumor efficacy of fiber-modified, midkine promoter-regulated oncolytic adenovirus in human malignant mesothelioma*. Cancer Sci, 2013. **104**(11): p. 1433-9.
38. Willmon, C., et al., *Vesicular stomatitis virus-induced immune suppressor cells generate antagonism between intratumoral oncolytic virus and cyclophosphamide*. Mol Ther, 2011. **19**(1): p. 140-9.
39. Willmon, C.L., et al., *Expression of IFN-beta enhances both efficacy and safety of oncolytic vesicular stomatitis virus for therapy of mesothelioma*. Cancer Res, 2009. **69**(19): p. 7173-20.
40. Kawasaki, Y., et al., *Replication-competent retrovirus vector-mediated prodrug activator gene therapy in experimental models of human malignant mesothelioma*. Cancer Gene Ther, 2011. **18**(8): p. 571-8.
41. Li, H., et al., *Oncolytic measles viruses encoding interferon beta and the thyroidal sodium iodide symporter gene for mesothelioma virotherapy*. Cancer Gene Ther, 2010. **17**(8): p. 550-8.
42. Silberhumer, G.R., et al., *Genetically engineered oncolytic Newcastle disease virus effectively induces sustained remission of malignant pleural mesothelioma*. Mol Cancer Ther, 2010. **9**(10): p. 2761-9.
43. Gauvrit, A., et al., *Measles virus induces oncolysis of mesothelioma cells and allows dendritic cells to cross-prime tumor-specific CD8 response*. Cancer Res, 2008. **68**(12): p. 4882-92.
44. Zhu, Z.B., et al., *Targeting mesothelioma using an infectivity enhanced survivin-conditionally replicative adenoviruses*. J Thorac Oncol, 2006. **1**(7): p. 701-11.
45. Robinson, B.W., C. Robinson, and R.A. Lake, *Localised spontaneous regression in mesothelioma -- possible immunological mechanism*. Lung Cancer, 2001. **32**(2): p. 197-201.
46. Anraku, M., et al., *Impact of tumor-infiltrating T cells on survival in patients with malignant pleural mesothelioma*. J Thorac Cardiovasc Surg, 2008. **135**(4): p. 823-9.
47. Leigh, R.A. and I. Webster, *Lymphocytic infiltration of pleural mesothelioma and its significance for survival*. S Afr Med J, 1982. **61**(26): p. 1007-9.
48. Cedres, S., et al., *Analysis of expression of programmed cell death 1 ligand 1 (PD-L1) in malignant pleural mesothelioma (MPM)*. PLoS One, 2015. **10**(3): p. e0121071.
49. Mansfield, A.S., et al., *B7-H1 expression in malignant pleural mesothelioma is associated with sarcomatoid histology and poor prognosis*. J Thorac Oncol, 2014. **9**(7): p. 1036-40.
50. Hassan, R., et al., *Major cancer regressions in mesothelioma after treatment with an anti-mesothelin immunotoxin and immune suppression*. Sci Transl Med, 2013. **5**(208): p. 208ra147.
51. Brahmer, J.R., et al., *Safety and activity of anti-PD-L1 antibody in patients with advanced cancer*. N Engl

- J Med, 2012. **366**(26): p. 2455-65.
52. Borghaei, H., et al., *Nivolumab versus Docetaxel in Advanced Nonsquamous Non-Small-Cell Lung Cancer*. N Engl J Med, 2015. **373**(17): p. 1627-39.
53. Rizvi, N.A., et al., *Activity and safety of nivolumab, an anti-PD-1 immune checkpoint inhibitor, for patients with advanced, refractory squamous non-small-cell lung cancer (CheckMate 063): a phase 2, single-arm trial*. Lancet Oncol, 2015. **16**(3): p. 257-65.
54. Weber, J.S., et al., *Nivolumab versus chemotherapy in patients with advanced melanoma who progressed after anti-CTLA-4 treatment (CheckMate 037): a randomised, controlled, open-label, phase 3 trial*. Lancet Oncol, 2015. **16**(4): p. 375-84.
55. Robert, C., et al., *Nivolumab in previously untreated melanoma without BRAF mutation*. N Engl J Med, 2015. **372**(4): p. 320-30.
56. Robert, C., et al., *Ipilimumab plus dacarbazine for previously untreated metastatic melanoma*. N Engl J Med, 2011. **364**(26): p. 2517-26.
57. Hodi, F.S., et al., *Improved survival with ipilimumab in patients with metastatic melanoma*. N Engl J Med, 2010. **363**(8): p. 711-23.
58. Calles, A., et al., *Expression of PD-1 and its ligands, PD-L1 and PD-L2, in smokers and never smokers with KRAS mutant lung cancer*. J Thorac Oncol, 2015.
59. Llosa, N.J., et al., *The vigorous immune microenvironment of microsatellite instable colon cancer is balanced by multiple counter-inhibitory checkpoints*. Cancer Discov, 2015. **5**(1): p. 43-51.
60. Lyford-Pike, S., et al., *Evidence for a role of the PD-1:PD-L1 pathway in immune resistance of HPV-associated head and neck squamous cell carcinoma*. Cancer Res, 2013. **73**(6): p. 1733-41.
61. Tarhini, A.A., et al., *Tumor associated PD-L1 expression pattern in microscopically tumor positive sentinel lymph nodes in patients with melanoma*. J Transl Med, 2015. **13**(1): p. 319.
62. Alley, E., et al., *Clinical safety and efficacy of pembrolizumab (MK-3475) in patients with malignant pleural mesothelioma: preliminary results from KEYNOTE-001*. AACR 2015, (abstract # CT103).
63. Calabro, L., et al., *Tremelimumab for patients with chemotherapy-resistant advanced malignant mesothelioma: an open-label, single-arm, phase 2 trial*. Lancet Oncol, 2013. **14**(11): p. 1104-11.
64. Calabro, L., et al., *Efficacy and safety of an intensified schedule of tremelimumab for chemotherapy-resistant malignant mesothelioma: an open-label, single-arm, phase 2 study*. Lancet Respir Med, 2015. **3**(4): p. 301-9.
65. Hegmans, J.P., et al., *Immunotherapy of murine malignant mesothelioma using tumor lysate-pulsed dendritic cells*. Am J Respir Crit Care Med, 2005. **171**(10): p. 1168-77.
66. Hegmans, J.P., et al., *Consolidative dendritic cell-based immunotherapy elicits cytotoxicity against malignant mesothelioma*. Am J Respir Crit Care Med, 2010. **181**(12): p. 1383-90.
67. Krug, L.M., et al., *WT1 peptide vaccinations induce CD4 and CD8 T cell immune responses in patients with mesothelioma and non-small cell lung cancer*. Cancer Immunol Immunother, 2010. **59**(10): p. 1467-79.
68. Hudson, A.L., et al., *Establishing a panel of chemo-resistant mesothelioma models for investigating chemo-resistance and identifying new treatments for mesothelioma*. Sci Rep, 2014. **4**: p. 6152.
69. Kamb, A., *What's wrong with our cancer models?* Nat Rev Drug Discov, 2005. **4**(2): p. 161-5.
70. Kim, J.B., *Three-dimensional tissue culture models in cancer biology*. Semin Cancer Biol, 2005. **15**(5): p. 365-77.
71. Kalra, N., et al., *Mesothelioma patient derived tumor xenografts with defined BAP1 mutations that mimic the molecular characteristics of human malignant mesothelioma*. BMC Cancer, 2015. **15**: p. 376.
72. Barbone, D., et al., *Vorinostat eliminates multicellular resistance of mesothelioma 3D spheroids via restoration of Noxa expression*. PLoS One, 2012. **7**(12): p. e52753.
73. Barbone, D., et al., *The Bcl-2 repertoire of mesothelioma spheroids underlies acquired apoptotic multicellular resistance*. Cell Death Dis, 2011. **2**: p. e174.
74. Ruppen, J., et al., *A microfluidic platform for chemoresistive testing of multicellular pleural cancer spheroids*. Lab Chip, 2014. **14**(6): p. 1198-205.
75. Gordon, G.J., et al., *Preclinical studies of the proteasome inhibitor bortezomib in malignant pleural mesothelioma*. Cancer Chemother Pharmacol, 2008. **61**(4): p. 549-58.
76. Sartore-Bianchi, A., et al., *Bortezomib inhibits nuclear factor-kappaB dependent survival and has potent in vivo activity in mesothelioma*. Clin Cancer Res, 2007. **13**(19): p. 5942-51.
77. Wang, Y., et al., *Targeted proteasome inhibition by Velcade induces apoptosis in human mesothelioma and breast cancer cell lines*. Cancer Chemother Pharmacol, 2010. **66**(3): p. 455-66.
78. Patterson, M.J., et al., *Assessing the function of homologous recombination DNA repair in malignant*

79. pleural effusion (MPE) samples. *Br J Cancer*, 2014. **111**(1): p. 94-100.
80. Xiang, X., et al., *The development and characterization of a human mesothelioma in vitro 3D model to investigate immunotoxin therapy*. *PLoS One*, 2011. **6**(1): p. e14640.
81. Kim, K.U., et al., *A novel in vitro model of human mesothelioma for studying tumor biology and apoptotic resistance*. *Am J Respir Cell Mol Biol*, 2005. **33**(6): p. 541-8.
82. Wilson, S.M., et al., *mTOR mediates survival signals in malignant mesothelioma grown as tumor fragment spheroids*. *Am J Respir Cell Mol Biol*, 2008. **39**(5): p. 576-83.
83. Jongsma, J., et al., *A conditional mouse model for malignant mesothelioma*. *Cancer Cell*, 2008. **13**(3): p. 261-71.
84. Kane, A.B., *Animal models of malignant mesothelioma*. *Inhal Toxicol*, 2006. **18**(12): p. 1001-4.
85. Stathopoulos, G.T. and I. Kalomenidis, *Animal models of malignant pleural effusion*. *Curr Opin Pulm Med*, 2009. **15**(4): p. 343-52.
86. Lo Iacono, M., et al., *Targeted next-generation sequencing of cancer genes in advanced stage malignant pleural mesothelioma: a retrospective study*. *J Thorac Oncol*, 2015. **10**(3): p. 492-9.
87. Guo, G., et al., *Whole-exome sequencing reveals frequent genetic alterations in BAP1, NF2, CDKN2A, and CUL1 in malignant pleural mesothelioma*. *Cancer Res*, 2015. **75**(2): p. 264-9.
88. De Rienzo, A., et al., *Gender-Specific Molecular and Clinical Features underlie Malignant Pleural Mesothelioma*. *Cancer Res*, 2015.
89. LaFave, L.M., et al., *Loss of BAP1 function leads to EZH2-dependent transformation*. *Nat Med*, 2015. **21**(11): p. 1344-9.



# Chapter 2

## Chemical Profiling of Primary Mesothelioma Cultures Defines Subtypes with Different Expression Profiles and Clinical Responses.

Laurel M. Schunselaar\*, Josine M.M.F. Quispel-Janssen\*, Yongsoo Kim, Costantine Alifrangis, Wilbert Zwart, Paul Baas and Jacques Neefjes

\*equal contribution

Clin Cancer Res. 2018 Apr; 24(7):1761-1770



## **Abstract**

**Purpose:** Finding new treatment options for patients with malignant pleural mesothelioma is challenging due to the rarity and heterogeneity of this cancer type. The absence of druggable targets further complicates the development of new therapies. Current treatment options are therefore limited and prognosis remains poor.

**Experimental design:** We performed drug screening on primary mesothelioma cultures to guide treatment decisions of corresponding patients that were progressive after first- or second-line treatment.

**Results:** We observed a high concordance between in vitro results and clinical outcomes. We defined three subgroups responding differently to the anticancer drugs tested. In addition, gene expression profiling yielded distinct signatures that segregated the differently responding subgroups. These genes signatures involved various pathways, most prominently the fibroblast growth factor pathway.

**Conclusions:** Our primary mesothelioma culture system has proved to be suitable to test novel drugs. Chemical profiling of primary mesothelioma cultures allows personalizing treatment for a group of patients with a rare tumor type, where clinical trials are notoriously difficult. This personalized treatment strategy is expected to improve the poor prospects of mesothelioma patients.

## **Keywords**

Mesothelioma, clinical responses, genetic profile, FGFR, personalized treatment

## Translational relevance

Mesothelioma or asbestos cancer is a tumor with a poor prognosis. Three mesothelioma subtypes have been defined based on morphology, and no effective treatment is available. Here, we describe a system allowing the culture of primary mesothelioma cells for drug testing and genetic analyses. On the basis of drug sensitivities, we define three new mesothelioma subtypes with a concomitant different gene expression profile, including FGF pathway. Translating the results of the primary cultures to the treatment of a small set of patients correctly predicted clinical responses. Chemical profiling of patients with mesothelioma allows identification of subgroups separated by the feature most relevant to patients; drug responses. The corresponding genetic analysis identifies the FGF pathway for targeting in a defined mesothelioma subgroups.

## Introduction

Malignant pleural mesothelioma (MPM) is a rare but aggressive tumor arising from mesothelial cells in the pleural cavity. It usually presents with pain or dyspnea, caused by pleural fluid or shrinkage of the hemithorax [1]. Palliative chemotherapy consisting of a platin and antifolate combination is considered standard of care and gives a modest survival advantage of around 3 months [2]. Further systemic treatment can be offered to fit patients, but thus far, studies in second-line failed to detect a survival benefit. Response rates in different second-line therapies range between 0% and 20% [3], which urges the need for more effective treatments.

Using genetic profiling to define drivers in cancer amendable to targeting by small molecular drugs has been successful in other types of tumors. MPM, however, has only a few mutations and none of these present as a likely target for therapy. Most genetic mutations found in MPM are loss of tumor suppressor genes, like CDKN2A, NF2 and BAP1, rather than activation of oncogenes [4]. The absence of druggable molecular targets in MPM hinders the development of more dedicated and effective therapies [5-9].

Based on histology, three types of mesothelioma are recognized: an epithelioid, a sarcomatoid, and a biphasic or mixed type [10]. Epithelioid mesothelioma comprises the largest group and has a better outcome than the sarcomatoid and mixed type. Regarding response to treatment, epithelioid mesothelioma is a heterogeneous disease. To increase the effectivity of current therapies, it is vital to find ways to more accurately profile this group of patients for personalized treatment and new therapeutic options.

Long-established cell lines are commonly used for in vitro drug screens to select compounds

for further clinical development [11]. However, their resemblance to primary tumors is questionable because cells change pheno- and genotypically during their adaptation to tissue culture conditions [12-15]. This can have a profound influence on their responses to anticancer drugs [16, 17]. The use of cell lines in drug development programs did not yield any active drugs for patients with mesothelioma. One example is the VANTAGE-014 trial, which was based on positive results from established cell lines [18]. This study exemplifies the difficulty of conducting clinical trials in a rare disease like mesothelioma [19](12). In this placebo-controlled trial that evaluated the HDAC-inhibitor vorinostat in second or third line, the time to accrue 661 patients with mesothelioma from 90 international centers was 6 years. Unfortunately, there was no clinical benefit from treatment with vorinostat in this very large study [20]. This trial stresses the need for in vitro drug testing conditions that reflect genuine mesothelioma tumors more accurately. Primary mesothelioma cultures may provide a valuable model for personalized drug selection for patients with mesothelioma because they recapitulate the original tumor far more accurately than long-established MPM cell lines [21, 22].

We established a method of profiling primary mesothelioma cultures with commonly used anticancer drugs and validated the results in corresponding patients. We distinguished three groups, not by means of genetic parameters, but based on the drug response patterns, which are ultimately more relevant to the patient. We found that the three “chemical” profiles were associated with three distinct gene expression profiles relating to the FGFR pathway. Indeed, FGFR inhibition blocked proliferation of primary mesothelioma cultures, providing proof-of-concept of chemical profiling as a method to reveal novel sensitivities to targeted agents.

## **Materials and Methods**

### **Patients**

All patients provided written informed consent for the use and storage of pleural fluid, tumor biopsies, and germ line DNA. Separate informed consent was obtained to use the information from the drug screens for making treatment decisions. The study was conducted in accordance with the Declaration of Helsinki and approved by Netherlands Cancer Institute review board. Diagnosis was determined on available tumor biopsies and confirmed by the Dutch Mesothelioma Panel, a national expertise panel of certified pathologists who evaluate all patient samples suspected of mesothelioma.

### **Culture method**

Short-term primary mesothelioma cultures were generated by isolating tumor cells from pleural fluid. Within half an hour after drainage, the pleural fluid was centrifuged at 1,500

rpm for 5 minutes at room temperature (RT). When the cell pellet was highly contaminated with erythrocytes, it was incubated with erythrocyte lysis buffer (containing 150 mmol/L  $\text{NH}_4\text{Cl}$ , 10 mmol/L potassium bicarbonate and 0.2 mmol/L EDTA) for 10 minutes at RT. Cells were resuspended in Dulbecco's Modified Eagle Medium (DMEM, Gibco) supplemented with penicillin/streptomycin and 8% fetal calf serum. The cells were seeded in T75 flasks at a quantity of  $10 \times 10^6$ ,  $15 \times 10^6$  or  $20 \times 10^6$  cells and incubated at  $37^\circ\text{C}$  at 5%  $\text{CO}_2$ . Medium was refreshed depending on metabolic activity of the cells, usually twice a week. Cells were cultured for a maximum period of 4 weeks.

### **Comparative genome hybridization (CGH)**

To ensure that our cultures consisted mainly of tumor cells, we performed CGH on a number of cultures. CGH was performed as described by Schouten and colleagues [23]. Tumor DNA was labeled with Cy3, and female pooled reference DNA (G1521, Promega) was labeled with Cy5 using the ENZO labeling kit for BAC arrays (ENZ-42670, ENZO Life Sciences). Unincorporated nucleotides were removed with the Qiagen MinElute PCR Purification Kit (28004, Qiagen). Subsequently, tumor and reference DNA were pooled and pelleted using an Eppendorf Concentrator (5301, Eppendorf). The pellets were resuspended in hybridization mix (NimbleGen Hybridization Kit, Roche Nimblegen) and the sample loaded on the array. Hybridization was at  $42^\circ\text{C}$  for 40 to 72 hours (Maui Hybridization System, BioMicro Systems). Slides were washed three times (Roche NimbleGen Wash Buffer Kit) and scanned at  $2 \mu\text{m}$  double pass using an Agilent High Resolution Microarray Scanner (Scanner model: G2505C, Agilent). The resulting image files were further analyzed using NimbleScan software (Roche Nimblegen). Grids were aligned on the picture manually and per channel pair files generated. The NimbleScan DNACopy algorithm was applied at default settings and the unaveraged DNACopy text files were used for further analyses.

### **Drug screens**

Drug screens were performed in biological duplicate after 1 and 2 weeks of culture. Seven single agents (cisplatin, carboplatin, oxaliplatin, vinorelbine, gemcitabine, pemetrexed and doxorubicin) and five combinations (cisplatin + pemetrexed, cisplatin + gemcitabine, carboplatin + pemetrexed, oxaliplatin + gemcitabine and oxaliplatin + vinorelbine) were used. Cells were seeded in a flat bottom 96-wells plate at a density of 5,000 cells/well. After overnight incubation, chemotherapeutics in a concentration range of  $50 \mu\text{mol/L}$  to 5 nmol/L were added in technical triplicates. After 72 hours of incubation with the drugs, the cytotoxicity was measured with a metabolic activity assay (Cell Titer blue G8081, Promega). Fluorescent readout was performed with the Envision Multilabel Reader (Perkin Elmer).

### **Interpretation dose-response curves**

Classification of cultures in three groups. The classification of cultures in three groups was

based on results from all drugs and drug combinations screened. For three concentrations (10 nmol/L, 1  $\mu$ mol/L, and 50  $\mu$ mol/L), cell survival cutoff was determined. Cell survival cutoff for a drug concentration of 10 nmol/L was set at  $\geq 90\%$  cell survival, for 1  $\mu$ mol/L at  $\geq 70\%$ , and for 50  $\mu$ mol/L at  $\geq 50\%$ . For each concentration, the number of drugs above the cutoff value was counted. A culture was defined as nonresponsive when for all three concentrations, five or more drugs were above the cell survival cutoff value. A culture was defined as an intermediate responder when for one or two concentrations, five or more drugs were above the cell survival cutoff value. When for all concentrations, less than five drugs were above the cell survival cutoff value, the culture was classified as a responder.

**In vitro response prediction.** An in vitro response prediction was made for each drug or drug combination individually. The in vitro response was correlated to the clinical response defined by RECIST modified for mesothelioma, thereby identifying patients with progressive disease, stable disease, and partial response. A test set of dose-response curves was used to determine cutoff points for area under the curve (AUC) values to predict clinical responses. Very low or very high drug concentrations were not expected to be clinically relevant. Therefore, the AUC was determined in a concentration range of 50 to 5,000 nmol/L (GraphPad Prism). An AUC level of less than 1,485 predicted a partial response. An AUC level higher than 2,970 predicted progressive disease. All AUC levels between these numbers predicted stable disease.

### **RNA isolation**

Total RNA was extracted using TRIzol reagent (15596-018, Ambion life technologies) according to the manufacturer's protocol. Typically, 1 mL of TRIzol reagent was used per  $1 \times 10^6$  cells. The total RNA pellet was air dried for 8 minutes, dissolved in an appropriate volume of nuclease-free water (AM9937, Ambion life technologies) and quantified using Nanodrop UV-VIS Spectrophotometer. Total RNA was further purified using the RNeasy MinElute Cleanup Kit (74204, Qiagen) according to the manufacturer's instructions. Quality and quantity of the total RNA was assessed by the 2100 Bioanalyzer using a Nano chip (Agilent). Total RNA samples having RIN  $>8$  were subjected to library generation.

### **RNA sequencing**

Strand-specific libraries were generated using the TruSeq Stranded mRNA sample preparation kit (Illumina Inc., San Diego, RS-122-2101/2) according to the manufacturer's instructions (Illumina, Part # 15031047 Rev. E). The libraries were analyzed on a 2100 Bioanalyzer using a 7500 chip (Agilent), diluted and pooled equimolar into a 10 nmol/L multiplexed sequencing pool and stored at  $-20^\circ\text{C}$ . The libraries were sequenced with 65-bp paired end reads on a HiSeq2500 using V4 chemistry (Illumina Inc.).

## **Gene expression analysis**

The raw sequencing data were aligned to a human reference genome (build hg38) using tophat 2.0, followed by measuring gene expression using our own protocol based on htseq count (lcount). Normalized count-per million (CPM) was measured using library sizes corrected with Trimmed mean of M-values (TMM) normalization with edgeR package [24]. For differentially expressed gene (DEG) identification, we used voom transformation [25] followed by empirical Bayes method with limma R package. Then, DEGs were identified as the genes with P values less than 0.005 and log<sub>2</sub> fold changes larger than 2. The voom-transformed log-CPM of DEGs was used in principal component analysis (PCA). For heatmap generation voom-transformed log-CPM of DEGs was standardized by mean centering and scaling with standard deviation. Genes were ordered based on hierarchical clustering with Pearson correlation as a similarity measure and ward linkage. ID number and corresponding fold changes of DEGs were uploaded in ingenuity pathway analysis (IPA; Qiagen Bioinformatics). Analysis was performed with 224 mapped IDs.

### **Stability assessment of differential gene expression analysis**

To assess the reliability of DEGs, we performed differential expression analysis with leaving out each of the responders and nonresponders. The P values and rankings of DEGs that were obtained with this analysis were used in the down-stream analysis. Further, for each of the held-out experiments, we obtained DEGs using same P values and fold-change cutoffs. For each of the DEG lists, hierarchical clustering analysis was performed, after which consensus of the clustering was obtained.

## **Results**

### **Profiling and characterization of primary mesothelioma cultures**

Between February 2012 and July 2016, 155 pleural fluids from 102 patients with a confirmed histological diagnosis of mesothelioma were collected for early passage primary cultures. Eighty-nine patients (87%) were male, the mean age was 67 years and most patients had an epithelial subtype, similar to the conventional distribution of mesothelioma subtypes. Forty-one patients were chemotherapy naïve at the time of cell isolation, and 61 patients had received one or more lines of treatment (Supplementary Table S1A). Figure 1A shows a flow chart of the pleural fluid pipeline depicting *in vitro* drug testing and subsequent clinical testing in patients. Eighty-one of the 155 isolations were suitable for further culture and drug screening, resulting in a take rate of 52%. These 81 isolations were derived from 57 patients. We failed to perform a drug screen for 45 patients. Patients' characteristics for both groups are given in Supplementary Table S1B and S1C. There was no significant difference between the two groups for age ( $P=0.05$ ), prior lines of treatment ( $P=0.54$ ), or histology ( $P=0.42$ ). There was a significant difference in gender ( $P=0.03$ ), however the number of female patients was too low to make conclusions about any effect of gender on success rate.

Failure was mainly due to too low tumor cell count isolated from the pleural fluid. The time between isolation of pleural fluid and the start of the first drug screen was generally 1 week. A biological duplicate screen was performed in the following week (Fig. 1B).

Because cultures may change over time, we assessed the stability of our cultures using CGH. While mesothelioma is generally characterized by very few mutations, they frequently show loss of the gene CDKN2A, located at the p16 locus on chromosome 9 [26-28]. This can be detected by CGH. There was no deletion of the p16 locus detected in samples of two patients. In the pleural fluid of three other patients, deletion of the p16 locus was detected in the first culture passages. At later passages, this deletion could not be detected anymore in two of the three patients. Because deletions cannot be repaired spontaneously, this suggests overgrowth of reactive mesothelial cells coisolated with the mesothelioma cells (Supplementary Fig. S2). These experiments validated the isolation and culture of primary mesothelioma cells and showed that drug screens should be performed during the first 3 weeks after isolation from patients, before overgrowth of other cells could be expected.

### **Chemical profiling identifies three mesothelioma subgroups**

Drug screening was performed on 81 different primary cultures with compounds selected on the basis of their current or historical use as treatment of patients with mesothelioma [2, 29-33]. Cisplatin, carboplatin, oxaliplatin, gemcitabine, vinorelbine, pemetrexed and doxorubicin have been tested as single agent and/or in combination. The different cultures showed marked differences in the dose-response profiles. This allowed clustering of the primary cultures in three different groups: so called “responders”, “nonresponders”, and “intermediate responders” (see Materials and Methods). The clustering is based on all drugs and drug combinations screened. We defined a “responder” as a culture responding to most of the chemotherapeutics screened (Fig. 2A; supplementary Fig. S3A). We defined a “non-responder” as a culture failing to respond to more than five of the drugs screened (Fig. 2B and supplementary Fig. S3B). An “intermediate responder” responded to some of the drugs, but not to all of them and visually did not fit in one of the other two categories (Fig. 2C; supplementary Fig. S3C). From the 81 cultures, six cultures classified as “responder”, 27 as “nonresponder” and 48 as “intermediate responders”. Thirty-one drug screens were performed on chemo-naïve cells. Fifty drug screens were performed on cells from patients that received one or more lines of treatments. The clustering in the three groups was not significant different for cells isolated from patients that had or had not received prior treatment ( $P=0.72$ ; supplementary Table S4A). These data suggested that primary mesothelioma cultures allow subdivision of tumors based on drug sensitivity without significant effects of earlier treatments of the corresponding patients.

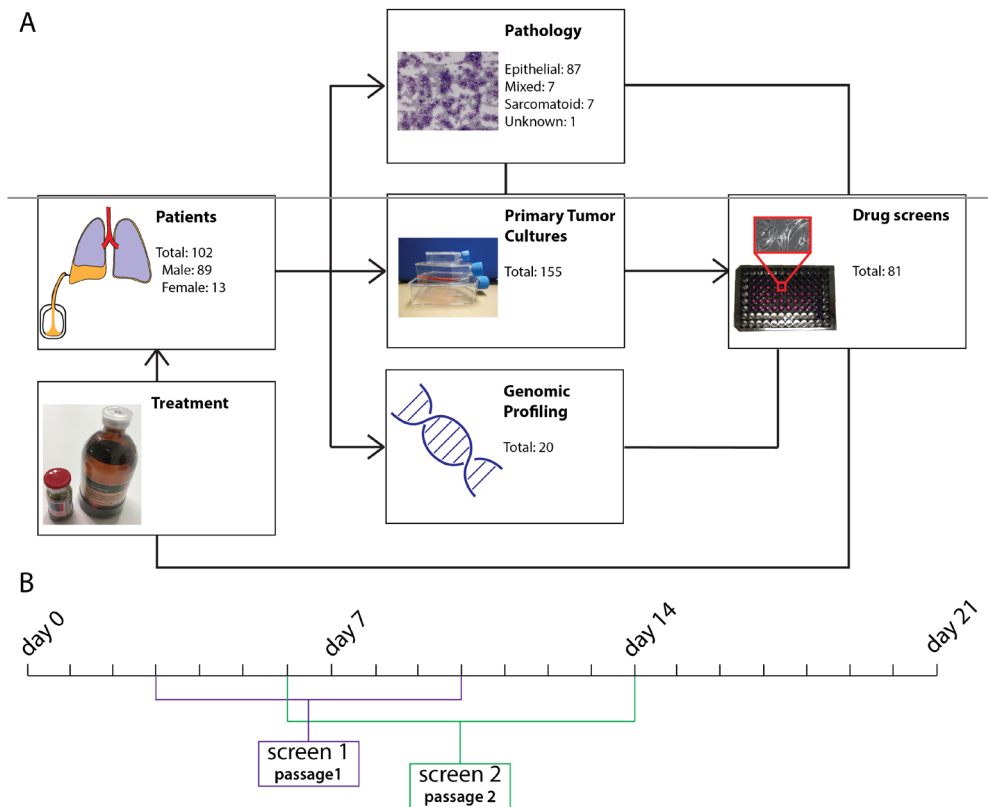


**Fig. 1. Flow chart and timeline of the chemical and genetic profiling of primary mesothelioma cultures.** **A)** Flow chart of the pleural fluid pipeline. Pleural fluid was extracted from 102 patients diagnosed with mesothelioma. The cultures were diagnosed with pathology and primary cultures were made. Twenty primary tumor cultures were genetically profiled. Eighty-one cultures were suitable for drug screening. The results from 11 drug screens were used in patient treatment. **B)** Timeline of drug screens using primary mesothelioma cultures. The first screen was started within 10 days after isolation (day 0), the biological duplicate screen was performed within one week after the first screen. The drug screening assays took five days and primary cultures were analyzed within three weeks after cell isolation from the pleural fluid

### Transcriptomic analyses reveal distinct genomic subclasses through chemical profiles

Between primary mesothelioma cultures, divergent responses to chemotherapeutic intervention were observed. To test whether there was a genomic basis for these three groups identified by chemical profiling, we performed RNA-seq on 20 primary mesothelioma samples, taken immediately after isolation and representing four “responder” samples, nine “nonresponder” samples, and seven samples from the “intermediate” group. We first identified a set of DEGs between responders and nonresponders with P values less than 0.005 and log<sub>2</sub> fold changes larger than 2 (see Material and Methods). A total of 133 genes were

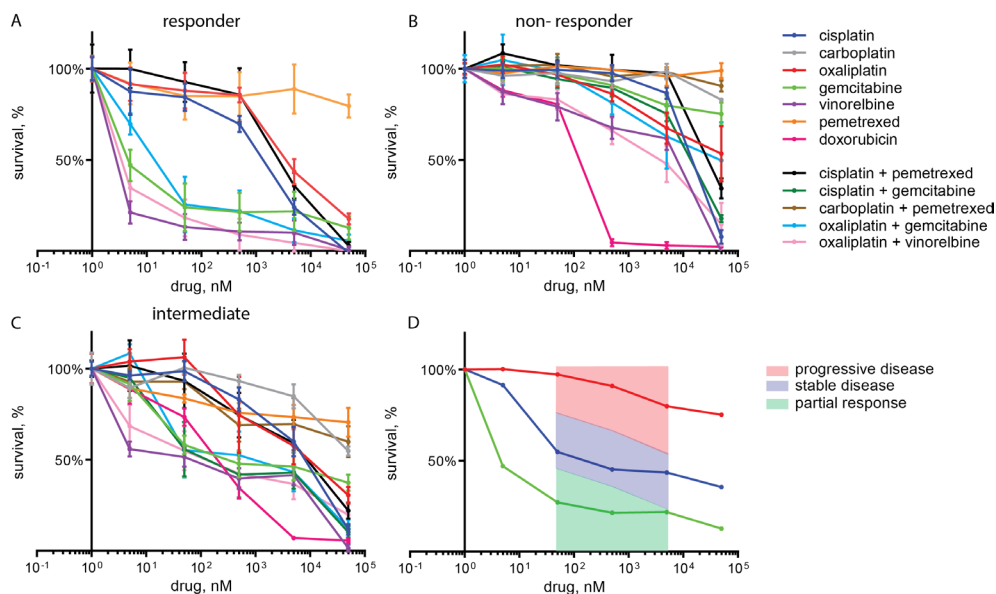
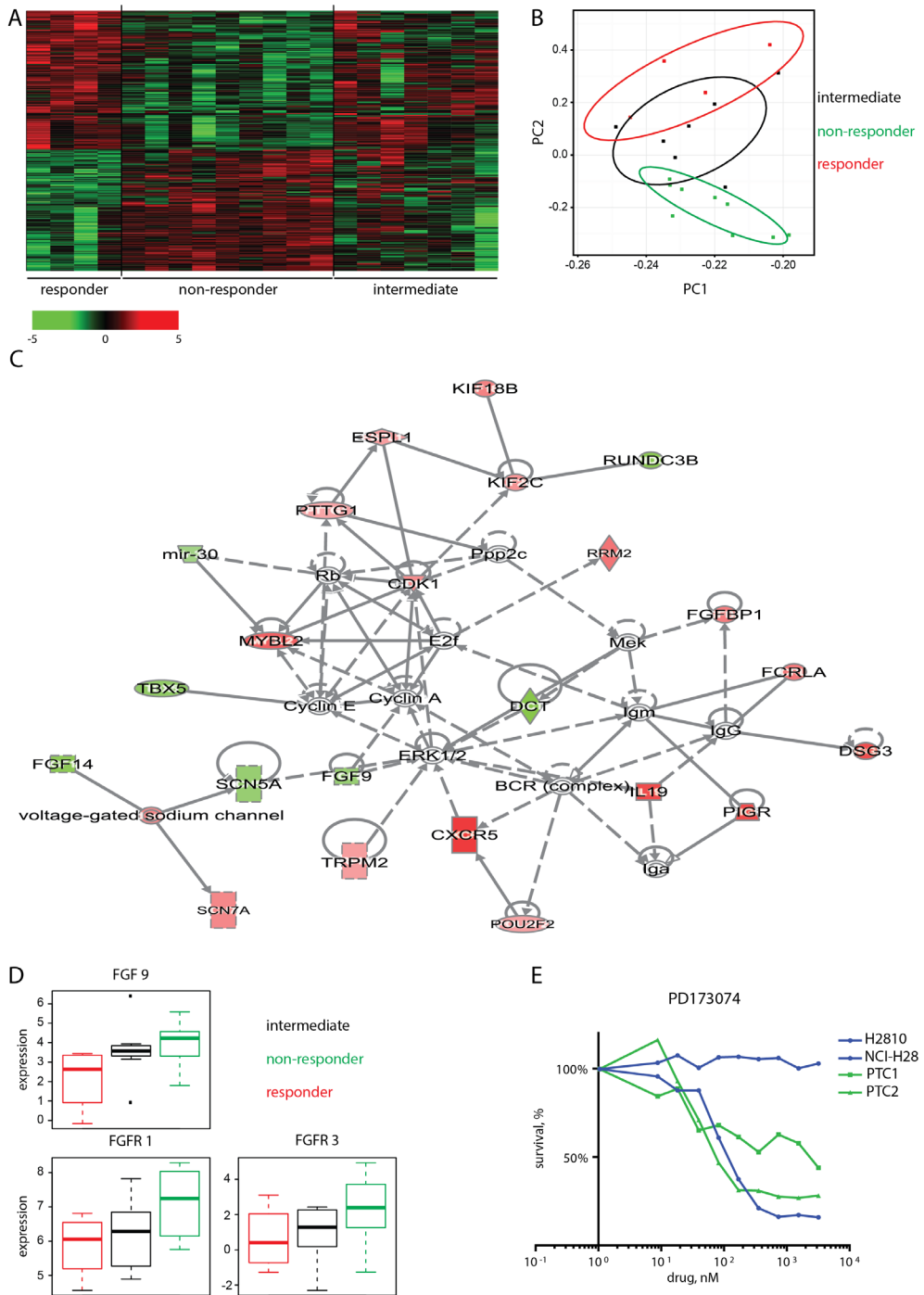


**Fig. 2. Dose response curves for various drugs depicted for the differently responding subgroups. A-C)** Dose-response curves of a responder, a non-responder and an intermediate responder are shown, as indicated. Drug screens were performed on chemo-naïve cells. Survival (mean  $\pm$ SD) is shown in relation to increasing concentrations of single agents and combinations, as indicated. **D)** Dose response curves for the drug gemcitabine screened in 3 different patients, a responder (green), an intermediate responder (blue) and a non-responder (red). Boxes indicate the AUC from which progressive disease (red), stable disease (blue) and partial response (green) is predicted. The AUC surface is pictured in the trend of the gemcitabine curves.

**Fig. 3. Gene expression profiling of the differently responding mesothelioma subgroups. A)** Heatmap showing 285 genes that are differentially expressed between 'responders' and 'non-responders'. Green bars depict genes that are downregulated, while red bars depict upregulated genes in 'non-responders'. The gene expression profile of the intermediate group is different from the expression profile of 'responders' and 'non-responders'. The list of genes is shown in Supplemental table. 2. **B)** Principal Component Analysis separates responders (red) from 'non-responders' (green). The intermediate group (black) locates between these groups. **C)** Ingenuity pathway analysis illustrating the most significant network containing 23 DEGs between 'responders' and 'non-responders'. Green: upregulated, red: downregulated DEGs in non-responders. **D)** Boxplot depicting gene expression of FGFR9 and interaction partners FGFR1 and FGFR3 in 'responders' (red), 'non-responders' (green) and 'intermediate responders' (black). The level of gene expression is indicated on the y-axis. Boxplot shows mean expression level with 75<sup>th</sup> (top) and 25<sup>th</sup> (bottom) percentile value. Whiskers indicate range of values. **E)** Dose-response curves of two non-responder cultures and reference cell lines NCI-H28 and H2810, treated with increasing concentrations of FGFR inhibitor PD-173074. Cell viability is measured.



downregulated, and 152 genes were upregulated in the “responder” group compared with the “nonresponder” group (supplementary Table S5). In differential gene expression analysis with leave-one-out cross validation, we confirmed that the 285 DEGs were consistently highly ranked and the cutoffs ( $P < 0.005$  and  $\log_2$  fold changes  $> 2$ ) provided genes that stably separated patients by response (supplementary Fig. S6). The “intermediate” group shows a signature that differs from both “responders” and “nonresponders”, also genetically defining it as a separate group (Fig. 3A). We observed the same trend in PCA on expression levels of DEGs (Fig. 3B; Materials and Methods). IPA on DEGs revealed 10 networks containing at least 7 DEGs. The top network with 23 DEGs contained the fibroblast growth factor (FGF) pathway (Fig. 3C). FGF9 was significantly upregulated in the nonresponder group (Fig. 3D). Because this pathway has been described previously in MPM [34], we analyzed gene expression of the preferred receptors for FGF9: FGFR3 and FGFR1. Gene expression of these receptors was also upregulated in the nonresponder group (Fig. 3D). The paired-end RNA-sequencing analysis did not reveal mutated expressed genes.

To test the relevance of the various components of the FGF pathway, primary mesothelioma cultures were exposed to compound PD-173074, an FGFR inhibitor with a high affinity for FGFR3 and FGFR1.

Two “nonresponder” primary mesothelioma cultures were sensitive to the FGFR-inhibitor (Fig. 3E). In mesothelioma cell lines, we also found a statistically significant correlation between elevated FGF9 mRNA expression and IC<sub>50</sub> to PD173074 ( $P = 0.0117$ ). These experiments show that chemical profiling of primary mesothelioma cultures allows identification of subgroups that are characterized by different expression profiles. In addition, new targets for treatment of mesothelioma subgroups can be identified, as is illustrated here for the FGF pathway.

### **Clinical implication of in vitro drug screens**

To study the correlation between in vitro drug screens and clinical outcome, we quantified drug sensitivity by calculating the AUC values of dose-response curves. The AUC was determined in a concentration range between 50 and 5,000 nmol/L. Lower or higher concentrations were not expected to be clinically relevant. In vitro response was determined for each drug or drug combination and was classified as the clinical responses: partial response, stable disease or progressive disease. Figure 2D illustrates dose-response curves for the drug gemcitabine in three different patients. The boxes indicate the AUC in which progressive disease, stable disease and partial response were predicted. We treated ten patients that were progressive after first- or second-line treatment, with the drug that was most effective based on the in vitro drug screen, that was performed on the patient’s primary mesothelioma cells (Table 1). Patient 1 was a 61-year-old woman with an epithelial-

type mesothelioma. Her frontline treatment consisted of the standard first-line combination of cisplatin and pemetrexed, which was followed by a surgical procedure consisting of a pleurectomy/decortication. Upon progression, the in vitro drug screen demonstrated oxaliplatin and vinorelbine as the most effective compounds and we predicted a partial response (Fig. 4A, patient 1). She was treated accordingly resulting in a partial response, as is shown in Fig. 4B. The second patient, a 52-year-old male with epithelial mesothelioma, was treated with cisplatin and pemetrexed, followed by a pleurectomy/decortication. Progression occurred 7 months after completion of his first-line therapy. The combination of oxaliplatin and gemcitabine was the most effective one and stable disease was predicted (Fig 4A, patient 2), which was indeed observed after clinical treatment with these drugs (Fig. 4B). Patient 3, a 36-year-old female patient with a mixed type of mesothelioma, had disease progression 4 months after her initial treatment with cisplatin, pemetrexed, and a pleurectomy/decortication. The in vitro drug screen showed a “nonresponder” profile and progressive disease was to be expected from treatment (Fig. 4A, patient 3). She was treated with consecutive courses of the best combination observed (carboplatin/gemcitabine and oxaliplatin/vinorelbine) but experienced disease progression after two courses of each combination (Fig. 4B) and died shortly thereafter. In vitro drug screen results and CT scans before and after treatment of patient 4 to 10 are depicted in Supplementary Fig. S7. For patient 8 to 10, in vitro response prediction correlated with the actual patient response. For patient 4, 6, 7, the patient response was better than predicted. Patient 5, a 71-year-old man with epithelial mesothelioma, was treated twice based on his chemosensitivity screen. After front-line treatment with carboplatin and pemetrexed, he was first treated with gemcitabine and later with vinorelbine. The clinical response for both treatments was stable disease. For gemcitabine, this was predicted based on the in vitro screen. For vinorelbine, however, the observed response was not as pronounced as was expected based on in vitro results (Supplementary Fig. S7). For patient 6, vinorelbine was selected as the best option to which oxaliplatin was added. Patient 7, 9, and 10 did not receive the most potent drug based on in vitro drug screen because of contro-indications for treatment with doxorubicin. Due to the patients’ history, vinorelbine or a combination with vinorelbine could not be given. From eleven drug screens, seven in vitro response predictions were correct. For the four that were not correctly predicted, the actual clinical response was better in three patients. These results suggest that the in vitro drug screens had added value in predicting actual individual patient responses to selected drugs.

## Discussion

Cancer treatment strategies are changing from general therapy regimens to more personalized treatment, often based on the genetic make-up of the tumor. Unfortunately, no druggable driver mutations have been identified in mesothelioma [5, 6, 8, 9, 35]. Therefore,

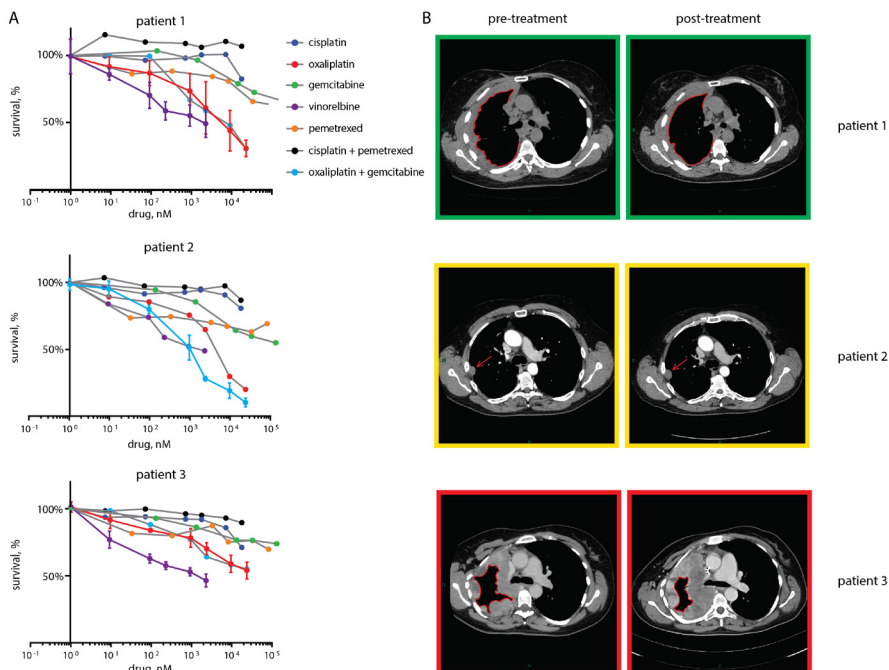


**Fig. 4. Dose-response curves and clinical responses of three patients.** **A)** Dose-response curves of primary mesothelioma cells isolated from patients 1-3 and treated with several single agents and combinations of cytotoxic drugs, as indicated. Cell viability measured after 72 hours of drug exposure as a function of increasing concentrations of several drugs and combinations is depicted. **B)** CT-scans of patient 1-3 before and after treatment with the drugs selected based on the in vitro drug screens. Response evaluation was done using modified RECIST for mesothelioma. Colored boxes around CT-scans indicate in vitro response prediction before treatment and the actual response after treatment. Green: partial response, yellow: stable disease, red: progressive disease. Patient 1 was treated with a combination of oxaliplatin and vinorelbine. The tumor rind indicated by the red line is irregular on her pre-treatment scan and is smaller and smoother on her post-treatment scan, indicating a partial response. Patient 2 received a combination of oxaliplatin and gemcitabine. The tumor nodule indicated by the red arrow, remains similar between the scans indicating stable disease. Patient 3 received successively carboplatin/gemcitabine and oxaliplatin/vinorelbine. The grey tumor rind on the pre-treatment scan -encircled by the red line- is larger on the post-treatment scan, which illustrates progressive disease.

**Table 1.** overview of patients treated based on their in vitro drug screen.

Patient	Gender	Histology	Drug	In vitro predicted response	Patient response
1	F	Epithelial	Oxaliplatin + vinorelbine	PR	PR
2	M	Epithelial	Oxaliplatin + gemcitabine	SD	SD
3	F	Mixed	Oxaliplatin + vinorelbine	PD	PD
4	M	Epithelial	Oxaliplatin + gemcitabine	SD	PR
5-1	M	Epithelial	Gemcitabine	SD	SD
5-2			Vinorelbine	PR	SD
6	M	Epithelial	Oxaliplatin + vinorelbine	PD	SD
7	M	Epithelial	Oxaliplatin + gemcitabine	PD	PR
8	M	Epithelial	Doxorubicine	SD	SD
9	M	Epithelial	Oxaliplatin + gemcitabine	PD	PD
10	M	Epithelial	Oxaliplatin + gemcitabine	SD	SD

F: Female, M: Male, green: PR - partial response, yellow: SD - stable disease, red: PD - progressive disease.

we “chemically” profiled primary mesothelioma cultures with common chemotherapeutic drugs and subsequently treated ten patients with the most effective drug or drug combination. This strategy has previously been successfully applied in lung cancer [36-38], ovarian cancer [39, 40], and breast cancer [41] and showed that in vitro drug responsiveness bears clinically relevant information for patient treatment efficacy.

For the patients treated in this study, we observed considerable overlap between the predicted drug responses in vitro and the corresponding clinical responses. Although the number of patients is too small to make definite conclusions, we present a system that can personalize the treatment of patients with mesothelioma, a heterogeneous disease, with a limited number of patients available for clinical trials and only one registered systemic therapy option.

In addition to predicting the best chemotherapeutic option for an individual patient, we identified “chemical profiles” corresponding to gene signatures that distinguished tumors resistant to most tested therapeutics, from tumors that were largely responsive. A third group with intermediate responses to drugs had an expression profile that was different from the responding and nonresponding group. We expected that drug screens performed on chemo-naïve cells would give a different chemosensitivity profile compared with drug screens performed on pretreated cells. However, no significant differences were detected in the three “chemical profiles” between these groups. This corresponds to results of Mujoomdar and colleagues who described similar results for chemo-naïve and pretreated biopsies treated in vitro with three single agents [42].

The different “chemical profiles” that we identified could not have been identified based on pathology without prior knowledge. In cancer types like prostate and breast cancer, gene expression profiles were successfully used to define subclasses. These were usually retrospectively correlated with prognostic features [43, 44], although one such a profile - the 70-gene signature in breast cancer - has recently been validated on the basis of a prospective study [45]. Our prospectively determined chemical profiles have predictive value, which - from the patients’ perspective - is the most important factor and clinically more relevant than prognostic values.

Of note, there are some limitations to our pipeline. The drug screening system was unable to test pemetrexed. Pemetrexed is an antifolate that inhibits multiple enzymes involved in the formation of nucleotides [46-49]. Pemetrexed activity is competed away by folate [46, 47, 50, 51]. The culture medium used in this system contained folate, probably at supra-physiological levels. Serum also contains a variety of folate, nucleosides, and nucleotides, which is expected to circumvent growth inhibition by pemetrexed [46, 52]. The presence of folate, nucleosides, and nucleotides in the culture system could explain why primary cultures were not sensitive to pemetrexed. Another limitation of the system is that the culture

does not include pharmacokinetics and dynamics of the different drugs. Every cell-based model lacks features of the original tumor like vasculature and tumor micro-environment, which makes it impossible to simulate pharmacokinetics and pharmacodynamics. On logical grounds, our system can also not be used for the testing of the recently introduced classes of immuno-oncology drugs. Our in vitro response prediction method is arbitrary and expanding with more patients would provide data to further define cutoffs for better drug response prediction.

Thus far, we have tested only chemotherapeutics that are commonly used in clinical practice because these allowed validation of the results in patients with mesothelioma. By further expanding the number and classes of compounds in the drug screen, we may not only be able to further characterize the more heterogeneous intermediate group, but also identify more suitable therapeutic options for the nonresponder patient population.

Our model will enable us to select drugs or drug combinations that are more likely to give a response in subgroups of patients. Because mesothelioma is a rare tumor type, such subgroups would probably not have been detected in clinical trials. Preselection of drugs and patients will help to optimize the design and success of clinical trials in this patient group.

We already have one example of a new drug selected on the basis of our method. Based on gene expression profiling, the FGF pathway appeared upregulated in the nonresponder patient population, for whom at this stage no active therapeutic options are available. Deregulated FGF signaling has been linked to cancer pathogenesis [53] and several groups have reported involvement of the FGF signaling cascade in mesothelioma [34, 54]. Because this pathway appeared selectively upregulated in the nonresponder patient population, preselected patients may derive specific benefit from therapeutic intervention using FGFR inhibitors, as we successfully illustrate in our primary cultures (Fig. 3E). Chemical profiling of primary mesothelioma cultures revealed three response groups corresponding to distinct gene signatures involving the FGF signaling cascade. We demonstrated considerable overlap between in vitro and in vivo responses suggesting that our pipeline represents a feasible method to personalize treatment that could ultimately improve the prospects of mesothelioma patients.

## **Acknowledgements**

The authors would like to acknowledge the NKI-AVL Core Facility Mocular Pathology and Biobanking (CFMPB) and the NKI-AVL Genomic Core Facility for supplying material and lab support. The authors thank Ultan McDermott for this data input. This work was supported by grants from the Dutch Cancer Society (KWF) assigned to P.Baas and J.Neefjes and a gravity program “Institute of Chemical Immunology” assigned to J. Neefjes

## References

1. Baas, P., et al., *Malignant pleural mesothelioma: ESMO Clinical Practice Guidelines for diagnosis, treatment and follow-up*. Ann Oncol, 2015. **26 Suppl 5**: p. v31-9.
2. Vogelzang, N.J., et al., *Phase III study of pemetrexed in combination with cisplatin versus cisplatin alone in patients with malignant pleural mesothelioma*. J Clin Oncol, 2003. **21**(14): p. 2636-44.
3. Buikhuisen, W.A., et al., *Second line therapy in malignant pleural mesothelioma: A systematic review*. Lung Cancer, 2015. **89**(3): p. 223-31.
4. Guo, G., et al., *Whole-exome sequencing reveals frequent genetic alterations in BAP1, NF2, CDKN2A, and CUL1 in malignant pleural mesothelioma*. Cancer Res, 2015. **75**(2): p. 264-9.
5. Bonelli, M.A., et al., *New therapeutic strategies for malignant pleural mesothelioma*. Biochem Pharmacol, 2017. **123**: p. 8-18.
6. Cheng, Y.Y., et al., *KCa1.1, a calcium-activated potassium channel subunit alpha 1, is targeted by miR-17-5p and modulates cell migration in malignant pleural mesothelioma*. Mol Cancer, 2016. **15**(1): p. 44.
7. Pignochino, Y., et al., *The combination of sorafenib and everolimus shows antitumor activity in preclinical models of malignant pleural mesothelioma*. BMC Cancer, 2015. **15**: p. 374.
8. Remon, J., et al., *Malignant pleural mesothelioma: new hope in the horizon with novel therapeutic strategies*. Cancer Treat Rev, 2015. **41**(1): p. 27-34.
9. Sekido, Y., *Molecular pathogenesis of malignant mesothelioma*. Carcinogenesis, 2013. **34**(7): p. 1413-9.
10. Churg A, Roggli VL, and G.-S.F.e. al., *Tumours of the pleura: mesothelial tumours*. , in *Pathology and Genetics of Tumours of the Lung, Pleura, Thymus and Heart*, B.E. Travis WD, Muller-Hermelink HK, Harris CC Editor. 2004, IARC, World Health Organization Classification of Tumours . Lyon, France. p. 128–136.
11. Garnett, M.J., et al., *Systematic identification of genomic markers of drug sensitivity in cancer cells*. Nature, 2012. **483**(7391): p. 570-5.
12. Daniel, V.C., et al., *A primary xenograft model of small-cell lung cancer reveals irreversible changes in gene expression imposed by culture in vitro*. Cancer Res, 2009. **69**(8): p. 3364-73.
13. Gillet, J.P., et al., *Redefining the relevance of established cancer cell lines to the study of mechanisms of clinical anti-cancer drug resistance*. Proc Natl Acad Sci U S A, 2011. **108**(46): p. 18708-13.
14. Roschke, A.V., et al., *Karyotypic complexity of the NCI-60 drug-screening panel*. Cancer Res, 2003. **63**(24): p. 8634-47.
15. Tveit, K.M. and A. Pihl, *Do cell lines in vitro reflect the properties of the tumours of origin? A study of lines derived from human melanoma xenografts*. Br J Cancer, 1981. **44**(6): p. 775-86.
16. Das, V., et al., *Pathophysiologically relevant in vitro tumor models for drug screening*. Drug Discov Today, 2015.
17. Eglén, R.M., A. Gilchrist, and T. Reisine, *The use of immortalized cell lines in GPCR screening: the good, bad and ugly*. Comb Chem High Throughput Screen, 2008. **11**(7): p. 560-5.
18. Paik, P.K. and L.M. Krug, *Histone deacetylase inhibitors in malignant pleural mesothelioma: preclinical rationale and clinical trials*. J Thorac Oncol, 2010. **5**(2): p. 275-9.
19. Garassino, M.C. and S. Marsoni, *A lesson from vorinostat in pleural mesothelioma*. Lancet Oncol, 2015. **16**(4): p. 359-60.
20. Krug, L.M., et al., *Vorinostat in patients with advanced malignant pleural mesothelioma who have progressed on previous chemotherapy (VANTAGE-014): a phase 3, double-blind, randomised, placebo-controlled trial*. Lancet Oncol, 2015. **16**(4): p. 447-56.
21. Szulkin, A., et al., *Characterization and drug sensitivity profiling of primary malignant mesothelioma cells from pleural effusions*. BMC Cancer, 2014. **14**: p. 709.
22. Chernova, T., et al., *Molecular profiling reveals primary mesothelioma cell lines recapitulate human disease*. Cell Death Differ, 2016. **23**(7): p. 1152-64.
23. Schouten, P.C., et al., *Platform comparisons for identification of breast cancers with a BRCA-like copy number profile*. Breast Cancer Res Treat, 2013. **139**(2): p. 317-27.
24. Robinson, M.D. and A. Oshlack, *A scaling normalization method for differential expression analysis of RNA-seq data*. Genome Biol, 2010. **11**(3): p. R25.
25. Law, C.W., et al., *voom: Precision weights unlock linear model analysis tools for RNA-seq read counts*. Genome Biol, 2014. **15**(2): p. R29.
26. Musti, M., et al., *Cytogenetic and molecular genetic changes in malignant mesothelioma*. Cancer Genet Cytogenet, 2006. **170**(1): p. 9-15.
27. Illei, P.B., et al., *Homozygous deletion of CDKN2A and codeletion of the methylthioadenosine phosphorylase gene in the majority of pleural mesotheliomas*. Clin Cancer Res, 2003. **9**(6): p. 2108-13.

28. Lopez-Rios, F., et al., *Global gene expression profiling of pleural mesotheliomas: overexpression of aurora kinases and P16/CDKN2A deletion as prognostic factors and critical evaluation of microarray-based prognostic prediction*. *Cancer Res*, 2006. **66**(6): p. 2970-9.
29. Ceresoli, G.L., et al., *Phase II study of pemetrexed plus carboplatin in malignant pleural mesothelioma*. *J Clin Oncol*, 2006. **24**(9): p. 1443-8.
30. Ceresoli, G.L. and P.A. Zucali, *Vinca alkaloids in the therapeutic management of malignant pleural mesothelioma*. *Cancer Treat Rev*, 2015. **41**(10): p. 853-8.
31. Kindler, H.L. and J.P. van Meerbeeck, *The role of gemcitabine in the treatment of malignant mesothelioma*. *Semin Oncol*, 2002. **29**(1): p. 70-6.
32. Schutte, W., et al., *A multicenter phase II study of gemcitabine and oxaliplatin for malignant pleural mesothelioma*. *Clin Lung Cancer*, 2003. **4**(5): p. 294-7.
33. Arrieta, O., et al., *First-line chemotherapy with liposomal doxorubicin plus cisplatin for patients with advanced malignant pleural mesothelioma: phase II trial*. *Br J Cancer*, 2012. **106**(6): p. 1027-32.
34. Schelch, K., et al., *Fibroblast growth factor receptor inhibition is active against mesothelioma and synergizes with radio- and chemotherapy*. *Am J Respir Crit Care Med*, 2014. **190**(7): p. 763-72.
35. Bueno, R., et al., *Comprehensive genomic analysis of malignant pleural mesothelioma identifies recurrent mutations, gene fusions and splicing alterations*. *Nat Genet*, 2016. **48**(4): p. 407-16.
36. Cortazar, P., et al., *Survival of patients with limited-stage small cell lung cancer treated with individualized chemotherapy selected by in vitro drug sensitivity testing*. *Clin Cancer Res*, 1997. **3**(5): p. 741-7.
37. Wilbur, D.W., et al., *Chemotherapy of non-small cell lung carcinoma guided by an in vitro drug resistance assay measuring total tumour cell kill*. *Br J Cancer*, 1992. **65**(1): p. 27-32.
38. Miyazaki, R., et al., *In Vitro Drug Sensitivity Tests to Predict Molecular Target Drug Responses in Surgically Resected Lung Cancer*. *PLoS One*, 2016. **11**(4): p. e0152665.
39. Holloway, R.W., et al., *Association between in vitro platinum resistance in the EDR assay and clinical outcomes for ovarian cancer patients*. *Gynecol Oncol*, 2002. **87**(1): p. 8-16.
40. Matsuo, K., et al., *Prediction of Chemotherapy Response With Platinum and Taxane in the Advanced Stage of Ovarian and Uterine Carcinosarcoma: A Clinical Implication of In vitro Drug Resistance Assay*. *Am J Clin Oncol*, 2010. **33**(4): p. 358-63.
41. Takamura, Y., et al., *Prediction of chemotherapeutic response by collagen gel droplet embedded culture-drug sensitivity test in human breast cancers*. *Int J Cancer*, 2002. **98**(3): p. 450-5.
42. Mujoomdar, A.A., et al., *Prevalence of in vitro chemotherapeutic drug resistance in primary malignant pleural mesothelioma: result in a cohort of 203 resection specimens*. *J Thorac Cardiovasc Surg*, 2010. **140**(2): p. 352-5.
43. Glinsky, G.V., et al., *Gene expression profiling predicts clinical outcome of prostate cancer*. *J Clin Invest*, 2004. **113**(6): p. 913-23.
44. van 't Veer, L.J., et al., *Gene expression profiling predicts clinical outcome of breast cancer*. *Nature*, 2002. **415**(6871): p. 530-6.
45. Cardoso, F., et al., *70-Gene Signature as an Aid to Treatment Decisions in Early-Stage Breast Cancer*. *N Engl J Med*, 2016. **375**(8): p. 717-29.
46. Zhao, R., et al., *Loss of reduced folate carrier function and folate depletion result in enhanced pemetrexed inhibition of purine synthesis*. *Clin Cancer Res*, 2005. **11**(3): p. 1294-301.
47. Suchy, S.L., et al., *Adaptation of a chemosensitivity assay to accurately assess pemetrexed in ex vivo cultures of lung cancer*. *Cancer Biol Ther*, 2013. **14**(1): p. 39-44.
48. Calvert, A.H., *Biochemical pharmacology of pemetrexed*. *Oncology (Williston Park)*, 2004. **18**(13 Suppl 8): p. 13-7.
49. Assaraf, Y.G., *Molecular basis of antifolate resistance*. *Cancer Metastasis Rev*, 2007. **26**(1): p. 153-81.
50. Zhao, R., F. Gao, and I.D. Goldman, *Marked suppression of the activity of some, but not all, antifolate compounds by augmentation of folate cofactor pools within tumor cells*. *Biochem Pharmacol*, 2001. **61**(7): p. 857-65.
51. Backus, H.H., et al., *Folate depletion increases sensitivity of solid tumor cell lines to 5-fluorouracil and antifolates*. *Int J Cancer*, 2000. **87**(6): p. 771-8.
52. Lorenzi, M., et al., *Plasma oxypurines in gastric and colorectal cancer*. *Biomed Pharmacother*, 1990. **44**(8): p. 403-7.
53. Touat, M., et al., *Targeting FGFR Signaling in Cancer*. *Clin Cancer Res*, 2015. **21**(12): p. 2684-94.
54. Marek, L.A., et al., *Nonamplified FGFR1 Is a Growth Driver in Malignant Pleural Mesothelioma*. *Mol Cancer Res*, 2014.

## Supplementary figures and tables

**Table S1** Patient characteristics

**A. Characteristics of all patients where cells could be isolated from pleural fluid.**

Patients (no.)	102
Male/ female (no./%)	89/ 13 (87%/ 13%)
Mean age (yrs)	67
Prior treatments lines: 0/ 1/ 2/ unknown	41/ 40/ 19/ 2 (40%/ 39%/ 19%/ 2%)
Histology: epithelioid/ sarcomatoid/ mixed/ unknown (no./ %)	87/ 7/ 7/ 1 (85%/ 7%/ 7%/ 1%)

For patients who had multiple cultures at different time points, the number of prior treatment lines was determined at the first successful culture. When we failed to perform a drug screen, the number of prior treatment lines was set at the first culture.

**B. Characteristics of patients with a successful drug screen**

Patients (no.)	57
Male/ female (no./%)	46/ 11 (81%/ 19%)
Mean age (yrs)	65
Prior treatments lines: 0/ 1/ 2/ unkown (no./%)	26/ 19/ 11/ 1 (46%/ 33%/ 19%/ 2%)
Histology: epithelioid/ sarcomatoid/ mixed/ unknown (no./%)	50/ 4/ 2/ 1 (88%/ 7%/ 4%/ 2%)

**C. Characteristics of patients where the drug screen failed.**

Patients (no.)	45
Male/ female (no./%)	43/2 (96%/ 4%)
Mean age (yrs)	68
Prior treatments lines: 0/ 1/ 2/ unknown (no./ %)	15/ 21/ 8/ 1 (33%/ 47%/ 18%/ 2%)
Histology: epithelioid/ sarcomatoid/ mixed/ unknown (no/%)	37/ 3/ 5/ 0 (82%/ 7%/ 11%/ 0%)

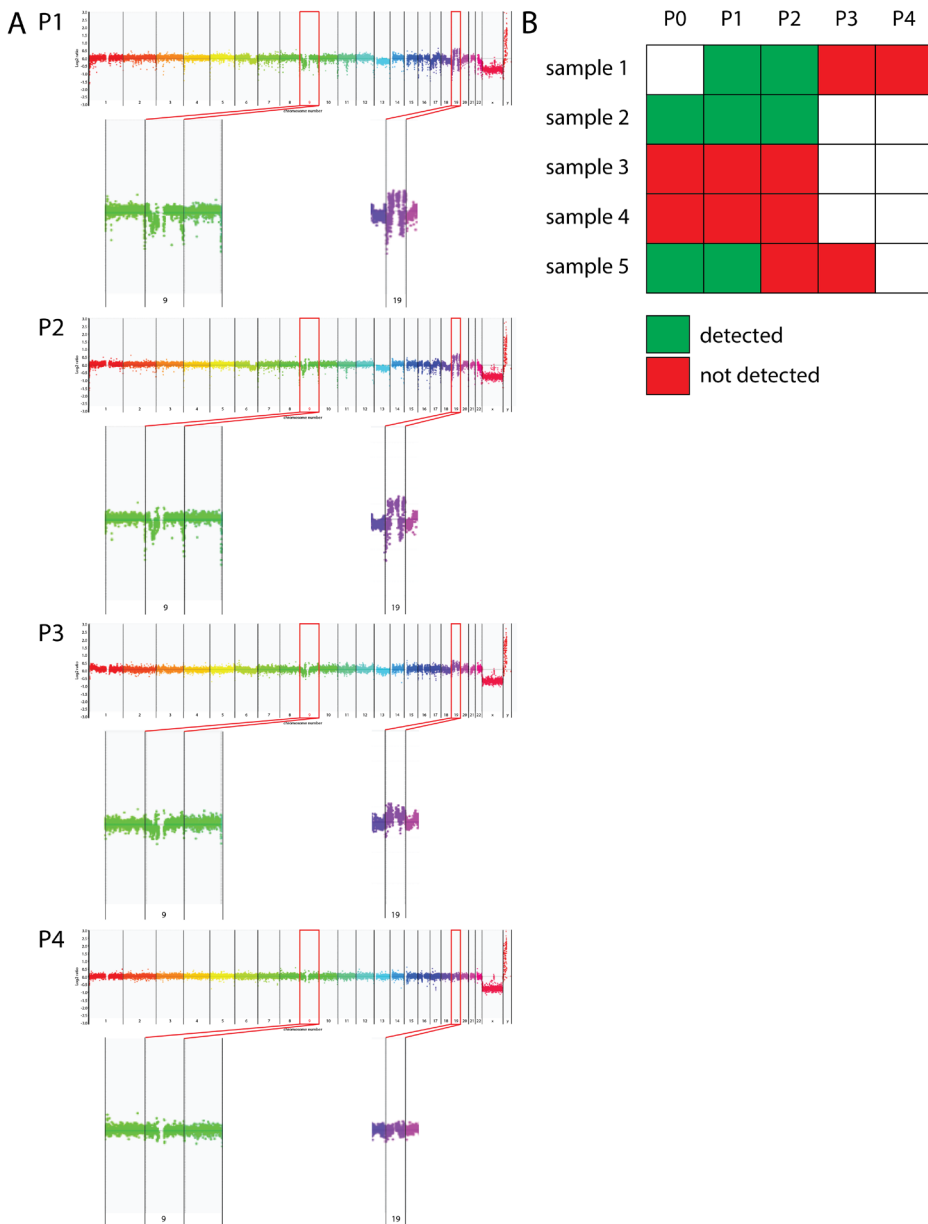


**Fig. S2. CGH profiles at different passages of a primary mesothelioma culture. A)** The  $\log_2$  ratio of copy number variations (CNV) is depicted for different chromosomes visualized on the x-axis, each chromosome in a different color. The overall profiles in the first two passages indicate the presence of malignant cells as is illustrated by deletion of the P16 locus on chromosome 9 (shown as an zoom-in in the inset). At higher passages the CNV is normalized indicating overgrowth by normal mesothelial cells. **B)** Overview of CDKN2A deletion for 5 patients. P1: passage 1, P2: passage 2, P3: passage 3, P4: passage 4. green: detected, red: not detected, white: not assessed. For patient 3 and 4 no deletion could be detected. For patient 1, 2 and 5 the CDKN2A deletion was detected in early passages. At later passages the deletion could not be detected for patient 1 and 5.

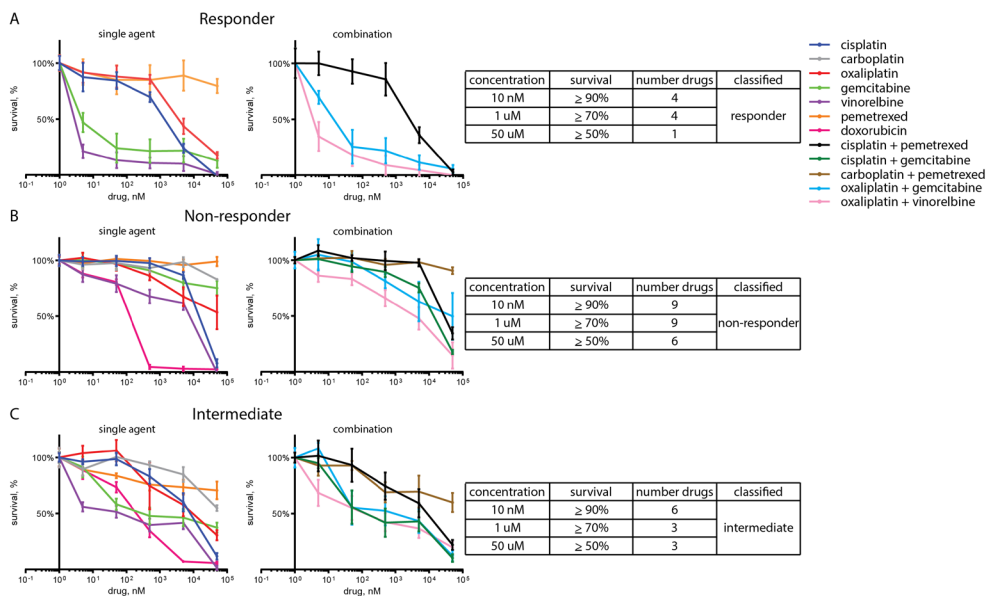


**Fig S3. Dose-response curves of single agents and combination depicted for the differently responding subgroups.** Dose-response curves of Fig. 2 separated to single agents and combinations are depicted for a responder **A)**, a non responder **B)** and an intermediate responder **C)**. Explanation for the subgroup definition is depicted next to the dose-response curves.

**Table S4 Drug screen classification characteristics**

	Non-treated		Treated	
	Number	Percentage	Number	Percentage
Drug screens	31	38%	50	62%
Responder	3	10%	3	6%
Intermediate	19	61%	29	58%
Non-responder	9	29%	18	36%

For the characteristics analyzed, there was no significant difference between these two groups ( $p=0.72$ )

**Table S5.** List of differential expressed genes.

Gene ID	Gene Symbol	Gene Name
ENSG00000163995	ABLIM2	actin binding LIM protein family member 2
ENSG00000100312	ACR	acrosin
ENSG00000174837	ADGRE1	adhesion G protein-coupled receptor E1
ENSG00000116771	AGMAT	agmatinase
ENSG00000165695	AK8	adenylate kinase 8
ENSG00000215267	AKR1C7P	aldo-keto reductase family 1 member C7, pseudogene
ENSG00000244301	AOX3P	
ENSG00000006453	BAIAP2L1	BAI1 associated protein 2 like 1
ENSG00000197299	BLM	Bloom syndrome RecQ like helicase
ENSG00000229106	BTBD6P1	BTB domain containing 6 pseudogene 1
ENSG00000221953	C1orf229	chromosome 1 open reading frame 229
ENSG00000128346	C22orf23	chromosome 22 open reading frame 23
ENSG00000225940	C5orf67	chromosome 5 open reading frame 67
ENSG00000118307	CASC1	cancer susceptibility candidate 1
ENSG00000246228	CASC8	cancer susceptibility candidate 8 (non-protein coding)
ENSG00000168491	CCDC110	coiled-coil domain containing 110
ENSG00000274736	CCL23	C-C motif chemokine ligand 23
ENSG00000272398	CD24	CD24 molecule
ENSG00000170312	CDK1	cyclin dependent kinase 1
ENSG00000100162	CENPM	centromere protein M
ENSG00000259430	CERS3-AS1	CERS3 antisense RNA 1
ENSG00000197748	CFAP43	cilia and flagella associated protein 43
ENSG00000172361	CFAP53	cilia and flagella associated protein 53
ENSG00000122966	CIT	citron rho-interacting serine/threonine kinase
ENSG00000144619	CNTN4	contactin 4
ENSG00000273509	CNTNAP3P1	contactin associated protein-like 3 pseudogene 1
ENSG00000124749	COL21A1	collagen type XXI alpha 1 chain
ENSG00000050767	COL23A1	collagen type XXIII alpha 1 chain
ENSG00000158525	CPA5	carboxypeptidase A5
ENSG00000109472	CPE	carboxypeptidase E
ENSG00000150938	CRIM1	cysteine rich transmembrane BMP regulator 1
ENSG00000169429	CXCL8	C-X-C motif chemokine ligand 8
ENSG00000160683	CXCR5	C-X-C motif chemokine receptor 5
ENSG000000080166	DCT	dopachrome tautomerase
ENSG00000165325	DEUP1	deuterosome assembly protein 1
ENSG00000267432	DNAH17-AS1	DNAH17 antisense RNA 1
ENSG00000118997	DNAH7	dynein axonemal heavy chain 7
ENSG000000007174	DNAH9	dynein axonemal heavy chain 9
ENSG00000134757	DSG3	desmoglein 3
ENSG00000198842	DUSP27	dual specificity phosphatase 27 (putative)
ENSG000001658891	E2F7	E2F transcription factor 7
ENSG00000186976	EFCAB6	EF-hand calcium binding domain 6
ENSG00000135373	EHF	ETS homologous factor
ENSG00000188316	ENO4	enolase family member 4
ENSG00000204334	ERICH2	glutamate rich 2
ENSG00000171320	ESCO2	establishment of sister chromatid cohesion N-acetyltransferase 2
ENSG00000264527	ESP33	uncharacterized locus ESP33
ENSG00000135476	ESPL1	extra spindle pole bodies like 1, separate
ENSG00000229007	EXOSC3P1	exosome component 3 pseudogene 1
ENSG00000198780	FAM169A	family with sequence similarity 169 member A
ENSG00000125804	FAM182A	family with sequence similarity 182 member A
ENSG00000175170	FAM182B	family with sequence similarity 182 member B
ENSG00000104059	FAM189A1	family with sequence similarity 189 member A1
ENSG00000269881	FAM234A	family with sequence similarity 234 member A
ENSG00000164616	FBXL21	F-box and leucine rich repeat protein 21 (gene/pseudogene)
ENSG00000132185	FCRLA	Fc receptor like A
ENSG00000181617	FD CSP	follicular dendritic cell secreted protein
ENSG00000230316	FEZF1-AS1	FEZF1 antisense RNA 1
ENSG00000275340	FGD5P1	FYVE, RhoGEF and PH domain containing 5 pseudogene 1
ENSG00000102466	FGF14	fibroblast growth factor 14
ENSG00000102678	FGF9	fibroblast growth factor 9

ENSG00000137440	FGFBP1	fibroblast growth factor binding protein 1
ENSG00000232774	FLJ22447	uncharacterized LOC400221
ENSG00000105255	FSD1	fibronectin type III and SPRY domain containing 1
ENSG00000123689	G0S2	G0/G1 switch 2
ENSG00000197093	GAL3ST4	galactose-3-O-sulfotransferase 4
ENSG00000227135	GCSAML-AS1	GCSAML antisense RNA 1
ENSG00000139278	GLIPR1	GLI pathogenesis related 1
ENSG00000140478	GOLGA6A	golgin A6 family member C
	(includes others)	
ENSG00000170775	GPR37	G protein-coupled receptor 37
ENSG00000138271	GPR87	G protein-coupled receptor 87
ENSG00000167914	GSDMA	gasdermin A
ENSG00000111305	GSG1	germ cell associated 1
ENSG00000075218	GTSE1	G2 and S-phase expressed 1
ENSG00000164588	HCN1	hyperpolarization activated cyclic nucleotide gated potassium channel 1
ENSG00000162639	HENMT1	HEN1 methyltransferase homolog 1
ENSG00000235527	HIPK1-AS1	HIPK1 antisense RNA 1
ENSG00000183598	HIST2H3D	histone cluster 2, H3d
ENSG00000212769	HMGN2P8	high mobility group nucleosomal binding domain 2 pseudogene 8
ENSG00000276975	HYDIN2	HYDIN2, axonemal central pair apparatus protein (pseudogene)
ENSG00000146678	IGFBP1	insulin like growth factor binding protein 1
ENSG00000142224	IL19	interleukin 19
ENSG00000254294	IMPDH1P6	inosine monophosphate dehydrogenase 1 pseudogene 6
ENSG00000123999	INHA	inhibin alpha subunit
ENSG00000183856	IQGAP3	IQ motif containing GTPase activating protein 3
ENSG00000170549	IRX1	iroquois homeobox 1
ENSG00000176049	JAKMIP2	janus kinase and microtubule interacting protein 2
ENSG00000184408	KCND2	potassium voltage-gated channel subfamily D member 2
ENSG00000235262	KDM5C-IT1	KDM5C intronic transcript 1
ENSG00000186185	KIF18B	kinesin family member 18B
ENSG00000116852	KIF21B	kinesin family member 21B
ENSG00000142945	KIF2C	kinesin family member 2C
ENSG00000237649	KIFC1	kinesin family member C1
ENSG00000124743	KLHL31	kelch like family member 31
ENSG00000137812	KNL1	kinetochore scaffold 1
ENSG00000205426	KRT81	keratin 81
ENSG00000233930	KRTAP5-AS1	KRTAP5-1/KRTAP5-2 antisense RNA 1
ENSG00000133317	LGALS12	galectin 12
ENSG00000186152	LILRP1	leukocyte immunoglobulin-like receptor pseudogene 1
ENSG00000170858	LILRP2	leukocyte immunoglobulin-like receptor pseudogene 2
ENSG00000180422	LINC00304	long intergenic non-protein coding RNA 304
ENSG00000214851	LINC00612	long intergenic non-protein coding RNA 612
ENSG00000237945	LINC00649	long intergenic non-protein coding RNA 649
ENSG00000242258	LINC00996	long intergenic non-protein coding RNA 996
ENSG00000271856	LINC01215	long intergenic non-protein coding RNA 1215
ENSG00000249667	LINC01259	long intergenic non-protein coding RNA 1259
ENSG00000249911	LINC01265	long intergenic non-protein coding RNA 1265
ENSG00000251396	LINC01301	long intergenic non-protein coding RNA 1301
ENSG00000227467	LINC01537	long intergenic non-protein coding RNA 1537
ENSG00000079435	LIPE	lipase E, hormone sensitive type
ENSG00000260868	LOC100128905	uncharacterized LOC100128905
ENSG00000234432	LOC100129484	uncharacterized LOC100129484
ENSG00000278909	LOC100130057	uncharacterized LOC100130057
ENSG00000237499	LOC100130476	uncharacterized LOC100130476
ENSG00000257545	LOC100287944	uncharacterized LOC100287944
ENSG00000250365	LOC101927124	uncharacterized LOC101927124
ENSG00000226747	LOC101927196	uncharacterized LOC101927196
ENSG00000250548	LOC101927780	uncharacterized LOC101927780
ENSG00000235834	LOC101928389	uncharacterized LOC101928389
ENSG00000255337	LOC101928424	uncharacterized LOC101928424
ENSG00000261465	LOC102723385	uncharacterized LOC102723385
ENSG00000230010	LOC105372550	uncharacterized LOC105372550

ENSG00000270171	LOC105376689	uncharacterized LOC105376689
ENSG00000233593	LOC105378853	
ENSG00000256050	LOC107984678	uncharacterized LOC107984678
ENSG00000234665	LOC403323	uncharacterized LOC403323
ENSG00000236780	LOC644838	uncharacterized LOC644838
ENSG00000230445	LRRC37A6P	leucine rich repeat containing 37 member A6, pseudogene
ENSG00000240720	LRRD1	leucine rich repeats and death domain containing 1
ENSG00000235448	LURAP1L-AS1	LURAP1L antisense RNA 1
ENSG00000187391	MAGI2	membrane associated guanylate kinase, WW and PDZ domain containing 2
ENSG00000234456	MAGI2-AS3	MAGI2 antisense RNA 3
ENSG00000078018	MAP2	microtubule associated protein 2
ENSG00000008735	MAPK8IP2	mitogen-activated protein kinase 8 interacting protein 2
ENSG00000199094	mir-30	microRNA 30a
ENSG00000208018	mir-645	microRNA 645
ENSG00000263463	MIR378I	microRNA 378i
ENSG00000162006	MSLNL	mesothelin-like
ENSG00000101057	MYBL2	MYB proto-oncogene like 2
ENSG00000250174	MYLK-AS2	MYLK antisense RNA 2
ENSG00000272916	NDST2	N-deacetylase and N-sulfotransferase 2
ENSG00000247809	NR2F2-AS1	NR2F2 antisense RNA 1
ENSG00000167693	NXN	nucleoredoxin
ENSG00000119547	ONECUT2	one cut homeobox 2
ENSG00000099985	OSM	oncostatin M
ENSG000000083454	P2RX5	purinergic receptor P2X 5
ENSG00000257950	P2RX5-TAX1BP3	P2RX5-TAX1BP3 readthrough (NMD candidate)
ENSG00000174740	PABPC5	poly(A) binding protein cytoplasmic 5
ENSG00000107719	PALD1	phosphatase domain containing, paladin 1
ENSG00000231806	PCAT7	prostate cancer associated transcript 7 (non-protein coding)
ENSG00000248383	PCDHAC1	protocadherin alpha subfamily C, 1
ENSG00000262576	PCDHGA4	protocadherin gamma subfamily A, 4
ENSG00000056487	PHF21B	PHD finger protein 21B
ENSG00000164530	PI16	peptidase inhibitor 16
ENSG00000153823	PID1	phosphotyrosine interaction domain containing 1
ENSG00000162896	PIGR	polymeric immunoglobulin receptor
ENSG00000127564	PKMYT1	protein kinase, membrane associated tyrosine/threonine 1
ENSG00000122861	PLAU	plasminogen activator, urokinase
ENSG00000137841	PLCB2	phospholipase C beta 2
ENSG00000136040	PLXNC1	plexin C1
ENSG00000240694	PNMA2	paraneoplastic Ma antigen 2
ENSG0000028277	POU2F2	POU class 2 homeobox 2
ENSG00000184486	POU3F2	POU class 3 homeobox 2
ENSG00000185250	PPIL6	peptidylprolyl isomerase like 6
ENSG00000119938	PPP1R3C	protein phosphatase 1 regulatory subunit 3C
ENSG00000158528	PPP1R9A	protein phosphatase 1 regulatory subunit 9A
ENSG00000068489	PRR11	proline rich 11
ENSG00000112812	PRSS16	protease, serine 16
ENSG00000206549	PRSS50	protease, serine 50
ENSG00000225706	PTPRD-AS1	PTPRD antisense RNA 1
ENSG00000164611	PTTG1	pituitary tumor-transforming 1
ENSG00000076344	RGS11	regulator of G-protein signaling 11
ENSG00000253006	RN7SKP283	
ENSG00000263974	RN7SL121P	RNA, 7SL, cytoplasmic 121, pseudogene
ENSG00000242853	RN7SL749P	
ENSG00000164197	RNF180	ring finger protein 180
ENSG00000251819	RNU6-322P	RNA, U6 small nuclear 322, pseudogene
ENSG00000221340	RNU6ATAC18P	
ENSG00000201558	RNVU1-6	RNA, variant U1 small nuclear 6
ENSG00000213228	RPL12P38	ribosomal protein L12 pseudogene 38
ENSG00000243422	RPL23AP49	ribosomal protein L23a pseudogene 49
ENSG00000171848	RRM2	ribonucleotide reductase regulatory subunit M2
ENSG00000160188	RSPH1	radial spoke head 1 homolog
ENSG00000105784	RUND3B	RUN domain containing 3B
ENSG00000160307	S100B	S100 calcium binding protein B
ENSG00000186193	SAPCD2	suppressor APC domain containing 2

ENSG00000183873	SCN5A	sodium voltage-gated channel alpha subunit 5
ENSG00000136546	SCN7A	sodium voltage-gated channel alpha subunit 7
ENSG00000135094	SDS	serine dehydratase
ENSG00000012171	SEMA3B	semaphorin 3B
ENSG00000232352	SEMA3B-AS1	SEMA3B antisense RNA 1 (head to head)
ENSG00000167680	SEMA6B	semaphorin 6B
ENSG00000057149	SERPINB3	serpin family B member 3
ENSG00000206073	SERPINB4	serpin family B member 4
ENSG00000101049	SGK2	SGK2, serine/threonine kinase 2
ENSG00000129946	SHC2	SHC adaptor protein 2
ENSG00000171241	SHCBP1	SHC binding and spindle associated 1
ENSG00000188991	SLC15A5	solute carrier family 15 member 5
ENSG00000103257	SLC7A5	solute carrier family 7 member 5
ENSG00000227258	SMIM2-AS1	SMIM2 antisense RNA 1
ENSG00000206754	SNORD101	small nucleolar RNA, C/D box 101
ENSG00000163071	SPATA18	spermatogenesis associated 18
ENSG00000150628	SPATA4	spermatogenesis associated 4
ENSG00000184005	ST6GALNAC3	ST6 N-acetylgalactosaminide alpha-2,6-sialyltransferase 3
ENSG00000127954	STEAP4	STEAP4 metalloredutase
ENSG00000169302	STK32A	serine/threonine kinase 32A
ENSG00000144834	TAGLN3	transgelin 3
ENSG00000182521	TBPL2	TATA-box binding protein like 2
ENSG00000089225	TBX5	T-box 5
ENSG00000240280	TCAM1P	testicular cell adhesion molecule 1, pseudogene
ENSG00000253304	TMEM200B	transmembrane protein 200B
ENSG00000165685	TMEM52B	transmembrane protein 52B
ENSG00000118503	TNFAIP3	TNF alpha induced protein 3
ENSG00000050730	TNIP3	TNFAIP3 interacting protein 3
ENSG00000188001	TPRG1	tumor protein p63 regulated 1
ENSG00000170893	TRH	thyrotropin releasing hormone
ENSG00000142185	TRPM2	transient receptor potential cation channel subfamily M member 2
ENSG00000157570	TSPAN18	tetraspanin 18
ENSG00000214391	TUBAP2	tubulin alpha pseudogene 2
ENSG00000276043	UHRF1	ubiquitin like with PHD and ring finger domains 1
ENSG00000093134	VNN3	vanin 3
ENSG00000075702	WDR62	WD repeat domain 62
ENSG00000154764	WNT7A	Wnt family member 7A
ENSG00000177752	YIPF7	Yip1 domain family member 7
ENSG00000169064	ZBBX	zinc finger B-box domain containing
ENSG00000221886	ZBED8	zinc finger BED-type containing 8
ENSG00000091656	ZFHX4	zinc finger homeobox 4
ENSG00000229956	ZRANB2-AS2	ZRANB2 antisense RNA 2 (head to head)

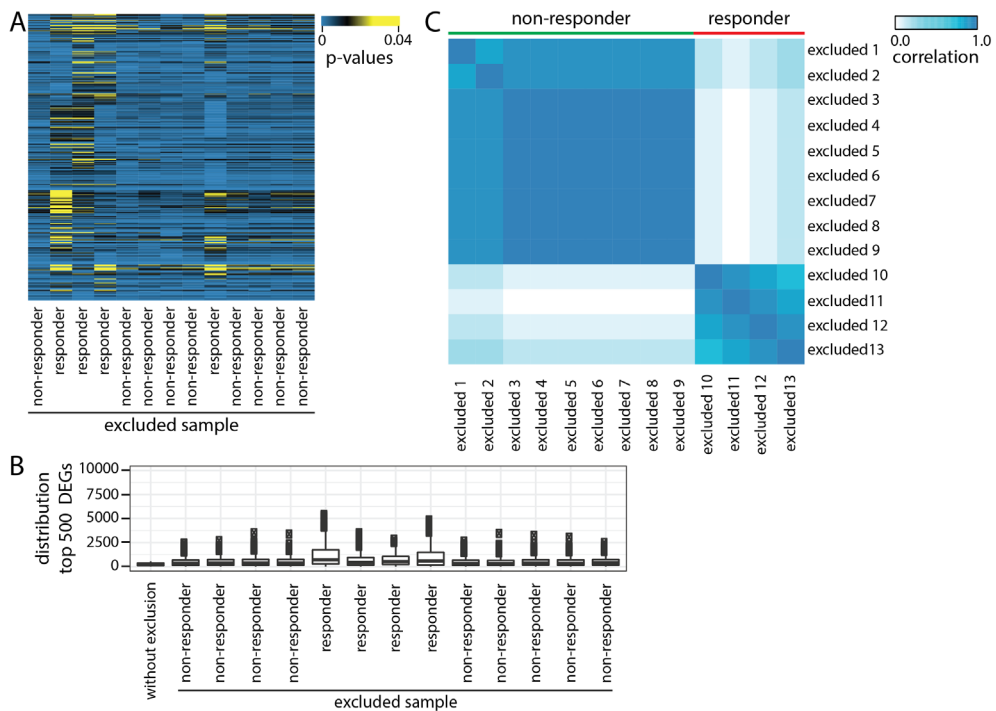


**Fig. S6. Stability assessment of differential gene expression analysis. A)** Heat map indicating P-values with leave one out cross-validation experiment. Columns are held out samples and rows are held-out genes. **B)** Ranks of DEGs in terms of P-values in the held-out experiment. **C)** Consensus clustering of samples with DEGs obtained from each of the held-out experiment. Color bar indicate patient group.

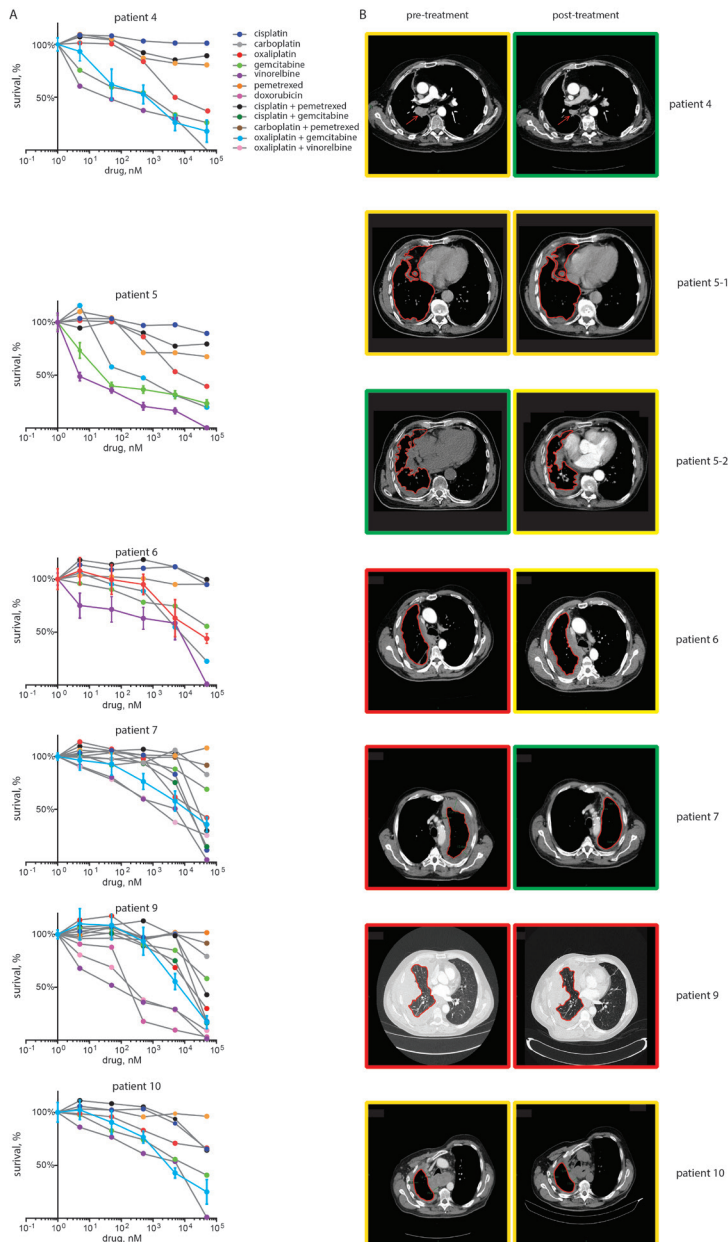


**Fig. S7. Dose-response curves and clinical responses.** **A)** Dose-response curves of primary tumor cultures performed for patient 4-7, 9 and 10. The chemotherapeutic agent that was given to the patient is depicted in color the rest of the screened chemotherapeutics is depicted with a gray line and colored dots. **B)** CT-scans of patient 4-7, 9 and 10 before and after treatment with the drugs selected based on the in vitro drug screen. Response evaluation was done using modified RECIST for mesothelioma. Colored boxes around CT-scans indicate in vitro response prediction before treatment and actual response after treatment. Green: partial response, yellow: stable disease, red: progressive disease. Tumor-rinds are indicated by red line.



# Chapter 3

## Comprehensive Pharmacogenomic Profiling of Malignant Pleural Mesothelioma Identifies a Subgroup Sensitive to FGFR Inhibition.

Josine M.M.F. Quispel-Janssen\*, Jitendra Badhai\*, Laurel M. Schunselaar\*, Stacey Price, Jonathan Brammeld, Francesco Iorio, Krishna Kolluri, Mathew Garnett, Anton Berns, Paul Baas, Ultan McDermott, Jacques Neefjes and Constantine Alifrangis  
\*equal contribution

Clin Cancer Res. 2018 Jan; 24(1):84-94



## Abstract

**Purpose:** Despite intense research, treatment options for patients with mesothelioma are limited and offer only modest survival advantage. We screened a large panel of compounds in multiple mesothelioma models and correlated sensitivity with a range of molecular features to detect biomarkers of drug response.

**Experimental design:** We utilized a high-throughput chemical inhibitor screen in a panel of 889 cancer cell lines, including both immortalized and primary early-passage mesothelioma lines, alongside comprehensive molecular characterization using Illumina whole-exome sequencing, copy-number analysis and Affymetrix array whole transcriptome profiling. Subsequent validation was done using functional assays such as siRNA silencing and mesothelioma mouse xenograft models.

**Results:** A subgroup of immortalized and primary MPM lines appeared highly sensitive to FGFR inhibition. None of these lines harbored genomic alterations of FGFR family members, but rather BAP1 protein loss was associated with enhanced sensitivity to FGFR inhibition. This was confirmed in a MPM mouse xenograft model and by BAP1 knockdown and overexpression in cell line models. Gene expression analyses revealed an association between BAP1 loss and increased expression of the receptors FGFR1/3 and ligands FGF9/18. BAP1 loss was associated with activation of MAPK signaling. These associations were confirmed in a cohort of MPM patient samples.

**Conclusion:** A subgroup of mesotheliomas cell lines harbor sensitivity to FGFR inhibition. BAP1 protein loss enriches for this subgroup and could serve as a potential biomarker to select patients for FGFR inhibitor treatment. These data identify a clinically relevant MPM subgroup for consideration of FGFR therapeutics in future clinical studies.

## Keywords

mesothelioma, FGFR, BAP1, biomarker

## Translational relevance

Malignant pleural mesothelioma (MPM) has limited treatment options and a dismal prognosis. To date, targeted therapies have proved ineffective, and no druggable genetic alterations have been identified. Selecting compounds for further clinical evaluation in this small and heterogeneous patient group is challenging. By combining high-throughput drug screens, comprehensive molecular characterization and functional assays in multiple mesothelioma models, we were able to identify an FGFR inhibitor-sensitive subgroup with BAP1 loss as a potential predictive biomarker. Loss of BAP1 is found in up to 64% of MPM tumors. These data suggest that a significant group of patients with mesothelioma may benefit from FGFR inhibition.

## Introduction

Malignant Pleural Mesothelioma (MPM) is a tumor arising from the pleural cavity and is strongly associated with occupational exposure to asbestos. Although strict regulation is in place in more than 50 countries, in parts of the world where there is still widespread usage of asbestos, most notably in South America, Russia and states of the former Soviet Republic, China and South-East Asia, the incidence of this disease is rising [1, 2]. MPM is highly refractory to conventional anticancer therapies, and the prognosis is poor; most patients die within a year of diagnosis. Surgery with curative intent is only possible in a highly selected group of patients and needs to be combined with chemotherapy. The only approved treatment, a combination of the cytotoxic agents cisplatin and pemetrexed, yields at best modest improvements in survival [3, 4]. Despite many clinical studies utilizing novel biological therapies, there are as yet no effective targeted therapies for this cancer [5, 6].

A recent comprehensive genomic analysis of 216 MPM samples found *BAP1*, *NF2*, *TP53*, *SETD2* and *CDKN2A* to be recurrently mutated or structurally rearranged [7]. The landscape is thus one of mutated tumor suppressor genes and alterations in pathways as diverse as Hippo, mTOR, and TP53, as well as histone methylation. Such loss-of-function oncogenic events are typically considered “undruggable”, but downstream programs of genes, activated as a consequence of such mutations, may themselves be tractable therapeutic targets. This is illustrated by NF2-deficient tumors with activated focal adhesion kinase (FAK). Defactinib, a FAK inhibitor, demonstrated efficacy in NF2-deficient tumors *in vitro* [8] but a subsequent clinical trial in mesothelioma was halted due to lack of efficacy. Other drugs tested to date that have failed to improve the outcome in MPM include EGFR inhibitors [9], Bcr-Abl inhibitors [10], thalidomide [11], bortezomib [12], and vorinostat [13]. In many of these studies, a subgroup of patients appeared to derive some benefit. However, in MPM, it has been difficult to elucidate reproducible biomarkers that identify these sensitive subgroups.

Some research groups have demonstrated coactivation of multiple RTK pathways in MPM tumors, which may provide a rationale for combination therapies with kinase inhibitors [14].

We aimed to utilize high-throughput chemical screening platforms alongside molecular characterization of immortalized and early-passage cell line models of MPM to uncover critical signaling pathways that may be amenable to therapeutic interrogation.

## **Materials and methods**

### **Cell lines and tissue culture**

Cells are grown and maintained in either RPMI or DMEM F/12 supplemented with 10% FBS and 1% penicillin/streptomycin. Cell lines were maintained at 37°C at 5% CO<sub>2</sub>. All cell lines have been verified by genotyping using short tandem repeat (STRs) profiling and Sequenom profiling of a panel of 92 single-nucleotide-polymorphisms.

### **Cell viability Assays**

Cells are trypsinized and counted before seeding at the optimal density for the well size (either 96- or 384-well plates were used) and duration of the assay. Seeding density was optimized by titration of the cells such that upon visual inspection of the control wells at the end of the assay, a confluency of 70% to 90% was observed allowing cells to grow in a linear phase. Adherent cell lines were seeded 24 hours before drug addition. The high-throughput chemical inhibitor screen was carried out using 384-well plates, and viability was measured 72 hours after drug addition with a 5-point serial fourfold concentration range of 265 compounds. All other viability assays were carried out using 96-well plates and a 9-point twofold dilution of the drugs. Drugs were all dissolved in DMSO, and DMSO was used only as a control condition. At the end of the experiment, cells were fixed with 4% paraformaldehyde. Following two washes with dH<sub>2</sub>O, 100ml of Syto60 nucleic acid stain (Invitrogen) was added to a final concentration of 1mmol/L (a 1/5,000 stock dilution), and plates were fixed for 1hour at room temperature. Quantification of fluorescent signal was achieved using a Paradigm (BD) plate reader using excitation/emission wavelengths of 630/695 nm. Data were analyzed by adjusting for background signals and normalizing each well to the DMSO-treated control.

### **High-throughput Screening Compounds**

Compounds were acquired from academic collaborators or commercial vendors. Each compound, its therapeutically relevant target substrate and pathway, and the minimum and maximum screening concentrations are listed in Supplementary Table S1. Compounds were stored as 10 mmol/L aliquots at -80°C and were subjected to a maximum of 5 freeze-thaw

cycles. Each of the agents was screened at a 5-point serial fourfold dilution to provide a 256-fold range from the lowest to highest concentration. The concentrations selected for each compound were based on *in vitro* data to cover the range of concentrations known to inhibit relevant kinase activity and cell viability.

### **Apoptosis assay**

Cells were seeded in a flat-bottom 384 wells plate at optimal cell density. After 24 hours, PD173074 and AZD 4547 in a concentration range between 0.007813 and 1  $\mu\text{mol/L}$  were added using a Tecan HP D300 Digital Dispenser. Five replicate wells were assayed for each condition. Phenylarsine oxide (20  $\mu\text{mol/L}$ ) was used as positive control condition. To assess apoptosis, 5  $\mu\text{mol/L}$  of IncuCyte caspase-3/7 green apoptosis assay reagent was added to the cells. Confluence and apoptosis levels were quantified by IncuCyte Zoom live-cell imaging systems from Essen bioscience. Relative apoptosis was calculated by dividing the confluence of fluorescent apoptotic cells by total confluence and normalized to the positive control condition.

### **Western Blots**

Cell monolayers were lysed on ice in NP40 Cell Lysis Buffer (Invitrogen) containing fresh protease and phosphatase inhibitors (Roche). Lysates were centrifuged at 13,000 rpm for 10 minutes and the supernatant used for analyses. Protein concentration was calculated from a standard curve of BSA using the BCA assay (calbiotech) according to the manufacturer's instructions. Equal protein concentrations were loaded on pre-cast 4% to 12% Bis-Tris SDS-PAGE Gels (Invitrogen), run at 200 V for 1 hour. Proteins were transferred onto a methanol activated PVDF membrane at 100 V for 1 hour or overnight at 30 V. Membranes were blocked in 5% milk for 1 hour before the addition of primary antibody at a concentration recommended. After overnight incubation with the primary antibody at 4°C, the membrane was washed three times in 0.1% TBS-T followed by incubation with the secondary antibody according to suppliers description at 1/2,500 dilution). Immunoblots were imaged using Pierce Supersignal Plus chemiluminescent kit on a gel imager (Syngene). Antibodies against BAP1, pERK, ERK, pFGFR (total) and pFGFR1 (all from Cell Signalling Technologies) and the polyclonal p-FGFR3 antibody sc-33041 (Santa Cruz Biotechnology) were used. Beta Tubulin was used as a loading control for Western blots. Phospho-RTK arrays (RD systems) and caspase-Glo 3/7 assay were used according to the manufacturer's instructions.

### **Establishment of early-passage primary mesothelioma tumor cell cultures**

All patients whose materials were used provided written informed consent for the use and storage of pleural fluid, tumor biopsies and germ line DNA. Diagnosis was made on tumor biopsies according to local IHC protocols and confirmed by the Dutch Mesothelioma Panel, a national expert panel of certified pathologists that evaluate all suspected mesothelioma

patient samples. Early-passage primary mesothelioma cultures were generated from tumor cells isolated from pleural fluid of patients at the Netherlands Cancer Institute. The pleural fluid was centrifuged at 1,500 rpm for 5 minutes at room temperature. Erythrocyte lysis buffer was used to remove erythrocytes if many were present. Cells were resuspended in Dulbecco's Modified Eagle Medium (DMEM, Gibco) supplemented with penicillin/streptomycin and 8% fetal calf serum. The cells were seeded in T75 flasks at a density of  $1 \times 10^6$  cells/mL and incubated at 37°C at a humidified 5% CO<sub>2</sub> atmosphere. Medium was refreshed depending on cell growth, usually twice a week. At seeding and during the first two passages, cytopspins were made and stained with HE and reviewed by our pathologist to determine the percentage of tumor cells. If the tumor percentage was over 70%, usually reached after one passage, living cell cultures were transported to the Wellcome Trust Sanger Institute within 6 hours for drug screening and genetic analysis. Cells were cultured for a maximum period of 4 weeks.

### **RNA interference and transfection**

Lipofectamine RNAiMAX (ThermoFisher) was used according to product guidelines for transfection with siRNA against FGFR3 (Thermo Fisher Silencer Select s5167 and s5169) or BAP1 (s15822) utilizing the protocol "forward transfection of mammalian cell lines". KIF11 siRNA (s7902) was used as a transfection (positive) control. Viability or protein expression were assayed as described above, at specified time points. H226 cell expressing a BAP1 stable construct, and BAP1 C91A mutant lines were a kind gift from K Kolluri (UCL, London).

### **Gene expression analyses**

Microarray data were generated on the Human Genome U219 96-Array Plate using the Gene Titan MC instrument (Affymetrix). The robust multi-array analysis (RMA) algorithm [15] was used to establish intensity values for each of 18562 loci (BrainArray v.10). We discarded transcripts with low sample variance and consolidated duplicated genes by averaging their expression values across duplicates. The resulting data were subsequently normalized ( $\mu=0$ ;  $\sigma=1$ ) sample-wise and gene-median centered. Raw data was deposited in ArrayExpress (accession: E-MTAB-3610). The RMA processed dataset is available at [www.cancerrxgene.org/gdsc1000/GDSC1000\\_WebResources/Home.html](http://www.cancerrxgene.org/gdsc1000/GDSC1000_WebResources/Home.html). The expression-level signal of each gene was normalized using a nonparametric kernel estimation of its cumulative density function as described in ref.[16]. Additionally, the normalized expression values were further tissue-centered using as grouping factors the cell line tissue labels of ref. [17].

### **MPM Mouse Xenograft Models**

All animal experiments were conducted according to institutional guidelines under protocol approved by the animal ethics committee of the Netherlands Cancer Institute. To establish xenografts, 3 million human mesothelioma cells (H2731 and MSTO211H) were implanted

subcutaneously into the right dorsal flank of 6- to 7-week-old female nude SCID mice. Mice were randomized into vehicle and drugs treatment groups, and treatment was initiated once the tumor volumes reached approximately 200 mm<sup>3</sup>. Tumor size was measured with calipers twice a week, and tumor volume was determined as  $a \times b^2 \times 0.5$ , where  $a$  and  $b$  were the large and small diameters, respectively.

## Results

### High-throughput chemical inhibitor screens in immortalized cell lines

A panel of 889 cancer cell lines was screened with 265 compounds that included targeted and cytotoxic compounds (for detail see <http://www.cancerrxgene.org/>). It was observed that three of 19 MPM lines (H2795, H2591, and MSTO-211H) had IC<sub>50</sub> values among the top 5% of cell lines showing highest sensitivity to the compound PD-173074, an FGFR1 and FGFR3 kinase inhibitor (Fig 1A; ref. 15). These three cell lines, together with two additional MPM lines (NCI-H28, resistant; MPP-89, partially sensitive) and an FGFR-dependent lung cancer cell line harboring amplification of FGFR1 (NCI-H1581), were rescreened with PD-173074 and were as sensitive to PD-173074 as the FGFR1-dependent lung cancer line NCI-1581 (Fig. 1B). Furthermore, this sensitivity was also seen with two more selective FGFR inhibitors, NVP-BGJ398 and AZD4547 (Supplementary Fig. S1). Sensitivity to PD-173074 in the MPM cell lines was confirmed by clonogenic survival assays (Fig. 1C). Although some sensitive lines died by apoptosis, as is shown by activated caspase activity with both PD-173074 and the multi-FGFR-targeted inhibitor AZD4547 (Fig. 1D and E), not all sensitive lines showed a dose incremental increase in this marker.

These data confirm previous findings [18] that a subset of MPM cell lines require FGF pathway activation for growth and survival, and that targeting this pathway could be a critical step in the control of these tumors.

### Drug sensitivity in early-passage MPM cultures

To test whether these observations could be reproduced in an independent cohort of primary mesothelioma cell lines, a panel of 11 pleural fluid-derived early-passage cultures from patients with MPM tumors were obtained and screened for viability using a panel of 48 small molecule inhibitors including PD-173074. Most of the early-passage cultures were resistant to virtually all agents (Supplementary Fig. S2). However, one MPM early-passage culture (NKI04) did demonstrate marked sensitivity to PD-173074. The sensitivity of NKI04 to FGFR inhibition was confirmed in a longer duration clonogenic survival assay, and the effect on cell viability was comparable to that seen in the FGFR1-amplified NCI-H1581 lung cancer cell line (Fig. 2A-C).

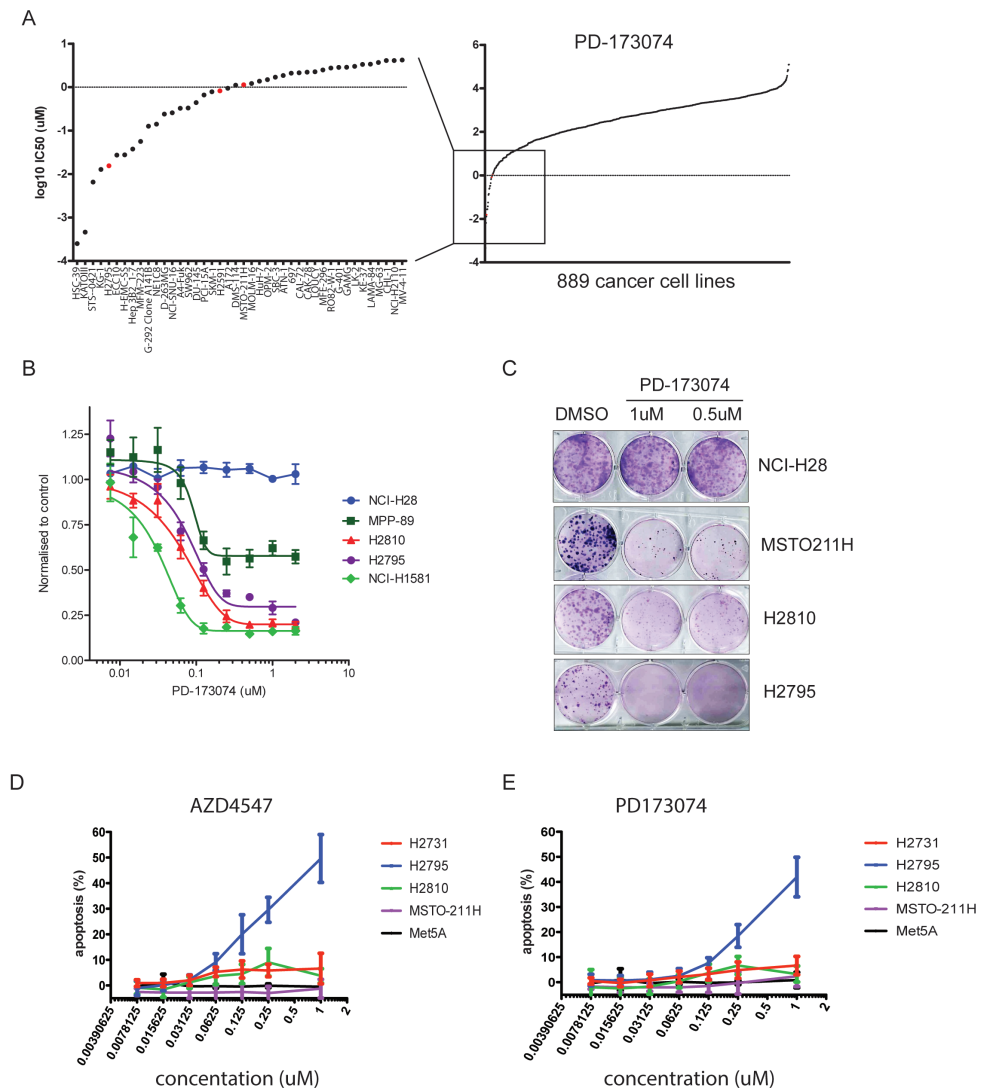


**Fig. 1. Sensitivity to FGFR inhibition in established mesothelioma cell lines. A)** Sensitivity to FGFR inhibitor PD173074 expressed as logIC<sub>50</sub> value (inhibiting concentration that kills 50% of the cells) of each different cell line. The enlargement shows the 5% most sensitive cell lines with amongst them mesothelioma cell lines depicted in red. **B)** Dose–response curves depicting the cell viability (mean SD) of different cell lines (y-axis) as a function of the dose of FGFR inhibitor PD-173074. NCI-H28, MPP-89, H2810, and H2795 are mesothelioma cell lines, while NCI-H1581 is an FGFR-dependent lung cancer cell line. **C)** Fourteen-day clonogenic survival assay of selected mesothelioma cell lines (NCI-H28, MSTO-211H, H2810, and H2795), treated with FGFR inhibitor PD-173074 at concentrations of 500 nmol/L and 1 mmol/L. **D)** FGFR inhibitor AZD4547 kills mesothelioma cell lines via induction of apoptosis as is demonstrated by an increase in caspase 3/7 activity after 48 hours of treatment with different doses of AZD4547 in a panel of MPM cell lines. **E)** FGFR inhibitor PD173074 kills mesothelioma cell lines via induction of apoptosis as is demonstrated by an increase in caspase3/7 activity after 48 hours of treatment with different doses of PD-173074 a panel of MPM cell lines.

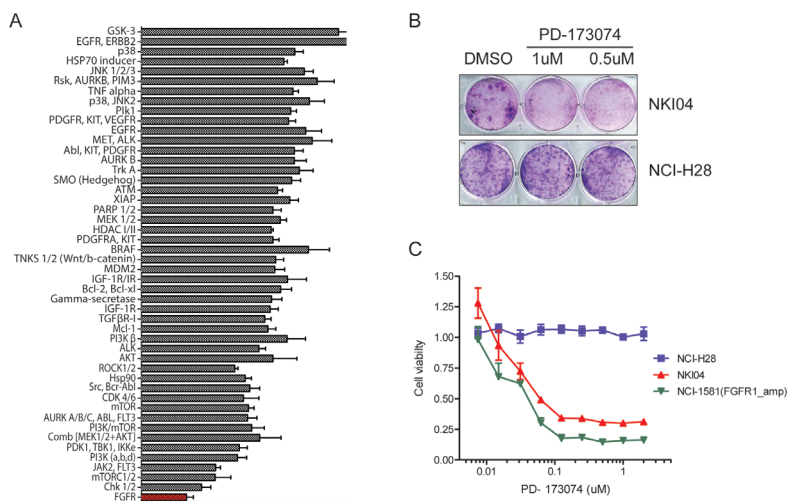


**Fig. 2. Sensitivity to FGFR inhibitors in primary mesothelioma lines. A)** Cell viability (mean SD) of primary mesothelioma line NKI04 after treatment with a fixed does of 48 different small molecule inhibitors. This cell line is most sensitive to FGFR inhibition. **B)** Fourteen-day clonogenic survival assay of primary mesothelioma line NKI04 compared with immortalized mesothelioma line NCI-H28 treated with FGFR inhibitor PD-173074 at concentrations of 500 nmol/L and 1 mmol/L. **C)** Cell viability (mean SD) of primary mesothelioma line NKI04 compared with immortalized mesothelioma line NCI-H28 and FGFR-dependent lung cancer cell line NCI-H1581 (y-axis), as a function of the concentration of FGFR inhibitor PD-173074. NCI-H28, MPP-89, H2810, and H2795 are mesothelioma cell lines.

### Molecular characterization of FGFR pathway signaling in cell lines and patient samples

In order to understand the basis for the observed sensitivity to FGFR inhibition, we analyzed whole-exome sequence and copy number array data for 21 MPM lines ([http://cancer.sanger.ac.uk/cell\\_lines](http://cancer.sanger.ac.uk/cell_lines)). There was no evidence of activating mutations or whole gene amplifications in any FGFR family member. RNA sequencing has been undertaken and shows no evidence of a fusion transcript involving any member of the FGFR family in any of the MPM cell lines (personal communication, M. Garnett). We then analyzed the corresponding gene expression data and focused on differential expression of FGFR and FGF family members in PD-173074-sensitive and -resistant MPM cell lines. Normalized expression of each of the FGF and FGFR family genes was correlated with sensitivity to PD-173074 to explore whether the variation in any single family member, either ligand or receptor, was associated with response to FGFR inhibition. We found a statistically significant correlation between elevated FGF9 mRNA expression and response to PD-173074 ( $P=0.0148$ ) and AZD4547 treatment ( $P=0.0098$ ; Fig. 3A). FGF9 is a secreted, high-affinity ligand for the FGFR3 receptor, with low affinity for the FGFR1 and FGFR2 receptors [19]. To determine whether a subset of MPM exhibits elevated

expression of the FGF9 ligand in patients, we analyzed gene expression from a panel of 53 assorted MPM and matched normal lung clinical samples (Fig. 3B; ref. [20]). Overall, we observed significantly higher FGF9 transcript levels in MPM tumors compared with pleura and lung normal tissue ( $P < 0.0001$ ). Therefore, similar to our observation in the MPM cell lines, a subset of patient samples also demonstrates high levels of FGF9 expression.

### **Modulation of FGF/FGFR function in MPM lines**

A possible premise for the observed sensitivity of MPM lines that express high levels of FGF9 would be activation of the FGFR3 receptor kinase in an autocrine loop and subsequent engagement of pro-survival downstream signaling pathways. Indeed, a comparison of phosphorylation status of 42 receptor tyrosine kinases between a small sample of MPM cell lines demonstrated increased phosphorylation of FGFR3 in the sensitive line H2795 but not in resistant lines Met-5A and NCI-H28 (Fig. 3C).

To further confirm a critical role for FGFR3, this transcript was silenced by siRNA in a panel of MPM cell lines and the direct effect on cell viability was measured. Transient siRNA-mediated silencing of the FGFR3 transcript reduced cell viability in all 3 FGFR inhibitor-sensitive cell lines, but not in the FGFR inhibitor-resistant lines. This indicates a dependency on FGFR3 mediated signaling of the FGFR inhibitor-sensitive lines (Fig. 3D). As would be expected, inhibition of FGFR3 by the specific inhibitors AZD4547 and BJJ398 decreased pERK levels (Fig. 3E), and this was also seen following siRNA-mediated silencing of FGFR3 in H2795 and MSTO-211H (Fig. 3F). The addition of FGF9 ligand to MPM cells lacking baseline FGFR3 activation was able to induce phosphorylation of FGFR3 and a change in the growth kinetics of this cell line in a dose-dependent fashion (Supplementary Fig. S5).

### **Role of BAP1 in modulating FGF pathway signaling**

Although we failed to identify genomic alterations in any member of the FGFR family that might explain the sensitivity to FGFR inhibition, we reasoned that this dependency might also be the consequence of other gene aberrations up- or downstream of FGFR3 signaling. We evaluated the gene expression and mutation database for other statistical associations explaining sensitivity to the FGFR inhibitor AZD4547 in the panel of MPM cell lines. We focused on driver mutations or copy-number alterations in three of the most frequently mutated genes in MPM, namely, *BAP1*, *NF2*, and *CDKN2A* [7]. We detected a weak but nonsignificant association between AZD4547 sensitivity and *BAP1* mutations in the sensitive cell lines (Fig. 4A). Given that loss of BAP1 protein expression might also occur through nonmutational mechanisms as previously described [21], we additionally characterized BAP1 protein status in these lines by Western blot analysis (Supplementary Figs. S3 and S4). When sensitivity to the AZD4547 was correlated with BAP1 protein expression (low/absent vs. expressed), there was a significant correlation between loss of BAP1 expression

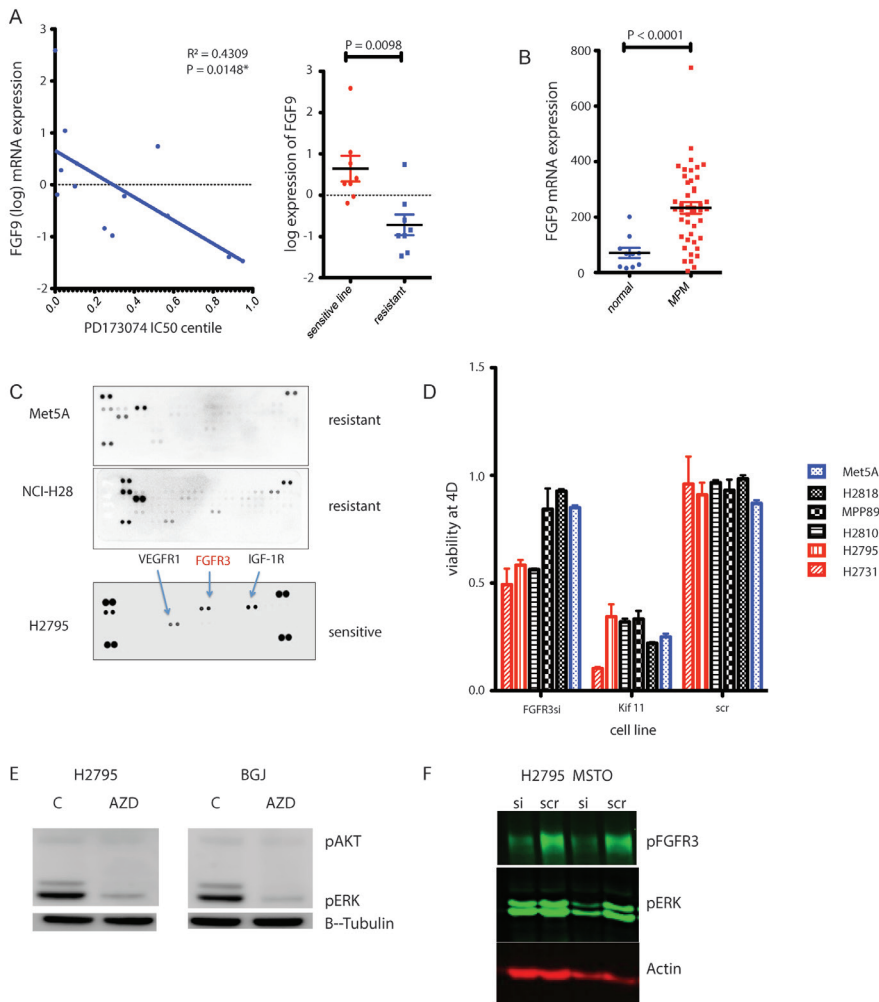


**Figure 3. FGFR inhibitor sensitivity is mediated by FGF axis signaling through FGF9 and FGFR3. A)** Scatterplot depicting sensitivity to FGFR inhibitor PD-173074 as a function of expression of FGF9. mRNA. Y-axis depicting log mRNA expression of FGF9 and x-axis showing centile of IC50 to PD173074 of individual MPM cell line in cell line screen. High FGF9 gene expression is significantly correlated to high sensitivity to FGFR inhibition. Right hand scatterplot showing FGF9 expression correlates with sensitivity to AZD4547. **B)** Expression of FGF9 in a set of MPM tumors, compared with normal lung and pleura, derived from GEO dataset GSE2549. The mean expression in MPM tumors is significantly higher than that of normal lung and pleura. **C)** Phospho-RTK array reveals phosphorylated-FGFR3 in FGFR inhibitor-sensitive cell line H2795 that is absent in two resistant lines (NCI-H28 and Met5a). **D)** Cell viability of MPM cell lines after silencing of the FGFR3 transcript demonstrates reduced viability of FGFR inhibitor-sensitive cell lines H2795, H2810, and H2731 compared with FGFR inhibitor-resistant lines Met5A, NCI-H2052, H2810, and MPP89. Viability at 4 days post transfection is compared with Kif11-positive control siRNA and scrambled negative control. **E)** Modulation of pERK signaling in H2795 cell line following 6 hours of exposure to DMSO (C) or 500 nmol/L AZD4547 or DMSO and 100 nmol/L BGJ398. **F)** siRNA-mediated knockdown of pFGFR3 in H2795 and MSTO211H, showing effect on pFGFR3 and pERK versus scrambled control.

and sensitivity ( $P=0.0208$ ; Fig. 4B).

### **Functional consequences of BAP1 modulation on FGFR signaling.**

Since silencing FGFR3 reduced cell viability in a subset of MPM lines, we next investigated whether this dependency on FGFR signalling was regulated by BAP1. BAP1 is a nuclear deubiquitinating enzyme with many unelucidated functions that might include modulation of the FGFR pathway. Silencing of BAP1 expression resulted in increased phosphorylation of FGFR3 (Figure 4C). Conversely, restoring BAP1 expression in the BAP1 null MPM line (Figure 4D) H226 resulted in a decrease in pFGFR and a modest increase in resistance to the FGFR inhibitor, AZD4547 (Figure 4E).

We observed increased expression at the protein level in the *BAP1* mutant cell lines of other RTK receptor genes and their appropriate ligands also known to be important in cell survival signaling in MPM such as PDGFRB, IGF1-R and MET [22] using phospho-RTK arrays (Supplementary Fig. S4A and S4B). The H226-null MPM cell line was transfected with a wild-type BAP1 construct and a functionally inactive C91A-mutant BAP1 construct. Gene expression analysis on these two lines was performed and Signaling Pathway Impact Analysis (SPIA) of the data (Supplementary Table S) demonstrated that among the most significantly activated pathways in BAP1-inactive cells is the “Bladder Cancer” pathway including FGFR3 (arrow, Supplementary Fig. S6A) illustrated in Supplementary Figure S6B [23]. In summary, the gene expression analysis demonstrates that BAP1 loss of function is associated with a transcriptional response upregulating not only FGFR signaling but also other RTKs such as PDGFRB, CMET and IGF1R, that may be important mediators of cell growth and survival. However, only FGFR inhibitors showed a significant viability effect as single agents. We analyzed gene expression data from a study of 51 mesothelioma tumor samples to see if a similar effect on the FGFR pathway was seen *in vivo* (40 *BAP1* wild-type and 11 mutant; GEO GSE29354; ref. [24]). Amongst members of the FGFR signaling family, *BAP1*-mutant tumors did indeed demonstrate increased expression of FGF18, FGFR2, and FGFR3 relative to *BAP1* wild-type tumors (Supplementary Table). To explore this association further in human tumors, we analyzed the available TCGA data and looked for the incidence of genetic and mRNA alterations of these genes in MPM tumors by *BAP1* status (Fig. 4F). This showed the majority of dysregulation (10 of 14) events in FGF9, FGF18, and FGFR3 occurred in the context of BAP1 gene of mRNA dysregulation.

### **FGFR inhibition in MPM xenograft model**

To assess the *in vivo* efficacy of targeting FGFR in MPM, we established a xenograft model using the FGFR inhibitor-sensitive MPM lines H2795 and MSTO-211H. Mice were treated with AZD4547, a selective inhibitor of FGFR1/2/3, which is currently being evaluated in clinical trials. We observed that treatment with AZD4547 resulted in significant growth

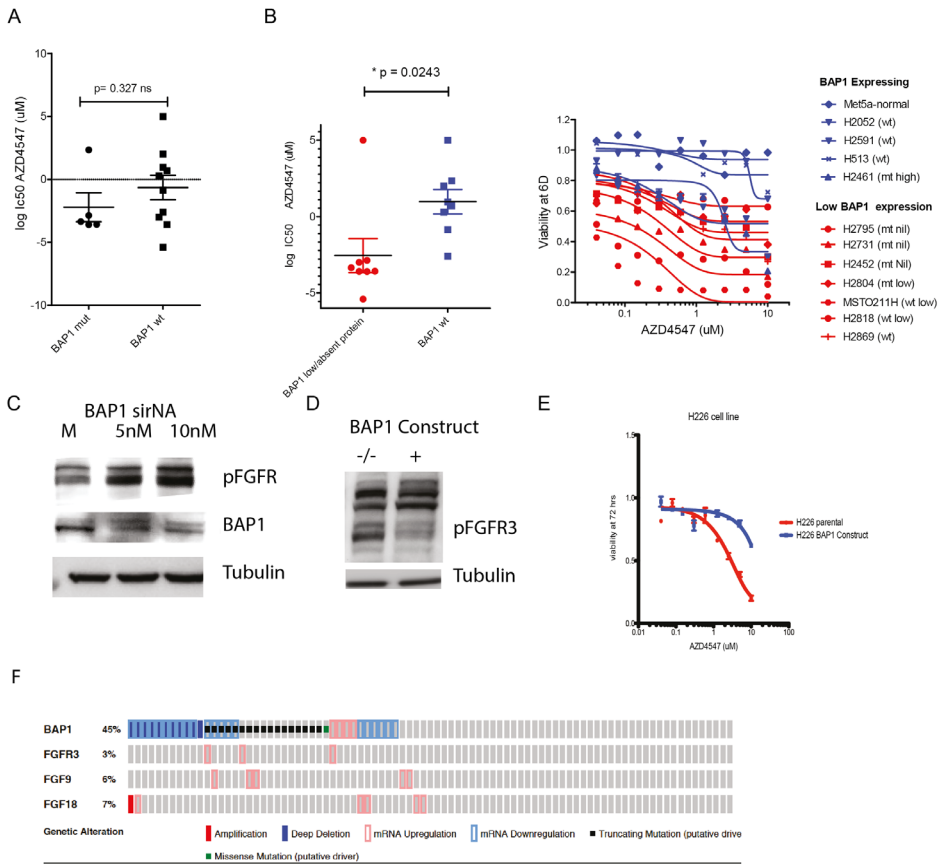


**Figure 4. Loss of BAP1 protein expression is correlated to FGFR inhibitor sensitivity.** **A)** Sensitivity to FGFR inhibitor AZD4547—expressed as  $\log IC_{50}$  value—of cell lines, grouped according to BAP1 mutation status. The mean  $\log IC_{50}$  value is not significantly different between the two groups. **B)** Sensitivity to FGFR inhibitor AZD4547 according to BAP1 protein expression. Red are cell lines with low or absent BAP1 protein. Blue lines have normal BAP1 protein expression. Sensitivity (left) is expressed as  $\log IC_{50}$  value (y-axis). The difference between the two groups is statistically significant. Cell viability (right) of different mesothelioma lines (y-axis) after treatment with FGFR inhibitor AZD4547 (x-axis). wt, wild-type; mt, mutant; high, high protein expression; low, low protein expression; nil, no protein expression. Right-hand panel showing dose–response curves of MPM cell lines treated with FGFR inhibitor AZD4547. Cell lines in red are lines with low or absent BAP1 protein expression. Blue lines have normal BAP1 protein expression. **C)** SiRNA-mediated depletion of BAP1 in H2052 at increasing siRNA doses of 5 and 10 nmol/L versus mock transfected (M) control. Western blot comparing pFGFR3 and BAP1 expression at these conditions. Tubulin as loading control. **D)** BAP1 overexpression in BAP1-null cell line H226. Western blot of BAP1 construct versus parental cell line baseline pFGFR levels with tubulin as loading control. **E)** Cell viability after treatment with increasing doses of FGFR inhibitor AZD4547 in parental cell line H226 BAP1-null (red) and in the same cell line with BAP1 construct (red). BAP1 overexpression increases cell viability after FGFR inhibition. **F)** Co-occurrence of somatic mutations in BAP1 and FGFR family members in MPM tumors in the TCGA cohort.

inhibition in the H2795- and MSTO-211H-derived tumors (Fig. 5A). Furthermore, AZD4547 treated tumors showed a reduction in pERK signaling by immunohistochemistry compared with vehicle control-treated tumors (Fig. 5B), indicating target engagement by the drug in this model. Caspase activation was also seen in drug-treated tumors suggesting apoptosis (Supplementary Fig. S7).

### Combination therapeutic screen

As the single-agent efficacy of FGFR inhibition was seen only in a subset of MPM cell lines, and because persistent pAKT pathway activation was seen in cell lines not responsive to FGFR inhibition, we hypothesized that a combination screen utilizing a PI3 kinase inhibitor may reveal useful synergies. We undertook an anchor-based combination screen in 15 MPM

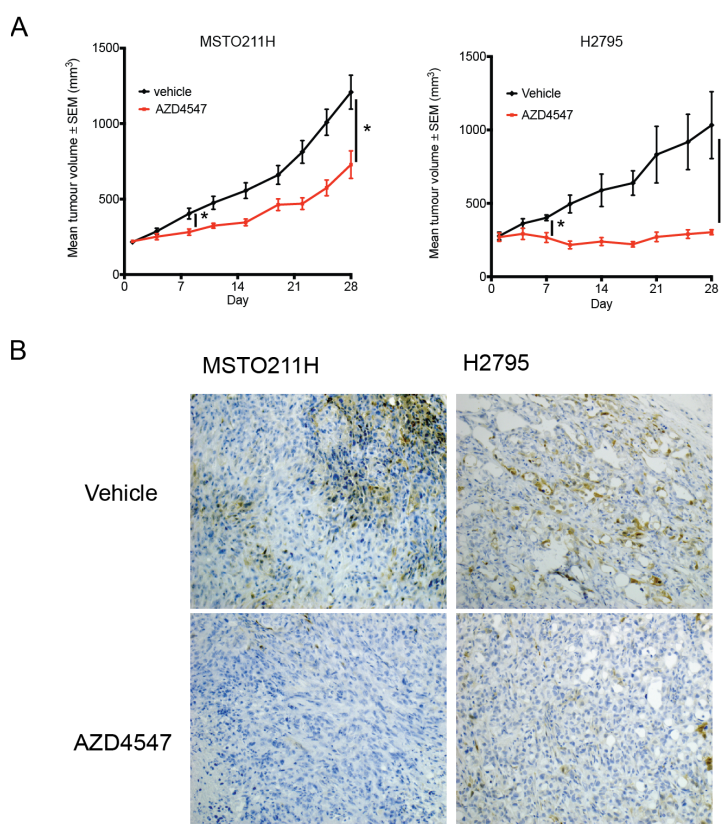


**Figure 5. Xenograft mouse model shows FGFR inhibition efficacy in vivo.** **A)** Xenograft mouse model using mesothelioma cell lines H2795 and MSTO211H. Mean tumor volume is depicted on the y-axis as a function of time (x-axis). Red lines indicate tumor growth in mice treated with FGFR inhibitor AZD4547, while the black lines indicate growth in vehicle-treated mice. **B)** Immunohistochemistry of AZD4547-versus vehicle control-treated xenograft tumors. ppERK expression in representative tumors in drug-treated versus vehicle control groups.

cell lines using 95 small-molecule inhibitors (see supplementary Table for details) selected to target many critical pathways in cancer, both as single agents and in combination with a fixed dose of the PI3 Kinase inhibitor AZD6482. The resulting difference in area under the curve (AUC) between single agent small-molecule inhibitor and the combination with AZD6482 was used to calculate synergy. The most recurrent synergistic interactions were seen with IGF1R inhibitor BMS-536924 and FGFR inhibitor PD-173074 (Supplementary Fig. S8A) with synergy observed in seven and six of 15 lines, respectively. Supplementary Fig. S8B shows a validation dose-response curve of the FGFRi-resistant NCI-H28 cell line showing minimal effect of BMS-536824 or AZD6482 alone, but reduced viability and pAKT reduction with the combination. This cytotoxicity is not seen in the mesothelial control cell line Met5a, suggesting that the synergy is not generic but cell line specific.

## Discussion

Because MPM is a rare and heterogeneous tumor, it is notoriously difficult to identify and characterize responding subgroups in clinical trials. Our work illustrates the application and possibilities of comprehensive pharmacogenomic profiling approaches in intractable cancers such as MPM. The finding of FGFR inhibitor sensitivity in a subgroup of immortalized MPM cell lines represents a potentially novel therapeutic approach for this tumor type. As immortalized cell lines may undergo genetic drift, we also confirmed our findings in primary mesothelioma early-passage lines.

Dysregulation of the FGFR pathway has been described in many cancer types [25, 26]. FGF9 signaling through FGFR3 has been shown to have a role in the development and progression of tumor cells in mouse models for NSCLC and prostate cancer [27]. In MPM cell line models, we observed that high levels of the ligand FGF9 were strongly correlated with sensitivity to the FGFR inhibitors PD-173074 and AZD4547. We hypothesize that the effects of FGF9 are mediated through FGFR3 signaling, as illustrated by modulation of downstream ERK phosphorylation upon chemical inhibition with small-molecule inhibitors of FGFR3 and knockdown of FGFR3. FGFR3 is conversely not phosphorylated in cell lines insensitive to FGFRi, and this phosphorylation can be induced by the addition of synthetic FGF9 ligand. Interestingly, there was variability in FGF9 mRNA expression levels among the MPM cell lines, similar to what is observed in tumors in previously published studies. Recently, other groups demonstrated efficacy of FGFR inhibition in preclinical models of MPM mediated by other FGF-pathway members such as FGFR1 [18, 28, 29]. We confirm the efficacy of a clinically utilized FGFR inhibitors including AZD4547 *in vivo* in MPM xenograft models. Furthermore, since undertaking these studies, early-phase clinical work with pharmacokinetic data has been published [30, 31] on AZD4547 and BGJ398. These have confirmed that the doses used in the *in vitro* work (100 nmol/L to  $\mu$ mol/L) here are achievable in plasma *in vivo* and are

able to modulate the target, with pharmacodynamic end points of target engagement with FRS2 downregulation and changes in serum phosphate levels seen.

FGF receptors and ligands are being targeted in clinical trials by both selective and nonselective FGFR TKI's and monoclonal antibodies [32] and AZD4547 has shown modest clinical activity in tumors with FGFR pathway aberrant activation [33]. In MPM dovitinib, a multitargeting kinase inhibitor with activity against FGFR has been trialed and has failed in small cohort of patients with MPM [34]. Because the data across tumor types demonstrate only a small group of patients responds to FGFR inhibition, it is crucial to find biomarkers that predict response to FGFR inhibition. Guagnano et al. integrated genomic and transcriptomic data of about 500 tumor cell lines with drug-sensitivity data to find predictive biomarkers for response to FGFR inhibitor NVP-BGJ398. A genetic alteration in one of the four FGF receptors was found in 7% of cell lines, but only about half of the cell lines with such an alteration was found to be sensitive [35].

We did not find any mutation, amplification, or fusion transcripts of the FGFR family in the inhibitor-sensitive MPM cell lines. The genes that were most recurrently altered in our MPM cell lines include *CDKN2A*, *BAP1* and *NF2*. The frequency at which these genes were mutated is broadly similar to those previously described in clinical MPM samples [6, 7].

We show that loss of *BAP1* expression was associated with sensitivity to FGFR inhibition. This finding was further validated with modulation of pFGFR signaling and dose-response kinetics to FGFR inhibition following siRNA-mediated knockdown and *BAP1* overexpression in MPM cell lines. Caveats with this association were also observed: NCI-H28 was one of the most resistant cell lines to FGFR inhibition but carried a *BAP1* homozygous deletion, suggesting that *BAP1* loss may enrich for FGFR inhibitor-sensitive cell lines but that some heterogeneity of drug response may still be observed. *BAP1* (BRCA-associated protein 1) is a nuclear deubiquinating enzyme that controls gene expression by interaction with numerous transcription factors and other complexes, including those of the double strand DNA-break repair machinery [36]. *BAP1* thus influences cell-cycle progression [37] and double-strand DNA break repair [38]. We show here that its loss may also affect gene expression of FGF pathway members, thereby enhancing signaling through this pathway.

The *BAP1* gene is inactivated by somatic mutation in 23% to 64% of patients with MPM and between 1% to 47% in other tumor types [24, 39-43]. Furthermore, *BAP1* protein levels are undetectable in about 25% of MPM with normal *BAP1* gene status, likely by epigenetic modification [24]. *BAP1* loss was observed to enrich for FGFR inhibitor-sensitive MPM lines, and expression of C91 hydrolase inactive mutant versus wild-type *BAP1* protein in the H226 cell line induced activation of FGFR3 signaling. We hypothesized that inactivation of *BAP1*

in MPM, possibly through its function as a ubiquitin hydrolase, induces changes in gene expression of both FGF family ligands and receptors to stimulate cell growth and survival.

We performed a combination drug screen to assess the impact of novel combinations of targeted therapies on MPM cell lines. On the 15 MPM cell lines screened, we found that FGFR and IGF1R inhibitors were the most recurrently synergistic with the PI3-kinase inhibitor AZD6482. This is the first time, to our knowledge, that both a single agent and combination therapeutic screen have been performed, which point to the primacy of the FGFR signaling pathway in MPM. Interestingly, one of the most resistant cell lines to FGFR inhibition was amenable to treatment with AZD6482 plus IGF1R inhibition with evidence of ablation of pAKT with the combination of drugs but not with either alone, implying true synergy. Previous studies have identified that multiple RTK's are active in MPM [14], and this has provided some rationale to consider combination therapies to overcome innate resistance to targeted therapies. It is also interesting to speculate as to whether IGF1R plus PI3K inhibition would be of use in acquired resistance to FGFR inhibitors.

## **Conclusion**

High-throughput drug screening revealed a subset of both immortalized and primary mesothelioma cell lines to be highly sensitive to FGFR-inhibition. This sensitivity was mediated through FGFR3 and was associated with loss of BAP1 protein expression. The high incidence of BAP1 protein loss in MPM tumors implies potential benefit from FGFR inhibition for a substantial subset of this patient group. In addition, our anchor-based screens revealed synergistic combinations that helped to overcome innate resistance to FGFR inhibition.

## References

1. van Meerbeeck, J.P., et al., *Malignant pleural mesothelioma: the standard of care and challenges for future management*. Crit Rev Oncol Hematol, 2011. **78**(2): p. 92-111.
2. Frank, A.L. and T.K. Joshi, *The global spread of asbestos*. Ann Glob Health, 2014. **80**(4): p. 257-62.
3. Baas, P., et al., *Malignant pleural mesothelioma: ESMO Clinical Practice Guidelines for diagnosis, treatment and follow-up*. Ann Oncol, 2015. **26** Suppl 5: p. v31-9.
4. Vogelzang, N.J., et al., *Phase III study of pemetrexed in combination with cisplatin versus cisplatin alone in patients with malignant pleural mesothelioma*. J Clin Oncol, 2003. **21**(14): p. 2636-44.
5. Pinton, G., et al., *Therapies currently in Phase II trials for malignant pleural mesothelioma*. Expert Opin Investig Drugs, 2013. **22**(10): p. 1255-63.
6. Ladanyi, M., et al., *New strategies in pleural mesothelioma: BAP1 and NF2 as novel targets for therapeutic development and risk assessment*. Clin Cancer Res, 2012. **18**(17): p. 4485-90.
7. Bueno, R., et al., *Comprehensive genomic analysis of malignant pleural mesothelioma identifies recurrent mutations, gene fusions and splicing alterations*. Nat Genet, 2016. **48**(4): p. 407-16.
8. Shapiro, I.M., et al., *Merlin deficiency predicts FAK inhibitor sensitivity: a synthetic lethal relationship*. Sci Transl Med, 2014. **6**(237): p. 237ra68.
9. Govindan, R., et al., *Gefitinib in patients with malignant mesothelioma: a phase II study by the Cancer and Leukemia Group B*. Clin Cancer Res, 2005. **11**(6): p. 2300-4.
10. Mathy, A., et al., *Limited efficacy of imatinib mesylate in malignant mesothelioma: a phase II trial*. Lung Cancer, 2005. **50**(1): p. 83-6.
11. Baas, P., et al., *Thalidomide in patients with malignant pleural mesothelioma*. Lung Cancer, 2005. **48**(2): p. 291-6.
12. Fennell, D.A., et al., *Phase II clinical trial of first or second-line treatment with bortezomib in patients with malignant pleural mesothelioma*. J Thorac Oncol, 2012. **7**(9): p. 1466-70.
13. Krug, L.M., et al., *Vorinostat in patients with advanced malignant pleural mesothelioma who have progressed on previous chemotherapy (VANTAGE-014): a phase 3, double-blind, randomised, placebo-controlled trial*. Lancet Oncol, 2015. **16**(4): p. 447-56.
14. Menges, C.W., et al., *A Phosphotyrosine Proteomic Screen Identifies Multiple Tyrosine Kinase Signaling Pathways Aberrantly Activated in Malignant Mesothelioma*. Genes Cancer, 2010. **1**(5): p. 493-505.
15. Irizarry, R.A., et al., *Exploration, normalization, and summaries of high density oligonucleotide array probe level data*. Biostatistics, 2003. **4**(2): p. 249-64.
16. Hanzelmann, S., R. Castelo, and J. Guinney, *GSVA: gene set variation analysis for microarray and RNA-seq data*. BMC Bioinformatics, 2013. **14**: p. 7.
17. Iorio, F., et al., *A Landscape of Pharmacogenomic Interactions in Cancer*. Cell, 2016. **166**(3): p. 740-754.
18. Marek, L.A., et al., *Nonamplified FGFR1 is a growth driver in malignant pleural mesothelioma*. Mol Cancer Res, 2014. **12**(10): p. 1460-9.
19. Zhang, X., et al., *Receptor specificity of the fibroblast growth factor family. The complete mammalian FGF family*. J Biol Chem, 2006. **281**(23): p. 15694-700.
20. Gordon, G.J., et al., *Identification of novel candidate oncogenes and tumor suppressors in malignant pleural mesothelioma using large-scale transcriptional profiling*. Am J Pathol, 2005. **166**(6): p. 1827-40.
21. Shah, A.A., T.D. Bourne, and R. Murali, *BAP1 protein loss by immunohistochemistry: a potentially useful tool for prognostic prediction in patients with uveal melanoma*. Pathology, 2013. **45**(7): p. 651-6.
22. Brevet, M., et al., *Coactivation of receptor tyrosine kinases in malignant mesothelioma as a rationale for combination targeted therapy*. J Thorac Oncol, 2011. **6**(5): p. 864-74.
23. Tarca, A.L., et al., *A novel signaling pathway impact analysis*. Bioinformatics, 2009. **25**(1): p. 75-82.
24. Bott, M., et al., *The nuclear deubiquitinase BAP1 is commonly inactivated by somatic mutations and 3p21.1 losses in malignant pleural mesothelioma*. Nat Genet, 2011. **43**(7): p. 668-72.
25. Dienstmann, R., et al., *Genomic aberrations in the FGFR pathway: opportunities for targeted therapies in solid tumors*. Ann Oncol, 2014. **25**(3): p. 552-63.
26. Helsten, T., et al., *The FGFR Landscape in Cancer: Analysis of 4,853 Tumors by Next-Generation Sequencing*. Clin Cancer Res, 2016. **22**(1): p. 259-67.
27. Suzuki, T., et al., *Multiple roles of extracellular fibroblast growth factors in lung cancer cells*. Int J Oncol, 2015. **46**(1): p. 423-9.
28. Schelch, K., et al., *Fibroblast growth factor receptor inhibition is active against mesothelioma and synergizes with radio- and chemotherapy*. Am J Respir Crit Care Med, 2014. **190**(7): p. 763-72.

29. Plones, T., et al., *Absence of amplification of the FGFR1-gene in human malignant mesothelioma of the pleura: a pilot study.* BMC Res Notes, 2014. **7**: p. 549.
30. Nogova, L., et al., *Evaluation of BGJ398, a Fibroblast Growth Factor Receptor 1-3 Kinase Inhibitor, in Patients With Advanced Solid Tumors Harboring Genetic Alterations in Fibroblast Growth Factor Receptors: Results of a Global Phase I, Dose-Escalation and Dose-Expansion Study.* J Clin Oncol, 2017. **35**(2): p. 157-165.
31. Gavine, P.R., et al., *AZD4547: an orally bioavailable, potent, and selective inhibitor of the fibroblast growth factor receptor tyrosine kinase family.* Cancer Res, 2012. **72**(8): p. 2045-56.
32. Touat, M., et al., *Targeting FGFR Signaling in Cancer.* Clin Cancer Res, 2015. **21**(12): p. 2684-94.
33. Paik, P.K., et al., *A Phase Ib Open-Label Multicenter Study of AZD4547 in Patients with Advanced Squamous Cell Lung Cancers.* Clin Cancer Res, 2017. **23**(18): p. 5366-5373.
34. Laurie, S.A., et al., *A phase II trial of dovitinib in previously-treated advanced pleural mesothelioma: The Ontario Clinical Oncology Group.* Lung Cancer, 2017. **104**: p. 65-69.
35. Guagnano, V., et al., *FGFR genetic alterations predict for sensitivity to NVP-BGJ398, a selective pan-FGFR inhibitor.* Cancer Discov, 2012. **2**(12): p. 1118-33.
36. Yu, H., et al., *The ubiquitin carboxyl hydrolase BAP1 forms a ternary complex with YY1 and HCF-1 and is a critical regulator of gene expression.* Mol Cell Biol, 2010. **30**(21): p. 5071-85.
37. Eletr, Z.M. and K.D. Wilkinson, *An emerging model for BAP1's role in regulating cell cycle progression.* Cell Biochem Biophys, 2011. **60**(1-2): p. 3-11.
38. Yu, H., et al., *Tumor suppressor and deubiquitinase BAP1 promotes DNA double-strand break repair.* Proc Natl Acad Sci U S A, 2014. **111**(1): p. 285-90.
39. Yoshikawa, Y., et al., *Frequent inactivation of the BAP1 gene in epithelioid-type malignant mesothelioma.* Cancer Sci, 2012. **103**(5): p. 868-74.
40. Nasu, M., et al., *High Incidence of Somatic BAP1 alterations in sporadic malignant mesothelioma.* J Thorac Oncol, 2015. **10**(4): p. 565-76.
41. Murali, R., T. Wiesner, and R.A. Scolyer, *Tumours associated with BAP1 mutations.* Pathology, 2013. **45**(2): p. 116-26.
42. Lu, C., et al., *The genomic landscape of childhood and adolescent melanoma.* J Invest Dermatol, 2015. **135**(3): p. 816-23.
43. Carbone, M., et al., *Combined Genetic and Genealogic Studies Uncover a Large BAP1 Cancer Syndrome Kindred Tracing Back Nine Generations to a Common Ancestor from the 1700s.* PLoS Genet, 2015. **11**(12): p. e1005633.

## Supplementary figures and tables

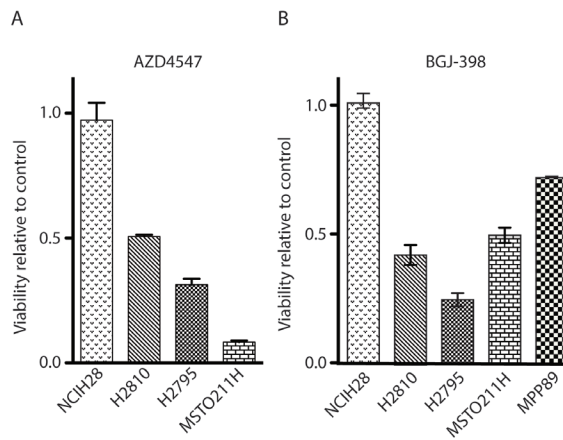


**Fig. S1. A subset of MPM cell lines respond to FGFR inhibition.** Cell viability of selected mesothelioma cell lines (NCI-H28, H2810, H2795, MSTO-211H and MPP-89) after 72 hours of treatment with **A)** AZD4547 at a fixed dose of 500 nmol/L and **B)** BGJ398 at a fixed dose of 300 nmol/L

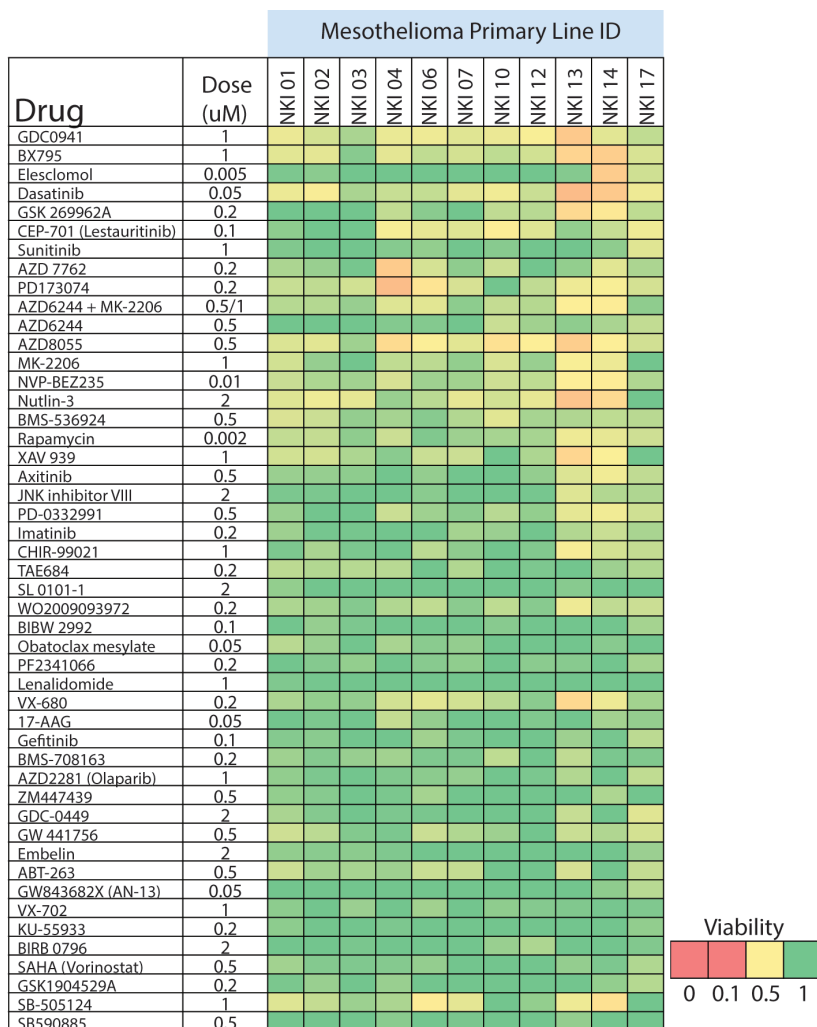


**Fig. S2. A subset of pleural fluid derived early passage primary cultures (EPL) respond to FGFR inhibition.** Cell viability of 11 early passage primary cultures (columns) after treatment with a fixed dose of 48 small molecular inhibitors (rows), depicted in a color scale (green: 100% cell viability; red: 0% cell viability).

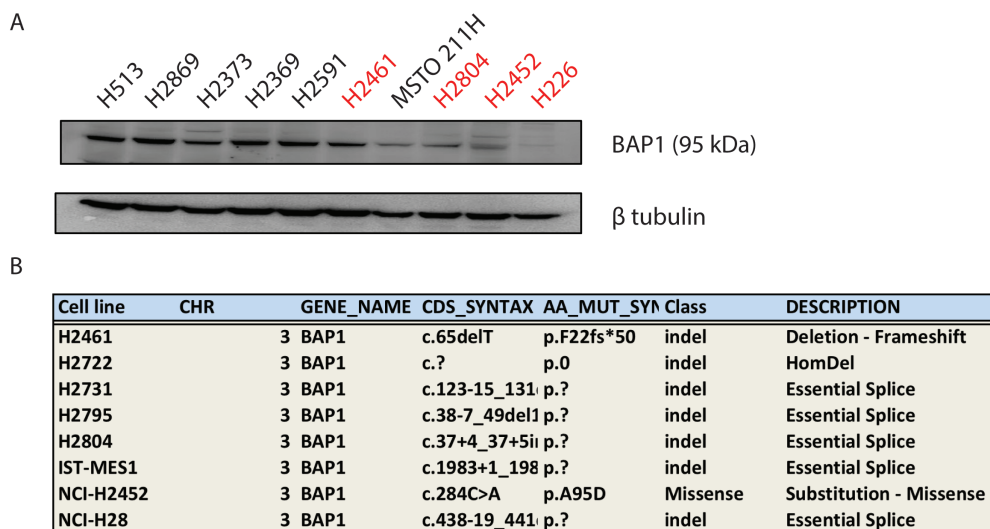


**Fig. S3. BAP1 mutation status does not correlate fully with protein expression. A)** Western Blot showing BAP1 protein expression in several MPM cell lines, both BAP1 wild type (black) and mutant lines (red). Beta tubulin represents the protein loading control. **B)** List of somatic mutations in BAP1 seen in MPM cell lines

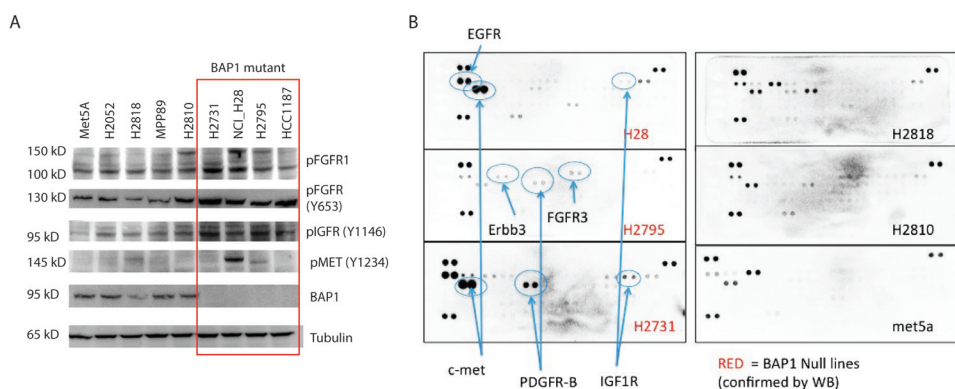


**Fig. S4. BAP1 null cell lines show increased activity of multiple tyrosine kinases. A)** Western Blot showing BAP1 protein expression in several MPM cell lines as well as activation in IGFR, MET, and FGFR. **B)** Phospho RTK array panel showing baseline RTK activation of BAP1 mutant (highlighted in red) versus wild type mesotheliomas.

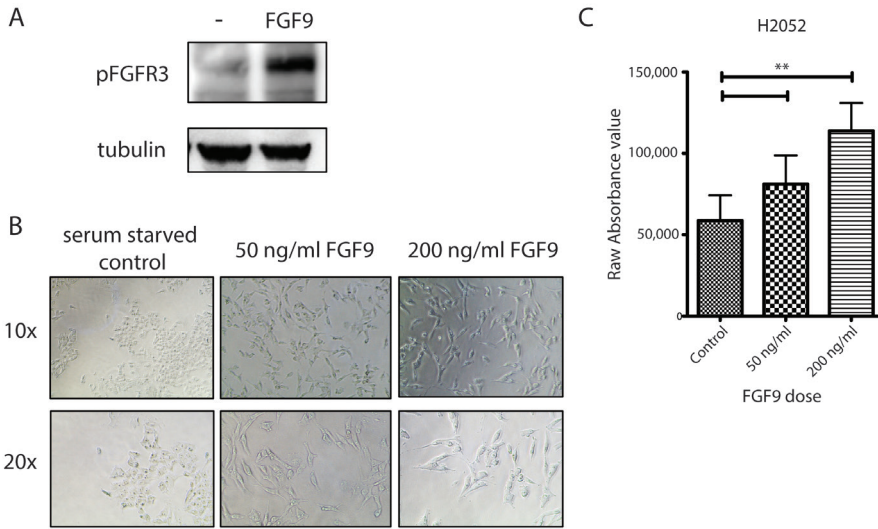


**Fig. S5. FGF 9 activated FGFR3 modulated growth and phenotype. A)** Western Blot of pFGFR in serum starved H2052 MPM cell line at baseline and with the addition of 50 ng/mL of recombinant FGF9 ligand after 1 hour. **B)** Light microscopy of H2052 cell line under serum starved conditions, and with the addition of FGF9 ligand at varying concentrations. **C)** Comparative viability of H2052 by syto 60 assay at baseline and following the addition of 50 ng/mL and 200 ng/mL FGF9 ligand.



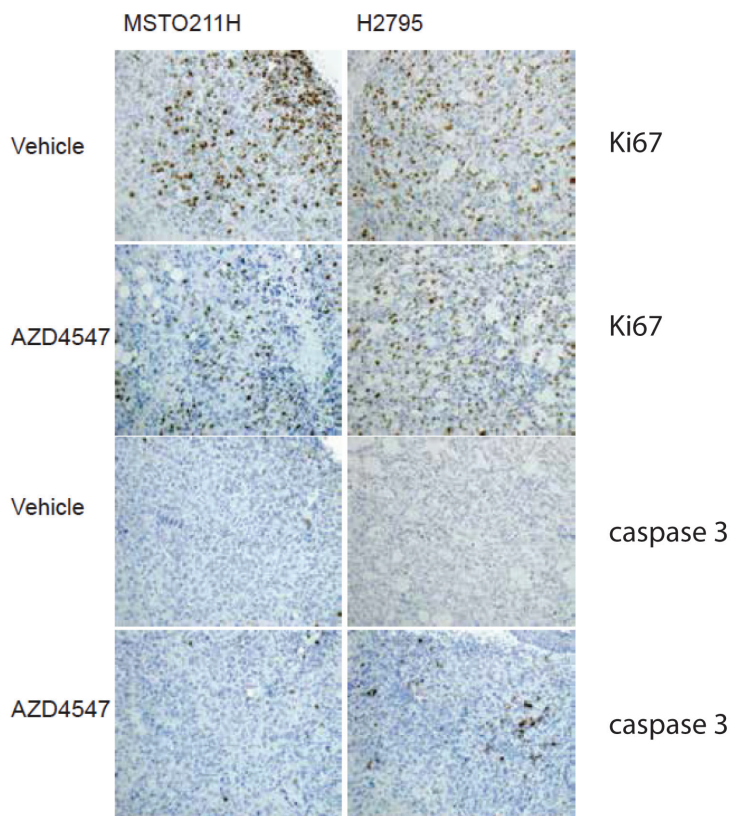


**Fig. S7. Xenograft tumor immunohistochemistry.** Immunohistochemistry for Caspase 3 and Ki67 in MPM xenograft tumors during vehicle control and AZD4547 treated conditions.

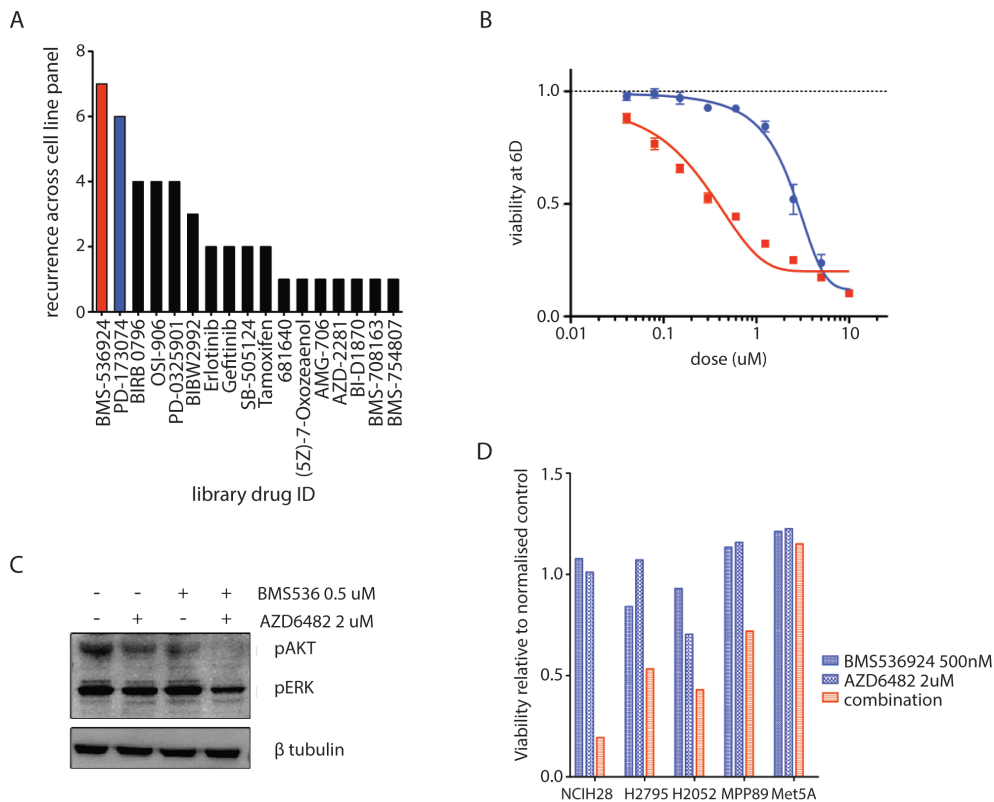


**Fig. S8. Combination drug screen of PI3Kinase inhibitor plus drug library in MPM cell lines. A)** Bar chart showing recurrent synergistic events in a combination screen PI3K inhibitor AZD6482 plus 95 small molecule inhibitors across 15 MPM cell lines. Most recurrent inhibitor PD-173074 ( $n=6$  cell lines). **B)** Validation of synergy between IGF1R inhibitor and PI3K inhibitor AZD6482 in NCO-H28 (FGFRi resistant cell line). Dose-response kinetics of BMS-536924 alone (blue) or with fixed dose (2uM) of AZD6482 (red). **C)** Immunoblot of NCI-H28 FGFRi resistant cell line treated with a combination of IGF1R inhibitor BMS-536924 and PI3L inhibitor AZD6482 showing loss of pAKT with combination treatment. **D)** Cell Titer Blue quantification of 2 week clonogenic survival assay of 5 MPM cell lines with EGF1R inhibitor BMS-536924 alone and in combination with PI3K inhibitor AZD6482.

**Table S1.** List of compounds used in the chemical inhibitor screen.

Identifier	Name	Synonyms	Brand name	Action	Clinical Stage	Putative Target	Targeted process/pathway
1	Erlotinib	AY-22989, Siroliimus, WY-090217	Tarceva	targeted	clinically approved	EGFR	EGFR signaling
3	Rapamycin		Rapamune	targeted	clinically approved	MTOR	TOR signaling
5	Sunitinib		Sutent	targeted	clinically approved	PDGFRB, KDR, KIT, FLT3	RTK signaling
6	PHA-665752	zLLL		targeted	experimental	MET	RTK signaling
9	MG-132	BMS-181339-01		targeted	experimental	Proteasome	other
11	Paclitaxel	11-deoxojervine	Taxol	cytotoxic	clinically approved	Microtubules	cytoskeleton
17	Cyclopamine			targeted	experimental	SMO	other
29	AZ628	BAY-43-9006		targeted	experimental	BRAF	ERK MAPK signaling
30	Sorafenib	MK-045, MK-0457, VX-68	Nexavar	targeted	clinically approved	PDGFRB, KDR, PDGFRA, KIT, FLT3	RTK signaling
32	VX-680	STI-571	MK-0457	targeted	in clinical development	AURKA, AURKB, AURKC, FLT3, ABL1, JAK2	mitosis
34	Imatinib	KIN001-017	Gleevec	targeted	clinically approved	ABL, KIT, PDGFR	ABL signaling
35	NVP-TAE684	PF-02341066	TAE684	targeted	experimental	ALK	RTK signaling
37	Crizotinib	Saracatinib, KIN001-045	Xalkori	targeted	in clinical development	MET, ALK	RTK signaling
38	AZD-0530	NSC 83265		targeted	in clinical development	SRC, ABL1	ABL signaling
41	S-Triyl-L-cysteine	Z-L-Norleucine-CHO		targeted	experimental	KIF11	mitosis
45	Z-LLNle-CHO	KIN001-005	na	targeted	experimental	g-secretase	other
51	Dasatinib	KIN001-013 (GNF-2 / 3-(6-(4-(trifluoromethoxy)phenylamino)pyrimidin-4-yl)benzamide)	Sprycel	targeted	clinically approved	ABL, SRC, KIT, PDGFR	ABL signaling
52	GNF-2	KIN001-019		targeted	experimental	ABL [T315I]	ABL signaling

Identifier	Name	Synonyms	Brand name	Action	Clinical stage	Putative target	Targeted process/pathway
53	GCP-60474	CINK4, KIN001-021		targeted	experimental	CDK1, CDK2, CDK5, CDK7, CDK9	cell cycle
54	CGP-082996	A770041, KIN001-111		targeted	experimental	CDK4	cell cycle
55	A-770041	KIN001-112	A770041	targeted	experimental	SRC family	other
56	WH-4-023	KIN001-123		targeted	experimental	SRC family, ABL	ABL signaling
59	WZ-1-84	KIN001-124		targeted	experimental	BMX	other
60	BI-2536	KIN001-126	NPK33-1-98-1	targeted	in clinical development	PLK1, PLK2, PLK3	mitosis
62	BMS-536924	KIN001-127	BMS-536924	targeted	experimental	IGF1R	IGFR signaling
63	BMS-509744	KIN001-128	BMS-509744	targeted	experimental	ITK	other
64	CMK		Chloromethylketone Rsk inhibitor	targeted	experimental	RSK	ERK MAPK signaling
71	Pyrimethamine		Daraprim	cytotoxic	clinically approved	Dihydrofolate reductase (DHFR)	DNA replication
83	JW-7-52-1	KIN001-139		targeted	experimental	MTOR	TOR signaling
86	A-443654	KIN001-134		targeted	experimental	AKT1, AKT2, AKT3	PI3K signaling
87	GW843682X	MS275	GW843682X (AN-13)	targeted	experimental	PLK1	mitosis
88	MS-275			targeted	in clinical development	HDAC	chromatin histone acetylation
89	Parthenolide	KIN001-135		targeted	in clinical development	NFKB1	other
91	KIN001-135			targeted	experimental	IKKE	other
94	TGX221	LDP-341, PS-341		targeted	experimental	PI3Kbeta	PI3K signaling
104	Bortezomib	XMD8-85	Velcade	targeted	clinically approved	Proteasome	other
106	XMD8-85	Seliciclib		targeted	experimental	MAP2K5 (ERK5)	other
110	Roscovitine	3-Phenyl-N-[2,2-trichloro-1-[[[8-quinolinylamino]thioxomethyl]amino]ethyl]-2-propanamide		targeted	in clinical development	CDKs	cell cycle
111	Salubrinal	Tykerb, Tyverb		targeted	experimental	GADD34-PP1C	other

119	Lapatinib	KIN001-155	Tykerb, Tyverb	targeted	clinically approved	ERBB2, EGFR	EGFR signaling
127	GSK269962A	Doxil, Rubex		targeted	experimental	ROCK1, ROCK2	cytoskeleton
133	Doxorubicin	VP-16	Adriamycin	cytotoxic	clinically approved	DNA intercalating	DNA replication
134	Etoposide	LY-188011	Etophophos	cytotoxic	clinically approved	TOP2	DNA replication
135	Gemcitabine		Gemzar	cytotoxic	clinically approved	DNA replication	DNA replication
136	Mitomycin C			cytotoxic	clinically approved	DNA crosslinker	DNA replication
140	Vinorelbine		Navelbine	cytotoxic	clinically approved	Microtubules	cytoskeleton
147	NSC-87877	ICI-176334		targeted	experimental	PTPBG (SHP-1), PTPN11 (SHP-2) ANDR (androgen receptor)	other
150	Bicalutamide	QS11	Casodex	targeted	clinically approved	ARFGAP	other
151	QS11	[2-(6,7-dimethoxyquinazolin-4-yl)-5-(pyridin-2-yl)-2H-1,2,4-triazol-3-amine]		targeted	experimental		other
152	CP466722	PKC 412		targeted	experimental		other
153	Midostaurin	CT 99021		targeted	experimental	ATM	Genome integrity
154	CHIR-99021	KIN001-192		targeted	in clinical development	KIT	RTK signaling
155	AP-24534	KIN001-193		targeted	experimental	GSK3B	WNT signaling
156	AZD6482	KIN001-204	Ponatinib	targeted	in clinical development	ABL	ABL signaling
157	JNK-9L	(KIN001-205)		targeted	in clinical development	PI3Kbeta	PI3K signaling
158	PF-562271	KIN001-206		targeted	experimental	JNK	JNK and p38 signaling
159	HG-6-64-1	JQ1		targeted	experimental	FAK	cytoskeleton
163	JQ1	JQ12		targeted	experimental	BRAFV600E, TAK, MAP4K5	ERK MAPK signaling
164	JQ12	Dimethylxalylglycine		targeted	experimental	BRD4	chromatin other
165	DMOG			targeted	experimental	HDAC	chromatin histone acetylation
166	FTI-277	AR-12		targeted	experimental	Prolyl-4-Hydroxylase Farnesyl transferase (FNTA)	other
167	OSU-03012	Shikonin		targeted	experimental	PDPK1 (PDK1)	PI3K signaling
170	Shikonin			not defined	in clinical development	unknown	other
171	AKT inhibitor VIII			targeted	in clinical development	AKT1, AKT2, AKT3	PI3K signaling

Identifier	Name	Synonyms	Brand name	Action	Clinical stage	Putative target	Targeted process/pathway
172	Embellin	FH535		targeted	in clinical development	XIAP	apoptosis regulation
173	FH535	PAC-1		not defined	experimental	unknown	other
175	PAC-1	IPA-3		targeted	in clinical development	CASP3 agonist	apoptosis regulation
176	IPA-3			targeted	experimental	PAK1, PAK2, PAK3	cytoskeleton
177	GSK-650394			targeted	experimental	SGK3	other
178	BAY 61-3606	5-Fluorouracil		targeted	experimental	SYK	other
179	5-Fluorouracil			cytotoxic	clinically approved	DNA antimetabolite	DNA replication
180	Thapsigargin			targeted	experimental	sarco-endoplasmic reticulum Ca <sup>2+</sup> -ATPases	other
182	Obatoclax Mesylate			targeted	in clinical development	BCL2, BCL2L1, MCL1	apoptosis regulation
184	BMS-754807	OSI-906	GX15-070	targeted	in clinical development	IGF1R	IGFR signaling
185	OSI-906	LG-100069, LGD-1069		targeted	in clinical development	IGF1R	IGFR signaling
186	Bexarotene		Targretin	targeted	clinically approved	Retinoic acid X family agonist	other
190	Bleomycin	DDE-28		cytotoxic	clinically approved	DNA damage	DNA replication
192	LFM-A13	GW-2580		targeted	experimental	BTK	other
193	GW-2580	VER-52296, NVP-AUY922		targeted	experimental	CSF1R (cFMS)	RTK signaling
194	AUY922	Phenformin		targeted	in clinical development	HSP90	other
196	Phenformin	Bryostatatin 1	imidodica_rbonimidi_c diamide, N-(2-ph_eny(ethyl))-NSC 339555	targeted	experimental	AAPK1 (AMPK) agonist	metabolism
197	Bryostatatin 1	GW786034		targeted	in clinical development	PRKC	other
199	Pazopanib	DacinoStat, NVP-LAQ824	Votrient	targeted	in clinical development	VEGFR, PDGFRA, PDGFRB, KIT	RTK signaling
200	LAQ824	GNF-PF-193		targeted	in clinical development	HDAC	chromatin histone acetylation

201	Epothilone B	GSK1904529A	EPO906 (ixabepilone, Patupilone)	cytotoxic	in clinical development	Microtubules	cytoskeleton
202	GSK-1904529A			targeted	experimental	IGF1R	IGFR signaling
203	BMS-345541			targeted	experimental	IKKB Farnesyl- transferase (FNTA)	other
204	Tipifarnib	Avagacestat	Zarnestra, IND58359, R115777	targeted	in clinical development	g-secretase	other
205	BMS-708163	INCB-18424		targeted	in clinical development		other
206	Ruxolitinib	AS601245	Jakafi	targeted	in clinical development	JAK1, JAK2, TYK2	other
207	AS601245	Ispinesib Mesylate		targeted	clinically approved		other
208	SB-715992			targeted	experimental	JNK	JNK and p38 signaling
211	TL-2-105			targeted	in clinical development	KIF11	mitosis
219	AT-7519	KIN001-201		targeted	experimental	CRAF	ERK MAPK signaling
221	TAK-715	KIN001-175		targeted	in clinical development	CDK9	cell cycle
222	BX-912	KIN001-167		targeted	in clinical development	p38a	JNK and p38 signaling
223	ZSTK474	KIN001-173		targeted	experimental	PDPK1 (PDK1)	PI3K signaling
224	AS605240			targeted	in clinical development	PI3K	PI3K signaling
225	Genentech Cpd 10			targeted	experimental	PI3Kgamma	PI3K signaling
226	GSK1070916			targeted	experimental	AURKA, AURKB	mitosis
228	KIN001-102	Enzastaurin		targeted	in clinical development	AURKB	mitosis
229	LY317615			targeted	experimental	AKT1	PI3K signaling
230	GSK429286A	KIN001-242		targeted	in clinical development	PRKCB (PKCbeta)	other
231	FMK			targeted	experimental	ROCK2	cytoskeleton
235	QL-XII-47			targeted	experimental	RSK	ERK MAPK signaling
238	CAL-101			targeted	experimental	BTK, BMX	other
				targeted	clinically approved	PI3Kdelta	PI3K signaling

Identifier	Name	Synonyms	Brand name	Action	Clinical stage	Putative target	Targeted process/pathway
245	UNC0638	Cabozantinib		targeted	experimental	G9a(EHMT2), GLP(EHMT1)	chromatin histone methylation
249	XL-184		Cometriq	targeted	clinically approved	VEGFR, MET, RET, KIT, FLT1, FLT3, FLT4, Tie2, AXL, CLK2, CNSK1E, FLT3, ULK1	RTK signaling
252	WZ3105			targeted	experimental	EPHB3, CAMK1	other
253	XMD14-99	Quizartinib, AC-220		targeted	experimental		RTK signaling
254	AC220			targeted	in clinical development	FLT3	RTK signaling
255	CP724714			targeted	in clinical development	ERBB2	EGFR signaling
256	JW-7-24-1			targeted	experimental	LCK	other
257	NPk76-II-72-1			targeted	experimental	PLK3	mitosis
258	STF-62247			not defined	experimental	stimulates autophagy	other
260	NG-25			targeted	experimental	MAP3K7 (TAK1)	other
261	TL-1-85			targeted	experimental	MAP3K7 (TAK1)	other
262	VX-11e			targeted	experimental	ERK	ERK MAPK signaling
263	FR-180204			targeted	experimental	ERK	ERK MAPK signaling
265	Tubastatin A			targeted	experimental	HDAC6	chromatin histone acetylation
266	Zibotentan, ZD4054	Sepantronium bromide		targeted	in clinical development	Endothelin A Receptor	other
268	YM155	XI-006		targeted	development	BIRC5 (Survivin)	apoptosis regulation
269	NSC-207895	4-(Butanoyloxymethyl)phenyl-(2E,4E,6E,8E)-3,7-dimethyl-9-(2,6,6-trimethylcyclohex-1-enyl)nona-2,4,6,8-tetraenoate		targeted	experimental	MDM4	p53 pathway
271	VNLG/124	HDAC-42		targeted	experimental	HDAC, RAR	chromatin histone acetylation
272	AR-42			targeted	in clinical development	HDAC	chromatin histone acetylation

273	CUDC-101			targeted	in clinical development	HDAC, EGFR	chromatin histone acetylation
274	PXD101, Belinostat	GSK525762A,		targeted	clinically approved	HDAC	chromatin histone acetylation
275	I-BET 151			targeted	experimental	BRD2, BRD3, BRD4	chromatin histone acetylation
276	CAY10603			targeted	experimental	HDAC6	chromatin histone acetylation
277	ABT-869	Linifanib		targeted	in clinical development	VEGFR and PDGFR family	RTK signaling
279	BIX02189			targeted	experimental	MAP2K5 (MEK5)	other
281	CH5424802			targeted	in clinical development	ALK	RTK signaling
282	EKB-569	Pelitinib		targeted	in clinical development	EGFR	EGFR signaling
283	GSK2126458	EX-8678		targeted	in clinical development	PI3K, MTOR	PI3K signaling
286	KIN001-236			targeted	experimental	TIE2	other
287	KIN001-244			targeted	experimental	PDPK1 (PDK1)	PI3K signaling
288	KIN001-055	WHI-P97, AC111GQE		targeted	experimental	JAK3, MNK1	other
290	KIN001-260	Bayer IKKb inhibitor		targeted	experimental	IKK	other
291	KIN001-266			targeted	experimental	MAP3K8 (COT)	other
292	Masitinib	AB1010		targeted	clinically approved	KIT	RTK signaling
293	MP470			targeted	in clinical development	PDGFR	RTK signaling
294	MPS-1-IN-1			targeted	experimental	MPS1	mitosis
295	NVP-BHG712			targeted	experimental	EPHB4	RTK signaling
298	OSI-930			targeted	in clinical development	KIT, VEGFR, PDGFR	RTK signaling
299	OSI-027	activebiochem A-1065		targeted	in clinical development	MTORC1/2	TOR signaling
300	CX-5461			targeted	experimental	RNA Pol I	other
301	PHA-793887			targeted	experimental	CDK-pan	cell cycle
302	PI-103			targeted	experimental	PI3Ka, PRKDC (DNAPK)	PI3K signaling
303	PIK-93			targeted	experimental	PI4K, PI3K	PI3K signaling

Identifier	Name	Synonyms	Brand name	Action	Clinical stage	Putative target	Targeted process/pathway
304	SB52334			targeted	experimental	ALK5	RTK signaling
305	TPCA-1			targeted	experimental	IKK	other
306	TG101348			targeted	in clinical development	JAK2	other
308	XL-880	GSK1363089, foretinib		targeted	in clinical development	MET	RTK signaling
309	Y-39983			targeted	experimental	ROCK	cytoskeleton
310	YM201636			targeted	experimental	FYV1	other
312	AV-951	Tivozanib		targeted	in clinical development	VEGFR	RTK signaling
326	GSK690693			targeted	experimental	AKT	PI3K signaling
328	SNX-2112			targeted	experimental	HSP90	other
329	QL-XI-92			targeted	experimental	DDR1	RTK signaling
330	XMD13-2			targeted	experimental	RIPK	other
<b>331</b>	QL-X-138			targeted	experimental	MNK2, PRKDC (DNAPK), MTOR, BTK, JAK3, CAIHK2B, CLK2, DYRK1A, MAST1, STK39	other
332	XMD15-27			targeted	experimental	LXR	other
333	T0901317			targeted	experimental	SIRT1	other
341	EX-527			targeted	experimental	CDK9	cell cycle
344	THZ-2-49			targeted	experimental	CDK9	cell cycle
345	KIN001-270			targeted	experimental	CDK9	cell cycle
346	THZ-2-102-1			targeted	experimental	CDK7	cell cycle
1001	AICAR	N1-( <i>b</i> -D-Ribofuranosyl)-5-aminoimidazole-4-carboxamide	AICAR	targeted	in clinical development	AAPK1 (AMPK) agonist	metabolism
1003	Camptothecin	7-Ethyl-10-Hydroxy-Camptothecin, SN-38	SN-38	cytotoxic	clinically approved	TOP1	DNA replication
1004	Vinblastine	Vinblastine sulphate	Vinblastine	cytotoxic	clinically approved	Microtubules	cytoskeleton

1005	Cisplatin	cis-Diammineplatinum(II) dichloride	Cisplatin	cytotoxic	clinically approved	DNA crosslinker	DNA replication
1006	Cytarabine	Ara-Cytidine, Arabinosyl Cytosine, U-19920	Cytarabine (AraC)	cytotoxic	clinically approved	DNA synthesis	DNA replication
1007	Docetaxel	RP-56976	Taxotere	cytotoxic	clinically approved	Microtubules	cytoskeleton
1008	Methotrexate		Methotrexate	cytotoxic	clinically approved	Dihydrofolate reductase (DHFR)	DNA replication
1009	ATRA	Tretinoin	Vesanoid	targeted	clinically approved	Retinoic acid and retinoid X receptor agonist	other
1010	Gefitinib	ZD-1839	Iressa	targeted	clinically approved	EGFR	EGFR signaling
1011	ABT-263			targeted	in clinical development	BCL2, BCL2L1, BCL2L2	apoptosis regulation
1012	Vorinostat	SAHA	Zolinza	targeted	clinically approved	HDAC inhibitor Class I, IIa, IIb, IV	chromatin histone acetylation
1013	Nilotinib		Tasigna	targeted	clinically approved	ABL	ABL signaling
1014	RDEA119	RDEA119		targeted	in clinical development	MAP2K1 (MEK1), MAP2K2 (MEK2)	ERK MAPK signaling
1015	CI-1040	PD-18435, PD-184352		targeted	in clinical development	MAP2K1 (MEK1), MAP2K2 (MEK2)	ERK MAPK signaling
1016	Temsirolimus	CCI-779	Torisel	targeted	clinically approved	MTOR	TOR signaling
1017	Olaparib	KU-0059436, AZD-2281	Lynparza	targeted	in clinical development	PARP1, PARP2	Genome integrity
1018	ABT-888	ABT-888		targeted	in clinical development	PARP1, PARP2	Genome integrity
1019	Bosutinib	SKI-606	Bosulif	targeted	clinically approved	SRC, ABL, TEC	ABL signaling
1020	Lenalidomide		Revlimid	targeted	clinically approved	TNFA	other
1021	Axitinib	AG-013736	Axitinib	targeted	in clinical development	PDGFR, KIT, VEGFR	RTK signaling
1022	AZD7762	AZD 7762		targeted	in clinical development	CHEK1, CHEK2	Genome integrity
1023	GW 441756			targeted	experimental	NTRK1	RTK signaling
1024	CEP-701	CEP-701	Lestaurtinib	targeted	in clinical development	FLT3, JAK2, NTRK1, RET	RTK signaling
1025	SB 216763	SB 216763		targeted	experimental	GSK3A, GSK3B	WNT signaling
1026	17-AAG	17-AAG	Telatinib	targeted	in clinical development	HSP90	other
1028	VX-702			targeted	in clinical development	p38	JNK and p38 signaling

Identifier	Name	Synonyms	Brand name	Action	Clinical stage	putative target	Targeted process/pathway
1029	AMG-706	AMG-706		targeted	in clinical development	VEGFR, RET, c-KIT, PDGFR	RTK signaling
1030	KU-55933		Motesanib Diphosphate	targeted	experimental	ATM	Genome integrity
1031	Elesclomol			targeted	in clinical development	HSP70	other
1032	Afatinib	Tovok, BIBW2992	Gilotrif	targeted	clinically approved	ERBB2, EGFR	EGFR signaling
1033	Vismodegib	GDC-0449	Erivedge	targeted	in clinical development	SMO	other
1036	PLX4720	Vemurafenib (derivative)	Zelboraf (derivative)	targeted	clinically approved	BRAF	ERK MAPK signaling
1037	BX-795	BX 795		targeted	in clinical development	TBK1, PDPK1, IKK, AURKB, AURKC	other
1038	NU-7441	NU-7432, KU-57788		targeted	experimental	PRKDC (DNAPK)	Genome integrity
1039	SL 0101-1			targeted	experimental	RSK, AURKB, PIM3	ERK MAPK signaling
1042	BIRB 0796		Doramapimod	targeted	experimental	p38, JNK2	JNK and p38 signaling
1043	JNK inhibitor VIII	JNK inhibitor VIII		targeted	experimental	JNK	JNK and p38 signaling
1046	681640,00	681640,00		targeted	experimental	WEE1, CHEK1	cell cycle
1047	Nutlin-3a	Nutlin-3a (-) enantiomer		targeted	in clinical development	MDM2	p53 pathway
1049	PD-173074	PD-173074		targeted	experimental	FGFR1, FGFR3	RTK signaling
1050	ZM-447439	ZM447439		targeted	experimental	AURKB	mitosis
1052	RO-3306			targeted	experimental	CDK1	cell cycle
1053	MK-2206			targete	in clinical development	AKT1, AKT2	PI3K signaling
1054	PD-0332991	PD-0332991		targeted	in clinical development	CDK4, CDK6	cell cycle
1057	NVP-BE2235	BEZ235		targeted	in clinical development	PI3K (Class 1) and MTORC1/2	PI3K signaling
1058	GDC0941			targeted	in clinical development	PI3K (class 1)	PI3K signaling
1059	AZD8055	AZD8055	pp242	targeted	in clinical development	MTORC1/2	TOR signaling
1060	PD-0325901	PD-0325901		targeted	in clinical development	MAP2K1 (MEK1), MAP2K2 (MEK2)	ERK MAPK signaling

1061	SB590885			targeted	experimental	ERK MAPK signaling
1062	AZD6244			targeted	in clinical development	ERK MAPK signaling
1066	AZD6482	WO2009093972		targeted	in clinical development	PI3K signaling
1067	CCT007093			targeted	experimental	PI3K signaling
1069	EHT 1864			targeted	experimental	other
1072	BMS-708163	Avagacestat		targeted	experimental	cytoskeleton
1091	BMS-536924	BMS-536924		targeted	in clinical development	other
1114	Cetuximab	Cetuximab	Erbix	targeted	experimental	IGFR signaling
1129	PF-4708671			targeted	clinically approved	EGFR signaling
1133	JNJ-26854165		Serdemetan	targeted	experimental	TOR signaling
1142	HG-5-113-01			targeted	in clinical development	p53 pathway
1143	HG-5-88-01			targeted	in clinical development	ABL signaling
1149	TW 37			targeted	experimental	EGFR signaling
1158	XMD11-85h			targeted	experimental	apoptosis regulation
1161	ZG-10			targeted	experimental	other
1164	XMD8-92			targeted	experimental	other
1166	QL-VIII-58			targeted	experimental	other
1170	CCT018159			targeted	experimental	TOR signaling
1175	AG-014699	PF-01367338		targeted	experimental	other
1192	GSK269962A	KIN001-155		targeted	experimental	other
1194	SB-505124	2-(5-Benzo[1,3]dioxol-5-yl-2-tert-butyl-3H-imidazol-4-yl)-6-methylpyridine hydrochloride hydrate		targeted	experimental	Genome integrity
1199	Tamoxifen			targeted	clinically approved	cytoskeleton
				targeted	clinically approved	ER
				targeted	clinically approved	other

Identifier	Name	Synonyms	Brand name	Action	Clinical stage	Putative target	Targeted process/pathway
1203	QL-XII-61			targeted	experimental	BTK	other
1218	JO1			targeted	experimental	BRD2, BRD3, BRD4	chromatin other
1219	PFI-1			targeted	experimental	BRD2, BRD3, BRD4	chromatin other
1230	IOX2			targeted	experimental	EGLN1	other
1236	UNC0638			targeted	experimental	G9a(EHMT2), GLP(EHMT1)	chromatin histone methylation
1239	YK 4-279			targeted	experimental	RNA helicase A	other
1241	CHIR-99021	CT 99021		targeted	experimental	GSK3B	WNT signaling
1242	(5Z)-7-Oxozeanol			targeted	experimental	MAP3K7 (TAK1)	other
1243	piperlongumine			not defined	experimental	Increases ROS levels	other
1248	FK866	APO866		targeted	experimental	NAMPT	metabolism
1259	BMN-673			targeted	experimental	PARP1	Genome integrity
1261	rTRAIL			targeted	experimental	TR10A (DR4), TR10B (DR5)	apoptosis regulation
1262	UNC1215			targeted	experimental	LMBL3	other
1264	SGC0946			targeted	experimental	Q8TEK3 (DOT1L)	chromatin histone methylation
1268	XAV 939	NVP-XAV 939		targeted	experimental	TNKS1 (tankyrase-1)	WNT signaling
1371	PLX4720 (rescreen)	Vemurafenib (derivative)	Zelboraf	targeted	experimental	BRAF	ERK MAPK signaling
1372	Trametinib	GSK1120212	Mekinist	targeted	clinically approved	MAP2K1 (MEK1), MAP2K2 (MEK2)	ERK MAPK signaling
1373	Dabrafenib	GSK2118436	Tafinlar	targeted	clinically approved	BRAF	ERK MAPK signaling
1375	Temozolomide	Temodar		cytotoxic	clinically approved	DNA alkylating agent	DNA replication
1377	Afatinib (rescreen)	Tovok, BIBW2992	Gilotrif	targeted	clinically approved	ERBB2, EGFR	EGFR signaling
1378	Bleomycin (50 uM)			cytotoxic	clinically approved	DNA damage	DNA replication
1494	SN-38	7-ETHYL-10-HYDROXY-CAMPTOTHECIN		cytotoxic	experimental	TOP1	DNA replication

	Olaparib	Olaparib		targeted	clinically approved in clinical development	PARP1, PARP2 MAP2K1 (MEK1), MAP2K2 (MEK2) ANDR (androgen receptor) MAP2K1 (MEK1), MAP2K2 (MEK2)	Genome integrity ERK MAPK signaling other
1495	Olaparib	Olaparib		targeted	clinically approved in clinical development	PARP1, PARP2 MAP2K1 (MEK1), MAP2K2 (MEK2) ANDR (androgen receptor)	ERK MAPK signaling other
1498	AZD6244			targeted	clinically approved	MAP2K1 (MEK1), MAP2K2 (MEK2)	ERK MAPK signaling
1502	Bicalutamide	ICI-176334	Casodex	targeted	experimental in clinical development	P13K NEDD8- activating enzyme	P13K signaling
1526	RDEA119 (rescreen)			targeted	in clinical development		
1527	GDC0941 (rescreen)			targeted			
1529	MLN4924			targeted			other

**Table S2.** SPIA pathway analysis performed highlighting significantly upregulated/downregulated pathways between BAP1 mutant and BAP1 wild type lines.  
Table size too big to fit page. Available upon request

**Table S3.** GEO data analysis of 40 BAP1wt vs. 11 BAP1mt mesothelioma tumors showing fold change in mRNA expression

ID	Adj. P value	P value	t	B	logFC	Gene symbol	Gene title
206987_x_at	<b>0.0467</b>	8.40E-06	-4.9297914	2,074	-1.55210916	FGF18	fibroblast growth factor 18
2111029_x_at	<b>0.0331</b>	3.23E-06	-5.200056	2,71569	-1.46628317	FGF18	fibroblast growth factor 18
2111485_s_at	<b>0.0173</b>	7.78E-07	-5.5953934	3,66039	-1.32935104	FGF18	fibroblast growth factor 18
203638_s_at	0.8387	9.17E-02	-1,7172855	-4,20483	-0,58459186	FGFR2	fibroblast growth factor receptor 2
208228_s_at	0.8261	7.39E-02	-1,822761	-4,07017	-0,57807812	FGFR2	fibroblast growth factor receptor 2
205110_s_at	0.7406	2.47E-02	-2,3120189	-3,35944	-0,57359639	FGF13	fibroblast growth factor 13
203639_s_at	0.8385	8.69E-02	-1,7439568	-4,17143	-0,42430659	FGFR2	fibroblast growth factor receptor 2
204379_s_at	0.7207	1.73E-02	-2,4574403	-3,12282	-0,30363692	FGFR3	fibroblast growth factor receptor 3
214284_s_at	0.7144	8.97E-03	-2,7123752	-2,68264	-0,2416635	FGF18	fibroblast growth factor 18
215404_x_at	0.7195	1.54E-02	2,5044305	-3,04406	0,32050106	FGFR1	fibroblast growth factor receptor 1



# Chapter 4

## Throphoblast Glycoprotein is Associated With a Favorable Outcome for Mesothelioma and a Target for Antibody Drug Conjugates

Laurel M. Schunselaar\*, Kim Monkhorst, Vincent van der Noort, Ruud Wijdeven, Dennis Peters, Wilbert Zwart, Jacques Neeffjes and Paul Baas  
J Thorac Oncol. 2018 Oct; 13(10):1577-1587



## Abstract

**Introduction:** The prognosis for patients with mesothelioma is poor, which prompts the need for the development of better treatment options. Antibody drug conjugates (ADCs) are gaining interest as a therapeutic strategy in mesothelioma. Trophoblast glycoprotein (5T4) is an oncofetal protein overexpressed in mesothelioma with low expression in normal tissue and therefore a good candidate for ADC treatment. Here, we evaluated and manipulated 5T4 as a suitable antigen for ADC targeted therapy in patients with mesothelioma.

**Methods:** Expression of the 5T4 antigen is evaluated in (primary) mesothelioma cell lines and biopsy specimens, and correlated with clinical outcome. Internalization was assessed in 5T4 expressing cells. The cytotoxicity of three different 5T4-targeting ADCs was tested on (primary) mesothelioma cells.

**Results:** 5T4 was expressed in 10 out of 12 (primary) cell lines. Most biopsy specimens stained positive for the 5T4 antigen, with marked differences in staining intensity and percentage of positive cells. High expression correlated with long progression-free survival. Both, free antibody and ADCs targeting 5T4, were internalized and entered lysosomal compartments. Cytotoxicity experiments showed that cell lines with a high expression for 5T4 were sensitive to two out of three ADCs. Lack of efficacy for the third ADC could be restored by neutralizing lysosomal compartments with chloroquine.

**Conclusion:** The 5T4 antigen is expressed in mesothelioma and 5T4-based ADCs are internalized in lysosomes. Two out of three ADCs were capable of killing the mesothelioma cells; the third ADC required additional lysosomal neutralization for its effect. 5T4-based ADC would be a selective strategy for the treatment of mesothelioma.

## Keywords

Malignant pleural mesothelioma, 5T4, Antibody-drug conjugate, treatment, Lysosome

## Introduction

Malignant pleural mesothelioma (MPM) is an aggressive tumor from mesothelial cells covering the pleural cavity. The prognosis for MPM is poor and most patients die within 2 years after diagnosis [1-4]. Standard of care chemotherapy, consisting of a platinum-based drug and anti-folate combination, gives a modest median survival benefit of at least 3 months [5, 6]. No further improved second-line therapy has been developed over the last 15 years.

Recently, antibody drug conjugates (ADCs) have gained substantial interest as a new strategy in the treatment of MPM. ADCs consist of monoclonal antibody chemically conjugated to a potent cytotoxic agent. They are developed to selectively target tumor cells, and as a result would minimize the toxicity in normal cells [7-9]. Conceptually, following binding of the antibody to the target antigen, the ADC will be internalized into tumor cells followed by the release of the toxin and elimination of the tumor cell (Fig. 1A). The toxin is released inside the lysosomes of the cells. Either a linker between toxin and antibody is constructed as a substrate for lysosomal proteases (the cleavable mechanism) or the full ADC is degraded (the noncleavable mechanism) to release the toxin. The cytotoxic agents that are mostly used in ADC technology are microtubule disrupting agents and DNA damaging agents (Fig. 1A) [7, 8, 10, 11].

Trophoblast glycoprotein (5T4) is an oncofetal cell surface glycoprotein, which plays a role in cell migration and epithelial-mesenchymal transition, and has been involved in wingless-type mouse mammary tumor virus (Wnt) signaling [12-16]. These functions may link to tumorigenesis, although 5T4 is not described as an oncogenic driver [8, 17]. 5T4 expression is limited in normal tissue, but overexpressed in various solid tumors, including lung, breast, ovarian, endometrial, bladder, pancreatic, colon and gastric cancers [18-22]. Upon antibody binding, 5T4 is rapidly internalized into cells, which is one important factor for ADC based-activity [16]. The first described 5T4 targeting ADC is A1-MMAF, an anti-5T4 immunoglobulin (Ig) G1 antibody that is conjugated by a maleimidocaproyl (mc) linker to monomethyl auristatin F (MMAF), an inhibitor of tubulin polymerization inducing G2/M cell cycle arrest and cell death [8, 10, 23]. A1-MMAF was highly potent in vitro and in vivo, and well tolerated in a phase I study performed in advanced solid tumors [23, 24].

Only one study has evaluated 5T4 expression in MPM cell lines, primary tumor cells in pleural fluid, and mesothelioma biopsy specimen [25]. We report that 5T4 is expressed at different levels in MPM cell lines and biopsy specimen, and internalizes to cathepsin B-positive lysosomes. High expression of 5T4 correlated with longer progression-free survival (PFS). We tested three different 5T4-ADCs and showed that they were cytotoxic in cell lines at a

5T4 antigen-dose-dependent manner. One ADC was lysosomally trapped and neutralization with chloroquine was required to release the drug from this site to induce cytotoxicity. We conclude that 5T4-mediated ADC therapy is a promising novel therapeutic option in a subset of patients with mesothelioma defined by high expression of 5T4.

## Materials and methods

### Patient samples

Biopsy specimens from patients with MPM were collected between 2009 and 2015 in the Netherlands Cancer Institute. All patients provided written informed consent for use and storage of their tumor biopsy specimens. Diagnosis was determined on available tumor biopsy specimens and confirmed by the Dutch Mesothelioma Panel, a national expertise panel of certified pathologist who evaluate all patient samples suspected of MPM.

### Cell lines

NCI-H2052, NCI-H2731, NCI-H2795, NCI-H2810, NCI-H2818 and MeT-5A were a kind gift of Professor McDermott from the Sanger Institute (Cambridgeshire, United Kingdom). Cells were cultured in Dulbecco's Modified Eagle Medium-F12 (Thermo Fisher Scientific, Waltham, Massachusetts) with 10% fetal calf serum (FCS) (Merck, Darmstadt, Germany). Cell lines VAMT and M28 were a kind gift of Professor C. Broaddus from the University of California, San Francisco. Cells were cultured in Dulbecco's Modified Eagle Medium (Thermo Fischer scientific) with 10% FCS. Isolating tumor cells from pleural fluid as described generated early passage cell lines NKI04, PV130913, PV180314, PV170614, and PV041214 [26]. LnCap cells were cultured in Roswell Park Memorial Institute solution (Life Technologies, Carlsbad, California) with 10% FCS. All cells were maintained at 37°C, 5% CO<sub>2</sub>.

### Preparation and characterization of ADC

Molecular anti-5T4 antibodies, H8 and A1 are produced in Expi293 cells according to manufactures instructions using commercially available pcDNA-based vector backbones (A14635, Life technologies) [23,27]. MMAF (T1006 LN-T-6871, Levana Biopharma, San Diego, California) is conjugated to H8 and A1 via a noncleavable mc linker as described [28]. Monomethyl auristatin E (MMAE) (T1004 LN-T-1458, Levana Biopharma) was conjugated to H8 via a valine-citrulline (vc) *p*-aminobenzylcarbamate linker that is cleaved by intracellular proteases such as cathepsin B as described [28].

### Immunohistochemistry

Immunohistochemistry (IHC) of the formalin-fixed paraffin-embedded biopsy specimens and cell lines was performed using a Discovery Ultra autostainer (Ventana Medical Systems, Oro Valley, Arizona). Paraffin sections were cut at 3 μm, heated at 75°C for 28 minutes and

deparaffinized with EZ prep solution (Ventana Medical Systems). Heat-induced antigen retrieval was performed using Cell Conditioning 1 (CC1, Ventana Medical Systems) for 64 minutes at 95°C. 5T4 was detected using clone EPR5529 (1/400 dilution, 1 hour at 37°C, AbCam, Cambridge, United Kingdom) and visualized using anti-rabbit HQ for 12 minutes at 37°C followed by anti-HQ HRP for 12 minutes at 37°C and the ChromoMap DAB detection kit (Ventana Medical Systems). Slides were counterstained with hematoxylin II and Bluing Reagent (Ventana Medical Systems). Staining was scored by a pathologist using H-score.

### **Western Blot**

Samples were lysed in radioimmunoprecipitation assay (RIPA) buffer (50 mmol/L Tris-Chloride, 1% nonylphenoxypolyethoxyethanol-40 [Sigma, St. Louis, Missouri], 0.5% sodium-deoxycholate [Sigma], 150 mmol/L sodium chloride, 1mmol/L ethylenediaminetetraacetic acid [Promega, Madison, Wisconsin], 1mmol/L ethyleneglycol-bis [ $\beta$ -aminoethyl ether] [VWR, Radnor, Pennsylvania] and protease/phosphatase inhibitors[Roche, Basel, Switzerland]), sonicated and centrifuged at 10,000 rpm for 15 minutes at 4°C. Membranes were stained with 5T4 (1:1,000, clone EPR5529, AbCam) and tubulin (1:6000, T9026, Sigma, St. Louis, Missouri) for 1 hour at room temperature (RT) or cathepsin B (1:1,000, clone D1C7Y, Cell Signaling, Danvers, Massachusetts) and actin (1:10,000, MAB1501R, Millipore, Burlington, Massachusetts) overnight at 4°C. Membranes were imaged by the Odyssey Classic imager (Li-Cor, Lincoln, Nebraska). Intensity of band was quantified using Image Studio Software (Li-Cor).

### **Confocal microscopy**

One hundred thousand cells were seeded on glass slides (13 mm diameter) and incubated with anti-5T4 monoclonal antibody (H8) for 1 hour at 4°C. Subsequently, cells were incubated for the indicated time, fixated in 3.7% formaldehyde (Merck) for 10 minutes, and permeabilized using 0.1% Triton X-100 (Merck). Staining was performed in 0.5% bovine serum albumin phosphate-buffered saline with antibodies against CD63 and Phalloidin-Alexa647 (Thermo Fisher scientific, Waltham, Massachusetts) [29]. 4',6-diamidino-2-phenylindole (DAPI) - containing Prolong Gold mounting medium (Thermo Fisher scientific) was used to mount the coverslips and detection of the nucleus. Images were acquired using a Leica TCS SP8 confocal microscope (Leica Microsystems, Wetzlar, Germany) at x63 magnification and quantified using Image J plugin Jacob for Pearson's coefficient calculations and processed using Adobe Photoshop and Illustrator (Adobe, San Jose, California).

### **Flow cytometry**

For expression experiments, 100,000 cells were incubated with 5  $\mu$ g/ml A1 or H8 antibody for 1 hour at 4°C. Cells were washed with phosphate-buffered saline/ 0.2% bovine serum albumin and incubated with secondary AlexaFluor488 (AF488) antibody (AffiniPure F(ab)2 fragment

goat anti human IgG-APC, 1:600, Jackson ImmunoResearch, West Grove, Pennsylvania) for 30 minutes at 4°C. Fluorescence intensities were measured by flow cytometry (BD Calibur, BD Bioscience, San Jose, California). To determine antibody binding capacity, human IgG calibrator (BioCytex, Marseille, France) was used according to manufactures protocol. For internalization experiments, H8 antibody was used with AF488 secondary antibody (1:8,000). Each antibody sample was prepared twice for total and quenched measurement. Cells were incubated at either 37°C to assess internalization or 4°C as control. After indicated incubation times, one sample was fixed in 3.7% formaldehyde. The other sample was quenched with anti-AF488 rabbit IgGAb (1:30 diluted Thermo Fisher scientific) for 30 minutes at 4°C after which it was fixed in 3.7% formaldehyde. Fluorescence intensity was determined by flow cytometry (BD Calibur, BD Bioscience, San Jose, California). Total signal was determined by the median fluorescence intensity of the unquenched sample corrected for the untreated cells (only AF488). Internalization signal was determined by the median fluorescence intensity of the quenched sample corrected for the untreated cells.

### **Cytotoxicity assay**

Cells were seeded in a flat bottom 96-well plate at appropriate cell density. After overnight incubation, ADC or MMAE were added in a concentration range of 1 ng/mL – 10 µg/mL and 0.001- 0.1 nmol/L, respectively. After 9 days of incubation, cytotoxicity was measured using a metabolic activity assay (Cell Titer blue G8081, Promenga, Madison, Wisconsin). Fluorescent readout was performed with the Envision Multilabel reader (Perkin Elmer, Waltham, Massachusetts). Percentage survival was calculated by dividing the fluorescent signal with the average mean fluorescence of control cells (0.1% dimethyl sulfoxide for ADC and 1% dimethylsulfoxide for MMAE).

### **Chloroquine reconstitution of drug activity**

Lysosomal trapping assay was performed with H8-mcMMAF and H8-vcMMAE as described in the cytotoxicity assay at concentration range between 1 ng/mL and 3.33 µg/mL. Each condition was prepared twice to compare cytotoxicity of ADC by itself with the cytotoxicity of ADC in combination with chloroquine. After 5 hours of incubation with the ADC, 10 µmol/L of chloroquine was added to the cells for 7 days. Cells were washed and incubated for an additional 48 hours after which cytotoxicity was measured.

### **Statistics**

Overall survival (OS) was defines as time from diagnosis until death of any cause. PFS was defined as time from start of firs-line treatment until radiological progression or death of any cause. Both are analyzed with the Kaplan-Meyer method and compared with the log-rank test. Patients not having the event of interest were right-censored at their day of last follow-up. Prognostic value for 5T4 H-score, age, sex, MPM subtype and disease control at 6 weeks

was assessed using Cox models, where disease control (defined as absence of progression) was not used in the model for PFS because of the overlap in definitions between disease control and PFS. 5T4 and age were continuous used in the multivariate analysis, whereas the hazard rate for 5T4 was determined per steps of 10 and age per 1 year.

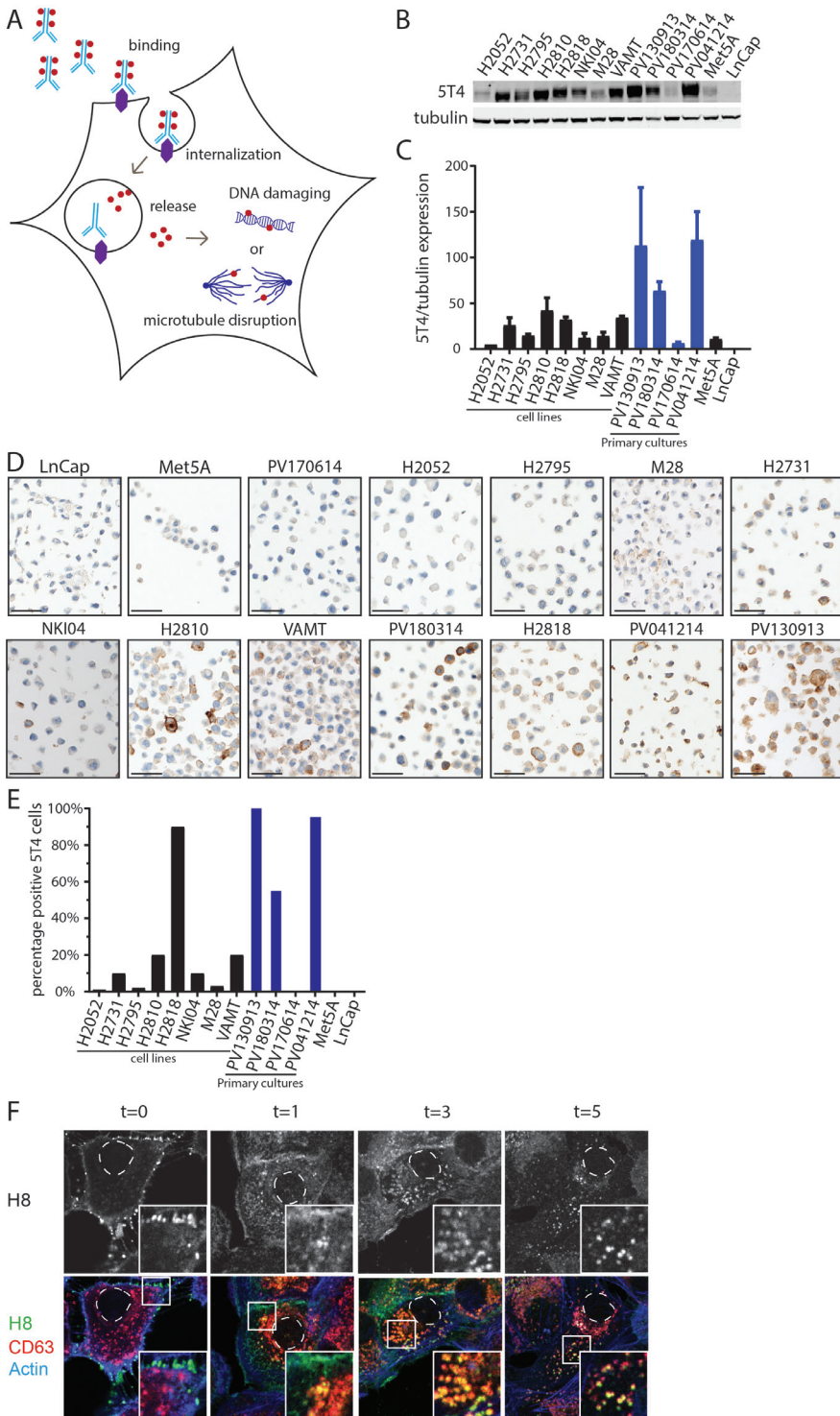
## Results

### Expression of 5T4 antigen in mesothelioma cell lines

To evaluate whether 5T4 is a suitable antigen for ADC-targeted therapy, we first analyzed 5T4 expression in eight human MPM tumor cell lines, four primary MPM tumor cell lines, and one human normal mesothelial cell line. As negative controls, the human prostate cancer LNCap and the melanoma SK-MEL30 cell lines were used. Seven of eight cell lines and three of four primary cell lines stained positive for 5T4 by Western blotting, including the sarcomatoid mesothelioma cell line VAMT. The normal mesothelial cell line, Met5A, expressed 5T4 at only very low levels (Fig. 1B and C). 5T4 expression in these cell lines was further confirmed using IHC, revealing strong plasma membrane and diffuse cytoplasmic expression for all cell lines that were positive based on Western blot analysis (Fig. 1D and E). The percentage of positive cells was variable between cell lines and stronger in primary MPM cultures as compared to the immortalized cell lines (Figure. 1D and E). To analyze 5T4 cell surface expression, the cells were analyzed by flow cytometry with two independent antibodies (also used in ADC technology): A1 and H8 [32, 27]. These data further confirmed 5T4 cell surface expression in the cell lines which were positive by Western blotting and IHC. Antibody binding capacity was stronger for the H8 antibody compared to the A1 antibody (Supplementary Fig. 1A). In summary, these data show that almost all MPM cell lines express 5T4 at the cell membrane albeit at different levels.

### Antibody-induced internalization of the 5T4 antigen in mesothelioma cell lines

5T4 is observed at the cell surface of MPM cell lines. Although this is a prerequisite for detection by the ADC, the antigen-antibody complex subsequently must internalize to release the associated toxin. To assess this, internalization of 5T4 upon binding by antibody H8 was determined in high 5T4 expressing cell lines: the epithelial cell line H2810, the sarcomatoid cell line VAMT and the primary cell line PV130913. Cells were incubated with AF488 (Jackson ImmunoResearch, West Grove, Pennsylvania) -labeled H8 antibody for 1 hour, after which internalization at 37°C was determined at different times. Quenching of the surface-bound AF488 labeled H8, with an anti-AF488 antibody, resulted in the fluorescence signal of the internalized H8-AF488 as quantified by flow cytometry. Quenching of the surface bound AF488 labeled H8 is incomplete as is evident from the 4°C controls (Supplementary Fig. 1B). This signal remained constant over time and represents the background of this assay. Internalization of the H8 antibody was observed in all three cell lines. Internalization is time



dependent and reached a maximum of 80% to 90% after 12 hours incubation for H2810 and VAMT cells, and a maximum of 100% internalization after 24 hours incubation for the primary cell line PV130913 (Supplementary Fig. 1B). As the cytotoxic drug will be activated in the lysosome, we next determined whether the ADCs ended up in the lysosome [8-11, 27]. After internalization of the H8-vcMMAE ADC, cells were stained for actin and the lysosomal marker CD63. Before internalization (0 hour) H8 is localized at the cell membrane, confirming the IHC results (Fig. 1D). After 1 hour, H8 is partly internalized into the cells and partly located at the cell surface. Over time, increasing internalization and colocalization of H8 with the lysosomal marker CD63 is observed, reaching complete H8 internalization after 5 hours of culture (Fig. 1F). These results indicate that H8 ADCs bind to the cell surface of mesothelioma cells followed by internalization and transport to the lysosomes.

### **Expression of the 5T4 antigen in MPM biopsies is associated with longer survival.**

For 5T4 to function as potential ADC-based drug target, there are two prerequisites: 1) expression in MPM; and 2) no expression in normal tissue. Therefore, we assessed the expression of the 5T4 antigen on 49 MPM biopsy specimens (34 epithelial, 8 mixed, and 7 sarcomatoid) and one tissue microarray containing different normal tissues including intestine, liver, kidney, prostate, and lung by IHC. Placenta was used as a positive control [16, 18, 22]. In line with cell line-based results (Fig. 1D), 5T4 localized to the plasma membrane in these biopsy specimens (Fig. 2A). 5T4 was not expressed in any of the normal tissues (Supplementary Fig. 2). For scoring the 5T4 expression, the H-score was used, in which staining intensity was scaled 0 to 3 for negative, weak positive, moderate positive, or strongly positive staining, respectively. The percentage of positive tumor cells was multiplied with the staining intensity giving an H-score between 0 and 300. 5T4 expression was observed in epithelial, mixed, as well as sarcomatoid mesothelioma (Fig. 2B). This indicates that 5T4-based ADC therapy is not restricted to one of the MPM subtypes. The median H-score in our patient cohort was 60. Based on this, two groups were differentiated, biopsy specimens with no to low expression of 5T4 (H-score  $\leq$ 60) (23 of 49), and biopsy specimens with a medium to high expression of 5T4 (H-score  $>$ 60) (26 of 49). Two examples of each group

**Figure 1. Expression and internalization of the 5T4 antigen in mesothelioma cells. A)** Model of the working mechanism of ADCs. When the antibody binds to the target it is internalized and the cytotoxic compound is released from the lysosomes. **B)** Expression of 5T4 by Western Blot in 12 mesothelioma cell lines and the normal mesothelial cell line Met5A. Prostate cancer cell line LnCap was used as negative control. **C)** Quantification of the Western Blot analysis, with 7 out of 8 cell lines (black) and 3 out of 4 primary cell lines (blue) staining positive for 5T4. Error bars indicate standard deviation from two independent experiments. **D)** Analysis of 5T4 expression using IHC showing strong plasma membrane and diffuse cytoplasmic expression (magnification: 20x, scalebar: 50  $\mu$ m). **E)** Quantification of IHC images. **F)** Internalization of H8-vcMMAE ADC (green) in the high 5T4 expressing cell line PV130913. At 0h, H8-vcMMAE is only expressed at the cell membrane, over time H8 is internalized and co-localization with lysosomal marker CD63 (red) is observed (Pearson's coefficient 0h: 0.19, 1h: 0.41, 3h: 0.55, 6h 0.56). Actin is depicted in blue and the dashed line indicates the nucleus.

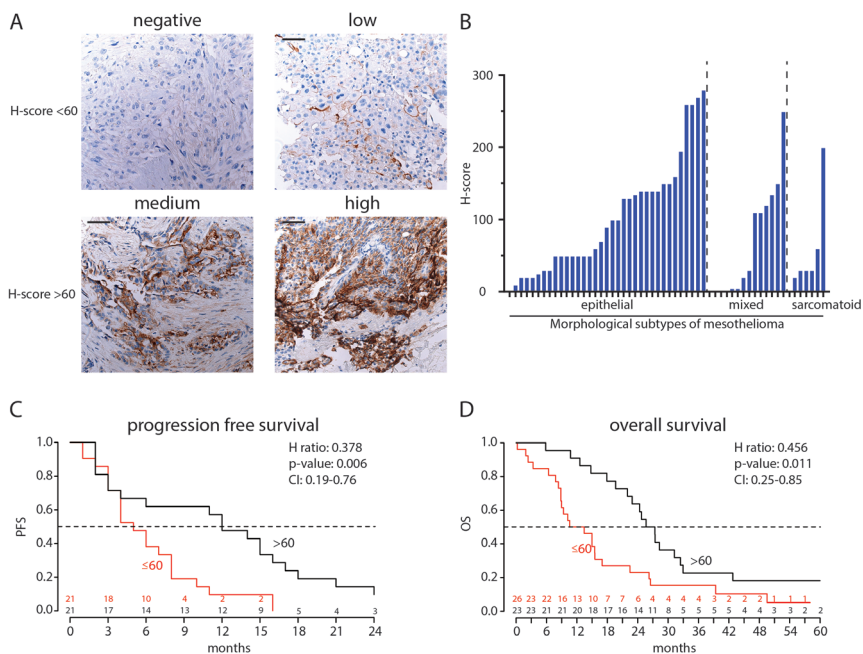


**Figure 2. Expression of the 5T4 antigen in mesothelioma biopsies correlates with survival. A)** Expression of 5T4 in mesothelioma biopsies (magnification: 40x, scalebar: 50  $\mu$ m). **B)** H-scores for all biopsies classified to the epithelial, mixed and sarcomatoid subtypes. **C)** Progression free survival analysis in patients with mesothelioma, with low (H-score  $\leq 60$ ) or high (H-score  $> 60$ ) 5T4 expression. P-value, Hazard rate and 95% confidence interval (CI) are indicated. **D)** Similar as C, but now with overall survival as event.

are depicted in Figure 2A. PFS and OS were determined for 42 and 49 patients, respectively. Median PFS for the patients with high 5T4 expression was 12 months (95% confidence interval [CI]: 4-18 months) versus 5 months (95% CI: 4-8 months) for the patients with low 5T4 expression. Median OS for the patients with high 5T4 expression was 26.5 months (95% CI: 22.9-33 months) versus 12 months (95% CI: 8.84-22.5 months) for patients with low 5T4 expression. Therefore, high 5T4 expression (H-score  $> 60$ ) was associated with longer PFS ( $p = 0.006$ , hazard ratio = 0.38, 95% CI: 0.19-0.76) and OS ( $p = 0.011$ , hazard ratio = 0.46, 95% CI: 0.25-0.85) in univariate analysis (Fig. 2 C and D) as well as in multivariate analysis using age, sex, histological subtype (epithelial versus nonepithelial) and (only in the case of OS) disease control (defined as absence of progression) after 6 weeks as covariates (Supplementary Table 1). Independent of 5T4, our analysis showed that the nonepithelial subtype is associated with shorter PFS and OS which was expected [30, 31]. Disease control at 6 weeks was also associated with longer OS.

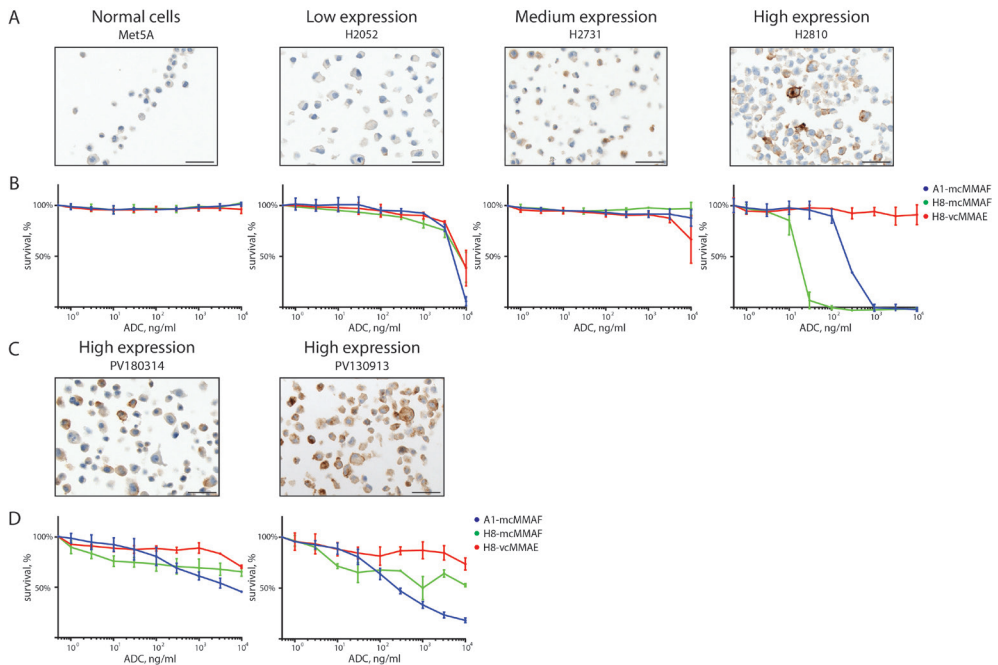


**Figure 3. Efficacy of 5T4 targeting ADCs in killing mesothelioma cells. A)** 5T4 expression by IHC for the different cell lines that were screened with ADCs. Cell lines are classified as normal mesothelial cells and low, medium or high 5T4 expression (magnification: 20x, scalebar: 50  $\mu$ m). **B)** Response curves indicating percentage of survival for cell lines Met5A, H2052, H2731 and H2810. Survival is depicted in relation to increasing concentration (ng/ml) of ADC; A1-mcMMAF (blue), H8-mcMMAF (green), H8-vcMMAE (red). Error bar indicates standard deviation from three independent measurements. **C)** 5T4 expression by IHC for two primary cell lines with high 5T4 expression. **D)** Response curves indicating percentage survival for cell lines PV180314 and PV130913. Survival is depicted in relation to increasing concentration (ng/ml) of ADC. Error bar indicates standard deviation from three independent measurements.

### Efficacy of 5T4 ADC-treatment in tumor cell killing

5T4 is expressed at the cell membrane of MPM cell lines and tumors, and high expression is associated with a favorable OS. To test whether 5T4 targeting ADC treatment is effective in MPM cell killing, we performed cytotoxicity experiments. To relate 5T4 ADC efficiency to 5T4 expression, four MPM cell lines and two primary cell lines were selected based on their 5T4 expression: normal mesothelial cells Met5A (no 5T4 expression), H2052 (low 5T4), H2731 (medium 5T4) and H2810, PV130913 and PV180314 (high 5T4 expression). We first tested the separate components of the ADC for their effect on toxicity. All cell lines were highly sensitive for the free toxin MMAE, a tubulin polymerization inhibitor and an uncharged analog of MMAF (Supplementary Fig 3A) [32]. The unconjugated 5T4 antibody did not affect cell survival, as was observed for the high expressing cell lines H2810 and PV130913 (Supplementary Fig. 3B). In total, three ADCs were tested. Two 5T4 antibodies

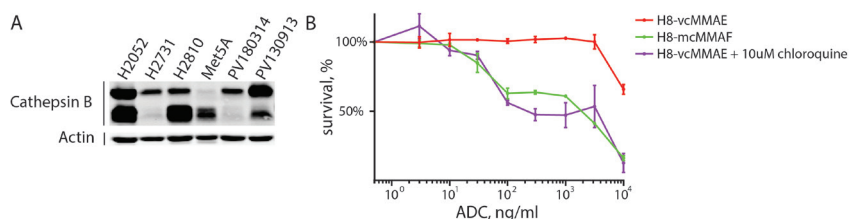


**Figure 4. Neutralizing lysosomal pH by chloroquine rescues ADC H8-vcMMAE mediated cell killing.** **A)** Western Blot analysis showing all cell lines express cathepsin B. **B)** Response curves of the high 5T4 expressing cell line H2810. Survival is depicted in relation to increasing concentration (ng/ml) ADC; H8-mcMMAF (green), H8-vcMMAE (red), H8-vcMMAE with 10  $\mu$ mol/L chloroquine (purple). Error bars indicate standard deviation from three independent measurements.

(A1 and H8) with the same linker and toxin were tested. A1-mcMMAF and H8-mcMMAF were conjugated by the same mc linker to MMAF [23]. Both ADCs must undergo complete proteolytic degradation to release the toxin [7, 10]. In addition, the H8 antibody was also coupled to a different linker-toxin combination. In this combination, H8 has a cleavable dipeptide vc linker that requires cleavage by the lysosomal protease cathepsin B to release the toxin [10, 28]. The normal mesothelial cell line Met5A, which does not express 5T4, was insensitive to any of the ADCs. Also the cell lines H2052 (low 5T4) and H2731 (medium 5T4) were insensitive to all ADCs. All high 5T4 expressing cell lines were sensitive to A1-mcMMAF and H8-mcMMAF, but not to H8-vcMMAE (Fig. 3). H8-mcMMAF performed superior over A1-mcMMAF, which is in concordance with 5T4 binding affinities of these antibodies, as deduced by flow cytometry (Supplementary Fig. 1A). Surprisingly, H8-vcMMAE was not active on these cells. We considered two options to explain this phenomenon: 1) the MPM cells did not express the lysosomal protease cathepsin B; or 2) the active drug is sequestered in lysosomes. Lysosomal sequestration is the accumulation of the active cytotoxic drug in acidic lysosomes, which is due to protonation of the toxin that as a result may not pass the lipid membrane of the lysosome and - as a consequence - fails to enter the cytosol where the drug is active [33]. Both options were tested. Western blot analysis showed that all cell lines express cathepsin B (Fig. 4), indicating that proteolytic cleavage of the drug, resulting in activation of the cytotoxic drug MMAE, could be achieved. Lysosomal sequestration was assessed by neutralizing acidic lysosomes in H8-vcMMAE-treated cells with 10  $\mu$ mol/L chloroquine (Fig. 4). MPM cells incubated with H8-vcMMAE were now efficiently killed in the same range as the H8-mcMMAE, indicating that lysosomal trapping of MMAE limits the effects of this ADC. In summary, both A1-mcMMAF and H8-mcMMAF are effective treatments in high-5T4 tumor cell killing, whereas H8-vcMMAE treatment requires addition of chloroquine for full potency.

## Discussion

Because of the poor prognosis of MPM, a pressing need exists for developing new treatment options. No druggable driver mutations have been identified, making targeted therapies difficult for patients with mesothelioma [34-36]. ADCs represent an interesting treatment option in which a cytotoxic agent is delivered to tumor cells via a cell-specific antibody based delivery [7, 8, 10, 11]. ADC therapy has been successfully applied in lymphoma and erb-b2 receptor tyrosine kinase 2 (Her2)-positive breast cancer [7, 11, 37, 38]. In mesothelioma, mesothelin has been evaluated as a target for ADC-based therapy, but the primary end point of PFS was not met in a phase II clinical trial [39, 40].

The cell surface protein 5T4 is highly expressed in MPM with limited expression in normal tissue, making this protein a suitable alternative candidate for ADC-based treatment [25]. In this report, we evaluated the potential use of 5T4-targeting ADC treatment in MPM by evaluating the expression and internalization of 5T4, determining correlations of 5T4 with patient prognostics and testing the efficacy of 5T4-targeting ADCs on MPM cells. We considered three different ADCs, in which we varied both the antibody as well as the linker-toxin combination.

Most cell lines and biopsy specimens stained positive for 5T4 regardless of MPM subtype, as reported before, indicating that 5T4-targeting ADCs could be of value for patients with MPM [25]. In our patient cohort, high 5T4 expression correlated with good survival, which is opposite to observations made in lung, colorectal, ovarian and gastric cancer [19-22]. This observation indicates that associations of 5T4 levels with outcome are tumor-type specific, which render it unlikely as a general driver of disease progression. However, most relevant is that 5T4 can be selectively targeted using ADCs, effectively yielding a targeted therapy for tumor types that would otherwise lack targeted therapeutics. As in lung cancer, 5T4-recognizing antibodies as well as ADCs rapidly internalize in MPM cells for intracellular transport to lysosomes [24]. The conjugation of H8 antibody to vcMMAE apparently did not alter its binding and internalization properties, consistent with the previously reported conjugation of A1 to mcMMAF [24]. This is not unexpected as the antigen recognition sites are not close to the cysteines to which the linker toxin is conjugated. The two Fab parts of the antibodies cluster the antigen and this likely accelerates endocytosis and lysosomal delivery [41].

We next tested the A1-mcMMAF ADC in MPM, which was previously reported to have antitumor activity in NSCLC and mammary cell line models. This ADC was active in various *in vivo* models and well tolerated in a phase I study [23, 24]. Next to this ADC, we generated two other ADCs by conjugating MMAF and MMAE to a second anti-5T4 antibody, H8. This

allowed us to assess the effect of different antibodies and the effect of different linker toxin conjugates on effectivity of the ADCs in eliminating 5T4-positive MPM cells. Two of the three ADCs were effective in high 5T4-expressing MPM cells, implying that sufficient quantities of drugs should be delivered to induce toxicity in the tumor cell. The current ADC tested will be of interest for MPM tumors expressing high amounts of 5T4, and this may be a biomarker for these ADCs.

We scored expression of 5T4 in biopsy specimens with the H-score because both percentage of positive cells as well as intensity of the staining were variable among tumors, and we believed that these variables were best-appreciated by using the H-index. Clearly, cell lines are more homogeneous in expression patterns, explaining why intensity of staining was similar among positive cells. These intrinsic differences render it challenging to compare expression of cells lines with biopsy specimens. Based on the responsiveness of 3 of 12 cell lines with high expression of 5T4, we expect that at least 25% of the tumors with the highest H-score will be responsive. However, further analyses using larger numbers of cell lines or primary tumor cultures are required to identify the optimal cut-off of 5T4 expression required for drug efficacy.

Changing the linker and drug used in ADC technology can also significantly alter the threshold of expression necessary for ADC efficacy, suggesting other 5T4 targeting ADCs could be effective in lower 5T4 expressing MPM cells [8]. Also, ADCs containing antibodies with a higher affinity than the ones we tested could be effective in lower 5T4-expressing MPM cells, although this could lead to unwanted killing of normal tissues that express low amounts of 5T4. We also noted effects of linkers on ADC activity. H8-vcMMAE was inactive in MPM cells. H8-vcMMAE was binding the target, and internalized into the cells, but sequestered into the lysosome which prevented release of the cytotoxic compound into the cytosol and abrogated cell killing. Neutralization of the lysosomes by chloroquine alleviated lysosomal trapping and facilitated the cytotoxic potential of the compound. Lysosomal sequestration of weak base chemotherapy is a known phenomenon in multi-drug resistance [33, 42]. Adding chloroquine to the treatment schedule after the toxin is released in the lysosomes could provide opportunities for ADC treatment; however, further research is required to assess the impact of lysosomal sequestration in more physiologically relevant systems.

An advantage of ADC-based treatment is the focused drug delivery limiting the toxicity to the target cell and minimizing side effects, which makes it possible to combine this treatment with other treatments. Especially combining ADCs with immune checkpoint inhibitors, which are under investigation in MPM, are expected to sustain the antitumor effect [7, 43]. In this study, we provide a first proof-of-concept of 5T4-based ADC monotherapy in MPM, in which 5T4 expression levels may be used as companion diagnostic tool to identify patient

populations who would be most eligible for this treatment. This ADC treatment targeting the 5T4 antigen could be a promising novel strategy in the treatment of MPM with high 5T4 expression.

## References

1. Martini, N., et al., *Pleural mesothelioma*. *Ann Thorac Surg*, 1987. **43**(1): p. 113-20.
2. Remon, J., et al., *Malignant mesothelioma: new insights into a rare disease*. *Cancer Treat Rev*, 2013. **39**(6): p. 584-91.
3. Suzuki, Y., *Pathology of human malignant mesothelioma--preliminary analysis of 1,517 mesothelioma cases*. *Ind Health*, 2001. **39**(2): p. 183-5.
4. van Zandwijk, N., et al., *Guidelines for the diagnosis and treatment of malignant pleural mesothelioma*. *J Thorac Dis*, 2013. **5**(6): p. E254-307.
5. Vogelzang, N.J., et al., *Phase III study of pemetrexed in combination with cisplatin versus cisplatin alone in patients with malignant pleural mesothelioma*. *J Clin Oncol*, 2003. **21**(14): p. 2636-44.
6. Zalcman, G., et al., *Bevacizumab for newly diagnosed pleural mesothelioma in the Mesothelioma Avastin Cisplatin Pemetrexed Study (MAPS): a randomised, controlled, open-label, phase 3 trial*. *Lancet*, 2016. **387**(10026): p. 1405-1414.
7. Lambert, J.M. and C.Q. Morris, *Antibody-Drug Conjugates (ADCs) for Personalized Treatment of Solid Tumors: A Review*. *Adv Ther*, 2017. **34**(5): p. 1015-1035.
8. Damelin, M., et al., *Evolving Strategies for Target Selection for Antibody-Drug Conjugates*. *Pharm Res*, 2015. **32**(11): p. 3494-507.
9. Erickson, H.K., et al., *Antibody-maytansinoid conjugates are activated in targeted cancer cells by lysosomal degradation and linker-dependent intracellular processing*. *Cancer Res*, 2006. **66**(8): p. 4426-33.
10. Sapra, P., et al., *Investigational antibody drug conjugates for solid tumors*. *Expert Opin Investig Drugs*, 2011. **20**(8): p. 1131-49.
11. Bouchard, H., C. Viskov, and C. Garcia-Echeverria, *Antibody-drug conjugates-a new wave of cancer drugs*. *Bioorg Med Chem Lett*, 2014. **24**(23): p. 5357-63.
12. Zhao, Y., et al., *Structural insights into the inhibition of Wnt signaling by cancer antigen 5T4/Wnt-activated inhibitory factor 1*. *Structure*, 2014. **22**(4): p. 612-20.
13. Kagermeier-Schenk, B., et al., *Waif1/5T4 inhibits Wnt/beta-catenin signaling and activates noncanonical Wnt pathways by modifying LRP6 subcellular localization*. *Dev Cell*, 2011. **21**(6): p. 1129-43.
14. Carsberg, C.J., K.A. Myers, and P.L. Stern, *Metastasis-associated 5T4 antigen disrupts cell-cell contacts and induces cellular motility in epithelial cells*. *Int J Cancer*, 1996. **68**(1): p. 84-92.
15. Spencer, H.L., et al., *E-cadherin inhibits cell surface localization of the pro-migratory 5T4 oncofetal antigen in mouse embryonic stem cells*. *Mol Biol Cell*, 2007. **18**(8): p. 2838-51.
16. Hole, N. and P.L. Stern, *A 72 kD trophoblast glycoprotein defined by a monoclonal antibody*. *Br J Cancer*, 1988. **57**(3): p. 239-46.
17. Stern, P.L., et al., *Understanding and exploiting 5T4 oncofoetal glycoprotein expression*. *Semin Cancer Biol*, 2014. **29**: p. 13-20.
18. Southall, P.J., et al., *Immunohistological distribution of 5T4 antigen in normal and malignant tissues*. *Br J Cancer*, 1990. **61**(1): p. 89-95.
19. Damelin, M., et al., *Delineation of a cellular hierarchy in lung cancer reveals an oncofetal antigen expressed on tumor-initiating cells*. *Cancer Res*, 2011. **71**(12): p. 4236-46.
20. Wrigley, E., et al., *5T4 oncofetal antigen expression in ovarian carcinoma*. *Int J Gynecol Cancer*, 1995. **5**(4): p. 269-274.
21. Naganuma, H., et al., *Oncofetal antigen 5T4 expression as a prognostic factor in patients with gastric cancer*. *Anticancer Res*, 2002. **22**(2b): p. 1033-8.
22. Starzynska, T., et al., *Prognostic significance of 5T4 oncofetal antigen expression in colorectal carcinoma*. *Br J Cancer*, 1994. **69**(5): p. 899-902.
23. Shapiro, G.I., et al., *First-in-human trial of an anti-5T4 antibody-monomethylauristatin conjugate, PF-06263507, in patients with advanced solid tumors*. *Invest New Drugs*, 2017. **35**(3): p. 315-323.
24. Sapra, P., et al., *Long-term tumor regression induced by an antibody-drug conjugate that targets 5T4, an oncofetal antigen expressed on tumor-initiating cells*. *Mol Cancer Ther*, 2013. **12**(1): p. 38-47.
25. Al-Taei, S., et al., *Overexpression and potential targeting of the oncofoetal antigen 5T4 in malignant pleural mesothelioma*. *Lung Cancer*, 2012. **77**(2): p. 312-8.
26. Schunselaar, L., et al., *Chemical profiling of primary mesothelioma cultures defines subtypes with different expression profiles and clinical responses*. *Clin Cancer Res*, 2017.
27. Boghaert, E.R., et al., *The oncofetal protein, 5T4, is a suitable target for antibody-guided anti-cancer*

- chemotherapy with calicheamicin. *Int J Oncol*, 2008. **32**(1): p. 221-34.
28. Doronina, S.O., et al., *Novel peptide linkers for highly potent antibody-auristatin conjugate*. *Bioconjug Chem*, 2008. **19**(10): p. 1960-3.
29. Vennegoor, C., et al., *Biochemical characterization and cellular localization of a formalin-resistant melanoma-associated antigen reacting with monoclonal antibody NK1/C-3*. *Int J Cancer*, 1985. **35**(3): p. 287-95.
30. Yap, T.A., et al., *Novel insights into mesothelioma biology and implications for therapy*. *Nat Rev Cancer*, 2017. **17**(8): p. 475-488.
31. Fennell, D.A., et al., *Statistical validation of the EORTC prognostic model for malignant pleural mesothelioma based on three consecutive phase II trials*. *J Clin Oncol*, 2005. **23**(1): p. 184-9.
32. Doronina, S.O., et al., *Enhanced activity of monomethylauristatin F through monoclonal antibody delivery: effects of linker technology on efficacy and toxicity*. *Bioconjug Chem*, 2006. **17**(1): p. 114-24.
33. Zhitomirsky, B. and Y.G. Assaraf, *Lysosomes as mediators of drug resistance in cancer*. *Drug Resist Updat*, 2016. **24**: p. 23-33.
34. Bonelli, M.A., et al., *New therapeutic strategies for malignant pleural mesothelioma*. *Biochem Pharmacol*, 2017. **123**: p. 8-18.
35. Remon, J., et al., *Malignant pleural mesothelioma: new hope in the horizon with novel therapeutic strategies*. *Cancer Treat Rev*, 2015. **41**(1): p. 27-34.
36. Bueno, R., et al., *Comprehensive genomic analysis of malignant pleural mesothelioma identifies recurrent mutations, gene fusions and splicing alterations*. *Nat Genet*, 2016. **48**(4): p. 407-16.
37. Senter, P.D. and E.L. Sievers, *The discovery and development of brentuximab vedotin for use in relapsed Hodgkin lymphoma and systemic anaplastic large cell lymphoma*. *Nat Biotechnol*, 2012. **30**(7): p. 631-7.
38. Krop, I.E., et al., *Trastuzumab emtansine versus treatment of physician's choice in patients with previously treated HER2-positive metastatic breast cancer (TH3RESA): final overall survival results from a randomised open-label phase 3 trial*. *Lancet Oncol*, 2017. **18**(6): p. 743-754.
39. Golfier, S., et al., *Anetumab ravtansine: a novel mesothelin-targeting antibody-drug conjugate cures tumors with heterogeneous target expression favored by bystander effect*. *Mol Cancer Ther*, 2014. **13**(6): p. 1537-48.
40. Kindler, H.L., et al., *Randomized Phase II Study of Anetumab Ravtansine or Vinorelbine in Patients with Malignant Pleural Mesothelioma in 18th World Conference on Lung Cancer*. 2017: Yokohama, Japan.
41. Ogris, M. and H. Sami, *Receptor Crosslinking in Drug Delivery: Detour to the Lysosome?* *Mol Ther*, 2015. **23**(12): p. 1802-4.
42. Giuliano, S., et al., *Resistance to sunitinib in renal clear cell carcinoma results from sequestration in lysosomes and inhibition of the autophagic flux*. *Autophagy*, 2015. **11**(10): p. 1891-904.
43. Muller, P., et al., *Microtubule-depolymerizing agents used in antibody-drug conjugates induce antitumor immunity by stimulation of dendritic cells*. *Cancer Immunol Res*, 2014. **2**(8): p. 741-55.

## Supplementary figures and tables

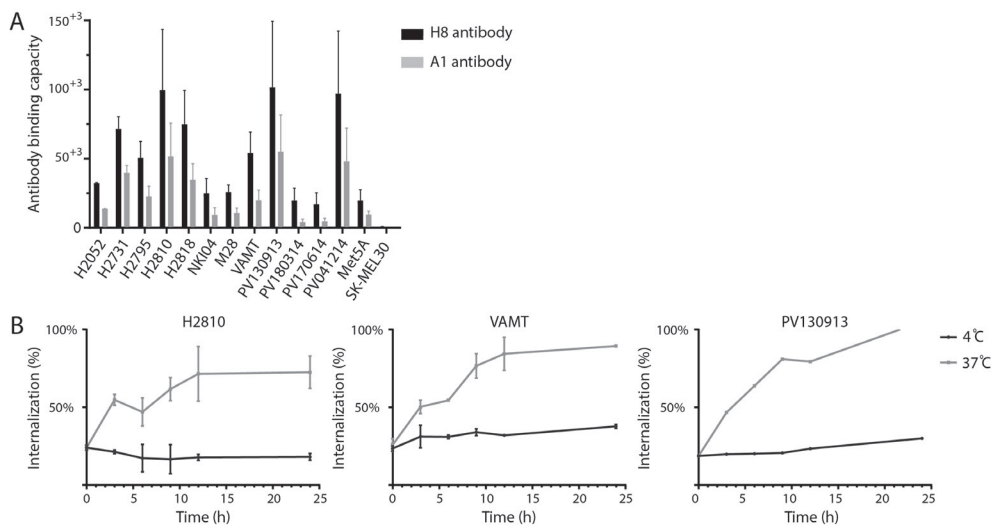


**Fig. S1. Expression and internalization of 5T4 by FACS analysis. A)** Antibody binding capacity of two anti-5T4 antibodies, H8 (black) and A1 (gray), in mesothelioma cells. The melanoma cell line SK-MEL30 was used as negative control. Error bars indicate standard deviation from two independent measurements. **B)** Internalization of the H8 antibody at 37°C (gray) in cell lines H2810, VAMT and PV130913. As control, cells were incubated at 4°C (black). Error bars indicate standard deviation from two (H2810) or three (VAMT) independent experiments.

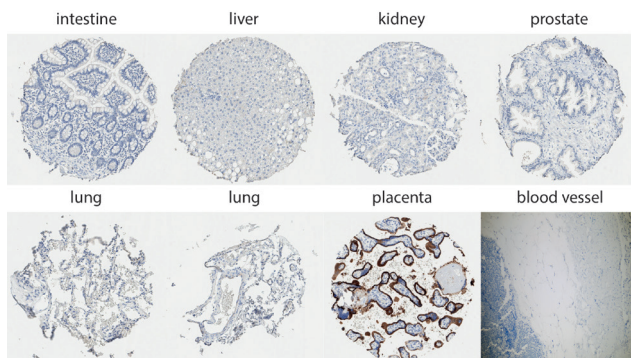


**Fig. S2. Expression of 5T4 in normal tissues.** 5T4 expression by IHC for normal tissues including intestine, liver, kidney, prostate, lung and a blood vessel. Placenta was used as a positive control (magnification 10x).

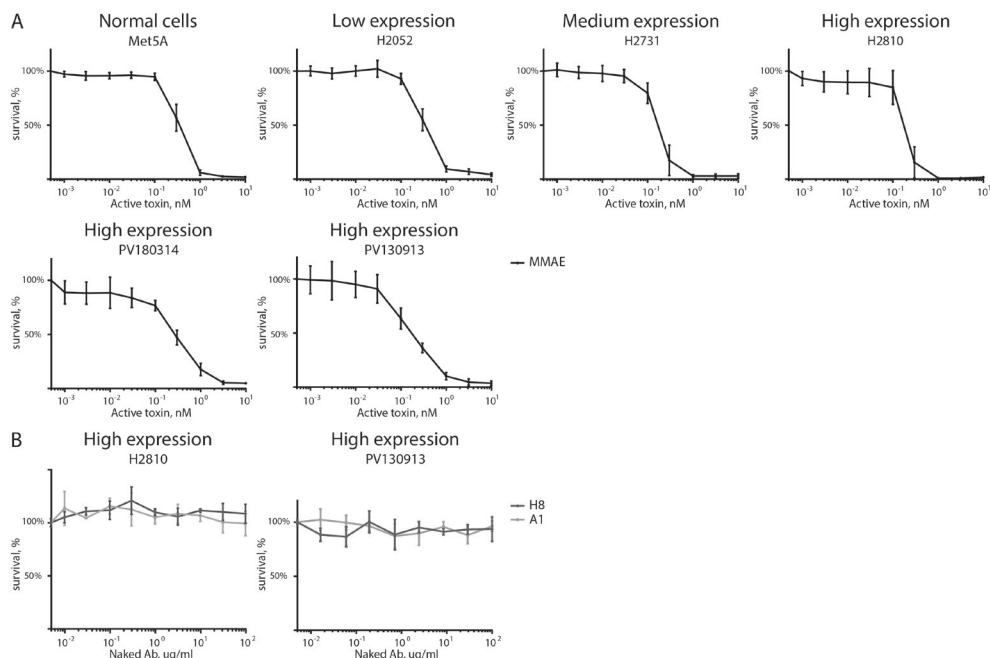


**Fig. S3. Efficacy of the free toxin and the unconjugated antibody.** **A)** Response to free toxin MMAE is depicted for all cell lines. Survival in relation to increasing concentrations (nmol/L) free toxin is depicted. Error bars indicate standard deviation from three independent measurements. **B)** Response curves for high 5T4 expressing cell lines H2810 and PV130913 are shown. Survival in relation to increasing concentrations ( $\mu\text{g/ml}$ ) unconjugated antibody is depicted. Error bars indicate standard deviation from two independent measurements.

**Table S1. Multivariate analysis**

**A) Multivariate analysis for progression free survival**

	Hazard rate	Confidence interval	P-value
H-score of 5T4	0.40	0.19-0.82	0.012
Age	1.00	0.96-1.04	0.957
Gender (male)	1.64	0.70-3.86	0.254
Non-epithelial subtype	2.18	0.97-4.89	0.058

**B) Multivariate analysis for overall survival**

	Hazard rate	Confidence interval	P-value
H-score of 5T4	0.53	0.25-1.14	0.104
Age	0.99	0.94-1.04	0.723
Gender (male)	4.13	1.39-12.30	0.011
Non-epithelial subtype	5.06	2.19-11.72	0.0002
Disease control rate	0.38	0.17-0.86	0.020

H-score of 5T4 and age were continuous used in the analysis, hazard rate, 95% confidence interval and P-value were determined per steps of 10 for 5T4 and per one year for age.



# Chapter 5

## Targeting BAP1: a New Paradigm for Mesothelioma

Laurel M. Schunselaar, Wilbert Zwart and Paul Baas  
Lung Cancer. 2017 Jul; 109:145-146



## **Abstract**

New treatment strategies for malignant pleural mesothelioma (MPM) are important. BAP1 mutations are present in 47-67% of the MPM tumors, making this a good target for treatment. Multiple functions of BAP1 are investigated in the preclinical situation. Due to many functions of BAP1, the phenotypic effect of BAP1 is diverse. Preclinical data on inhibitors reversing these phenotypic effects are promising. However, the mechanism of BAP1 is not fully elucidated yet and further research about the mechanism and possible inhibitors is necessary.

## **Keywords**

malignant mesothelioma, BAP1, mutation, loss, targeting, inhibitor.

Malignant mesothelioma (MM) is a rare but aggressive tumor arising in mesothelial cells lining the pleural and peritoneal cavity. MM has a poor prognosis and most patients die within the first 2 years after diagnosis [1-4]. A variety of new treatment strategies are currently being tested to improve the outcome of this disease. Besides immune-oncology (IO) therapies and anti-vascular agents which are under investigation, new avenues in the field of molecular genetics are also examined.

BRCA-associated protein 1 (BAP1) is one of the molecular targets that has been identified as a potential novel target in the treatment of MM. BAP1 has a number of regulatory functions in the cell, including its function as deubiquitinating enzyme (DUB) with predominantly nuclear localization. Through its deubiquitinase activity and the effects thereof on transcription, BAP1 functions as a tumor suppressor regulating target genes in transcription, cell cycle control, DNA damage repair and cellular differentiation [5-8]. BAP1 germline mutation in patients with mesothelioma was first reported in 2011 [9]. These patients are often diagnosed at an early age with a number of skin disorders including skin tumors and uveal melanomas. Furthermore, BAP1 mutation carriers are more likely to develop a peritoneal or pleural mesothelioma [10, 11]. For mesothelioma patients with a germline BAP1 mutation, prognosis seems to be better with a 5-year survival rate of 47%, when compared with 6.7% for patients who did not have the mutation [11].

Although germline mutations are rare in sporadic mesothelioma [12], somatic BAP1 aberrations are more common in mesothelioma tumors. About 47–67% of the mesothelioma tumors contain a BAP1 genetic aberration. BAP1 somatic mutations are more frequent in the epithelioid subtype than in the sarcomatoid subtype. Besides single point mutations in the BAP1 gene, copy number loss, rearrangements and multiple alterations are found as well [13-20]. The somatic BAP1 mutation can easily be identified with immunohistochemistry (IHC) and these observations are consistent with sequencing results [16, 17, 19].

### **BAP1 as a drug target in mesothelioma**

Based on the apparent causal role of BAP1 mutations in mesothelioma development, it would be interesting to identify therapeutic agents that reverse the phenotypic effects of BAP1 protein loss. BAP1 has many interaction partners that may function as attractive drug targets, along with downstream substrates of BAP1.

BAP1 together with ASXL1 forms a polycomb repressive deubiquitinase (PR-DUB) complex that deubiquitinates histone 2A (H2A) [5, 6, 8, 21]. Together with the polycomb repressor complex (PRC) that ubiquitinates histones, the PR-DUB takes care of the transcriptional balance and control. Loss of BAP1 causes significantly altered expression of several

polycomb target genes. For instance, alterations in the BAP1/ASXL1 interaction cause an increased ubiquitination of H2A leading to deregulation of cell cycle progression and hindered senescence [5]. The regulation of histones by BAP1 suggests that an interaction with histone deacetylase (HDAC) inhibitors could be beneficial. In MM, the effect of HDAC inhibitors on H2A is not known, but in uveal melanoma, HDAC inhibitors reduced levels of H2A ubiquitination in BAP1-depleted cells. One potential explanation for this reduction is the transcriptional repression of the PRC1 component BMI1 by HDAC inhibitors [22, 23]. Recently, it was found that BAP1 loss also reduces HDAC2 expression [24], and BAP1 knockdown in MM cell lines increases the sensitivity for HDAC inhibitors leading to cell death, a process known as synthetic lethality. The exact mechanism behind this sensitizing effect is not known, but these results indicate that HDAC inhibitors could be effective in patients with a BAP1 loss. However, in the VANTAGE 014 study, a phase III trial including 661 patients, the HDAC inhibitor vorinostat did not improve overall survival in an unselected group of patients compared with placebo [25]. From half of these patients material is still available and it would be important to correlate the BAP1 status with response to HDAC inhibition for these patients.

Enhancer of zeste homolog 2 (EZH2), an enzymatic subunit of the PRC2, is upregulated in MM [13, 26-28]. LaFave et al. [27] described that BAP1 loss leads to increased EZH2 levels in cell lines and BAP1-knockout mice. Although others could not observe a clear association between BAP1 loss and EZH2 upregulation in MM biopsies using immunohistochemistry, the development of EZH2 specific inhibitors is gaining interest of pharmaceutical companies [13, 28]. In MM cell lines, treatment with an EZH2 inhibitor decreased cell proliferation, reduced invasion and inhibited clonogenicity in soft agar. In line with these results, treatment with EZH2 inhibitors in MM-tumor bearing mice significantly reduced tumor size with no toxicity [26, 27]. Importantly, BAP1 mutant mice were more responsive to the EZH2 treatment compared with wild-type mice [26]. Also in other tumor types, phase I studies with EZH2 inhibitors showed promising results [28]. This approach is being tested in a phase 2, 2-part, single-arm study of tazemetostat 800 mg administered two times a day (BID) orally (NCT02860286). In the first part, unselected patients with MM will be entered, followed by patients with a BAP1 mutation. This can elucidate whether EZH2 inhibitors could be used as therapeutic agents that reverse the phenotypic effects of BAP1 protein loss in MM.

Another interaction partner of BAP1 is host cell factor 1 (HCF1), which plays a role in cell cycle progression by activating transcription of promoters bound by the E2F family. BAP1 deubiquitinates HCF1 and recently multiple groups showed that BAP1 mutation results in increased HCF1 ubiquitination, impairing E2F activation. Decreased activation of E2F causes problems in cell cycle progression and inhibition of cell growth [5, 7, 21, 29, 30]. Lower levels of HCF1 result in decreased interaction of BAP1 with transcription factor Yin Yang 1 (YY1),

which controls cellular proliferation. The latter interaction, however, is not yet described in MM [31]. These interaction partners may provide options for new therapeutic intervention strategies.

## **Conclusions**

Based on the prevalence of BAP1 mutations that cause BAP1 protein loss, it is important to identify therapeutic agents that reverse the phenotypic effects. Multiple interaction partners and proteins under the influence of BAP1 are described and preclinical data of inhibitors targeting these partners are promising. Since the exact molecular mechanism of BAP1 function is yet to be fully clarified, further research on BAP1 action may reveal even more therapeutic possibilities. Due to the many interaction partners and functions of BAP1, it could be wise to test combinations of therapeutic agents that can possibly reverse the phenotypic effect of BAP1 protein loss. BAP1 can be considered as one of the new, promising targets in MM and ongoing (clinical) research is in progress.

## References

1. Martini, N., et al., *Pleural mesothelioma*. *Ann Thorac Surg*, 1987. **43**(1): p. 113-20.
2. Suzuki, Y., *Pathology of human malignant mesothelioma--preliminary analysis of 1,517 mesothelioma cases*. *Ind Health*, 2001. **39**(2): p. 183-5.
3. van Zandwijk, N., et al., *Guidelines for the diagnosis and treatment of malignant pleural mesothelioma*. *J Thorac Dis*, 2013. **5**(6): p. E254-307.
4. Remon, J., et al., *Malignant mesothelioma: new insights into a rare disease*. *Cancer Treat Rev*, 2013. **39**(6): p. 584-91.
5. Wang, A., et al., *Gene of the month: BAP1*. *J Clin Pathol*, 2016. **69**(9): p. 750-3.
6. Bononi, A., et al., *Latest developments in our understanding of the pathogenesis of mesothelioma and the design of targeted therapies*. *Expert Rev Respir Med*, 2015. **9**(5): p. 633-54.
7. Misaghi, S., et al., *Association of C-terminal ubiquitin hydrolase BRCA1-associated protein 1 with cell cycle regulator host cell factor 1*. *Mol Cell Biol*, 2009. **29**(8): p. 2181-92.
8. Scheuermann, J.C., et al., *Histone H2A deubiquitinase activity of the Polycomb repressive complex PR-DUB*. *Nature*, 2010. **465**(7295): p. 243-7.
9. Testa, J.R., et al., *Germline BAP1 mutations predispose to malignant mesothelioma*. *Nat Genet*, 2011. **43**(10): p. 1022-5.
10. Ohar, J.A., et al., *Germline BAP1 Mutational Landscape of Asbestos-Exposed Malignant Mesothelioma Patients with Family History of Cancer*. *Cancer Res*, 2016. **76**(2): p. 206-15.
11. Baumann, F., et al., *Mesothelioma patients with germline BAP1 mutations have 7-fold improved long-term survival*. *Carcinogenesis*, 2015. **36**(1): p. 76-81.
12. Sneddon, S., et al., *Absence of germline mutations in BAP1 in sporadic cases of malignant mesothelioma*. *Gene*, 2015. **563**(1): p. 103-5.
13. Shinozaki-Ushiku, A., et al., *Diagnostic utility of BAP1 and EZH2 expression in malignant mesothelioma*. *Histopathology*, 2016.
14. Hida, T., et al., *BAP1 immunohistochemistry and p16 FISH results in combination provide higher confidence in malignant pleural mesothelioma diagnosis: ROC analysis of the two tests*. *Pathol Int*, 2016. **66**(10): p. 563-570.
15. Kato, S., et al., *Genomic Landscape of Malignant Mesotheliomas*. *Mol Cancer Ther*, 2016. **15**(10): p. 2498-2507.
16. Nasu, M., et al., *High Incidence of Somatic BAP1 alterations in sporadic malignant mesothelioma*. *J Thorac Oncol*, 2015. **10**(4): p. 565-76.
17. Yoshikawa, Y., et al., *Frequent inactivation of the BAP1 gene in epithelioid-type malignant mesothelioma*. *Cancer Sci*, 2012. **103**(5): p. 868-74.
18. Guo, G., et al., *Whole-exome sequencing reveals frequent genetic alterations in BAP1, NF2, CDKN2A, and CUL1 in malignant pleural mesothelioma*. *Cancer Res*, 2015. **75**(2): p. 264-9.
19. Lo Iacono, M., et al., *Targeted next-generation sequencing of cancer genes in advanced stage malignant pleural mesothelioma: a retrospective study*. *J Thorac Oncol*, 2015. **10**(3): p. 492-9.
20. Righi, L., et al., *BRCA1-Associated Protein 1 (BAP1) Immunohistochemical Expression as a Diagnostic Tool in Malignant Pleural Mesothelioma Classification: A Large Retrospective Study*. *J Thorac Oncol*, 2016. **11**(11): p. 2006-2017.
21. Eletr, Z.M. and K.D. Wilkinson, *An emerging model for BAP1's role in regulating cell cycle progression*. *Cell Biochem Biophys*, 2011. **60**(1-2): p. 3-11.
22. Landreville, S., et al., *Histone deacetylase inhibitors induce growth arrest and differentiation in uveal melanoma*. *Clin Cancer Res*, 2012. **18**(2): p. 408-16.
23. Bommi, P.V., et al., *The polycomb group protein BMI1 is a transcriptional target of HDAC inhibitors*. *Cell Cycle*, 2010. **9**(13): p. 2663-73.
24. Sacco, J.J., et al., *Loss of the deubiquitylase BAP1 alters class I histone deacetylase expression and sensitivity of mesothelioma cells to HDAC inhibitors*. *Oncotarget*, 2015. **6**(15): p. 13757-71.
25. Krug, L.M., et al., *Vorinostat in patients with advanced malignant pleural mesothelioma who have progressed on previous chemotherapy (VANTAGE-014): a phase 3, double-blind, randomised, placebo-controlled trial*. *Lancet Oncol*, 2015. **16**(4): p. 447-56.
26. Kemp, C.D., et al., *Polycomb repressor complex-2 is a novel target for mesothelioma therapy*. *Clin Cancer Res*, 2012. **18**(1): p. 77-90.
27. LaFave, L.M., et al., *Loss of BAP1 function leads to EZH2-dependent transformation*. 2015. **21**(11): p. 1344-9.

28. Kim, K.H. and C.W. Roberts, *Targeting EZH2 in cancer*. Nat Med, 2016. **22**(2): p. 128-34.
29. Bott, M., et al., *The nuclear deubiquitinase BAP1 is commonly inactivated by somatic mutations and 3p21.1 losses in malignant pleural mesothelioma*. Nat Genet, 2011. **43**(7): p. 668-72.
30. Machida, Y.J., et al., *The deubiquitinating enzyme BAP1 regulates cell growth via interaction with HCF-1*. J Biol Chem, 2009. **284**(49): p. 34179-88.
31. Yu, H., et al., *The ubiquitin carboxyl hydrolase BAP1 forms a ternary complex with YY1 and HCF-1 and is a critical regulator of gene expression*. Mol Cell Biol, 2010. **30**(21): p. 5071-85.



# Chapter 6

## General Discussion





Malignant pleural mesothelioma (MPM) is a malignancy of the mesothelial cells lining the pleura [1-4]. There are three histological subtypes of MPM: epithelioid (60% of the cases), sarcomatoid (20% of the cases) and biphasic (20% of the cases), the later containing both epithelial and sarcomatoid cells [5-7]. The occurrence of MPM is strongly associated with asbestos exposure. Due to the latency period between exposure and development of MPM, ranging from 20 to 50 years, MPM is still diagnosed. The incidence of MPM is slightly increasing over the last years and is not expected to decrease before 2020 [3, 8-10].

The treatment of MPM consist of the chemotherapeutic combination of cisplatin with pemetrexed. This combination showed an overall survival (OS) benefit of 16.1 months versus 9.3 months for patients who only received cisplatin [11, 12]. Since 2003, there are no new treatments licensed, even though there are many clinical trials conducted. An overview of these trials, till 2016, is given in **chapter 1**.

Finding new treatment strategies suitable for MPM is challenging. The mutational load in MPM is low/ intermediate and dominated by mutations in tumor suppressor genes rather than oncogenes. The tumor suppressor genes that are frequently mutated in MPM are cyclin-dependent kinase inhibitor 2A (CDKN2A), neurofibromina 2 (NF2) and BRCA associated protein 1 (BAP1) [13-18]. The absence of drugable molecular targets makes the search for targeted therapy very difficult. Heterogeneity is another explanation why a treatment, suitable for all patients with MPM, is difficult to find. Survival in MPM is associated with histological subtype [19, 20], indicating the impact that inter-patient heterogeneity can have on clinical trial results. It is therefore important to stratify on histological subtype in clinical trials. Recent findings also indicated that MPM could be a polyclonal tumor [21]. Although not a lot is known on this subject, a polyclonal origin would suggest high intra-tumor (genetic) heterogeneity, which is likely to contribute to unresponsiveness of MPM to most treatments.

## Personalized treatment

Personalized treatment can be more successful than finding a treatment strategy designed for all patients with MPM. In **chapter 2** we present a method of chemically profiling primary MPM cultures with commonly used anticancer drugs. Patients' own tumor cells, isolated from pleural fluid, were tested for multiple chemotherapeutics to select the best therapeutic option. Because therapy response forms the basis for therapy selection, the biology and the molecular mechanism of the tumor are less relevant and, for the same reason, it is not necessary to select patients with biomarkers.

Unfortunately, this method is not suitable for patients that do not develop pleural fluid.

Thereby, in 50% of the cases it was not possible to successfully screen the primary tumor culture, because of lack of tumor cells. The personalized treatment method is furthermore limited by the fact that it cannot test immuno-oncology drugs, due to the absence of the immune micro-environment.

We showed a strong correlation between the *in vitro* and *in vivo* response in the first ten patients that were treated based on their chemical profile. We foresee that this approach will lead to an improved selection of patients suitable for a specific treatment, especially when the number and classes of compounds is expanded and not restricted to commonly used anticancer drugs. In addition, this personalized treatment method may also prevent the use of therapies which are doomed to fail and will only lead to increased toxicity for the patient. However, further validation of this technology is necessary and currently ongoing in a phase II trial (PeRsOnalized treatment fOr patients with pleural eFFusions due to malignant pleural mesothelioma or lung cancer in second or third line (PROOF study)).

Besides personalizing treatment, based on all chemical profiles we could distinguish three groups, so called non-responders, intermediate responders and responders. It is expected that, with more chemical compounds, the intermediate group can be subdivided in two or even more groups. This unique way of classifying MPM, based on drug sensitivity, is not shown before. Transcriptomic analysis of these groups revealed corresponding gene signatures, which made it possible to identify new targets for the treatment of MPM subgroups. Focusing on the non-responder group, the group in which it is most important to find new treatment options, we identified that several genes playing a role in the fibroblast growth factor (FGF) pathway were upregulated. Elaborating on this, we treated non-responder cultures with FGF receptor (FGFR) inhibitors and showed they were highly sensitive. This shows chemical profiling of primary MPM cultures can help identifying new treatments for MPM.

## FGFR inhibitors

In a high throughput chemical inhibitor screen we identified that a subset of immortalized and primary cell lines were sensitive for FGFR inhibitors, as described in **chapter 3**. We showed that the sensitive lines were dependent on FGFR3 mediated signaling regulated by BAP1.

Our results are in line with others that showed patients with MPM could benefit from FGFR inhibitors [22-24]. It was published that FGF1 and 2 and FGFR1 were highly expressed in MPM biopsies [22-24]. Treatment of cell lines or mice with MPM tumors with FGFR inhibitors resulted in impairment of proliferation and a reduction of the tumor burden [22, 23]. This

indicates FGFR sensitivity is not only dependent on FGFR3 mediated signaling, but also on FGFR1 mediated signaling.

The only FGFR inhibitor that was tested in clinical trials with MPM was dovitinib. Dovitinib is a tyrosine kinase inhibitor (TKI) that predominantly inhibits vascular endothelial growth factor receptor, but also FGFRs [25]. The phase II study was halted due to minimal activity and poor tolerability [25]. It is possible that dovitinib was not potent enough to inhibit FGFR. However, another explanation in line with our results, is that only a selection of patients is sensitive to FGFR inhibitors. We showed BAP1 protein expression could serve as a biomarker for FGFR inhibitor therapy. Protein expression detected with immunohistochemistry was consistent with mutation data found by sequencing [26-28]. BAP1 is mutated in 47% to 67% of the tumors [13, 26-31] indicating FGFR inhibitors could be useful in a large group of patients with MPM.

## BAP1

The group of patients with somatic mutations in BAP1 could also benefit from other therapeutics. As we describe in **chapter 5**, BAP1 is a tumor suppressor gene with many regulatory functions in transcription, cell cycle control, DNA damage repair and cellular differentiation. The many interaction partners or downstream substrates of BAP1, such as histone 2A (H2A), enhancer of zeste homolog 2 (EZH2) and host cell factor 1 (HCF1), may function as attractive drug targets. However, the exact molecular mechanism of BAP1 function is not yet clarified and many interaction partners of BAP1 can also play a role in downstream signaling of NF2 and CDKN2A, two other tumor suppressor genes frequently mutated. It is also described that a subset of patients have mutations in two or three of these genes [14, 15]. This indicates the molecular mechanism of MPM, in which different pathways play a role, can be difficult to unravel.

Therefore, treating MPM is complicated and combining targeted therapies is necessary to optimize survival in MPM. In general, combination therapy is often based on a novel agent combined with an approved drug, or combining two approved drugs [32]. However, with new insights in the molecular pathways it will be more promising to combine two or even more novel agents.

Combining these novel agents will give challenges in which the molecular pharmacology of both drugs plays an important role. What is the optimal dose of each drug? How long should there be dosed and in which schedule? Also toxicity issues make combination therapy challenging. Overlapping toxicities of the individual drugs could lead to accumulation of toxicity and gives a narrow therapeutic window [32]. With a cocktail of therapies, the

pharmacology and toxicity issues become even more challenging. A good design of clinical trials is therefore very important.

## Antibody-drug conjugates

In chapter 1 we describe three developments that will improve prospects for patients with MPM: 1. personalized treatment (chapter 2), 2. better understanding of the genetic make-up of MPM (chapter 5) and 3. immunotherapy. One treatment strategy gaining more interest in MPM, was not described in this chapter: antibody-drug conjugates (ADCs). ADCs consist of a drug conjugated to an antibody targeting the tumor cells [33-35]. Anetumab ravtansine, a human anti-mesothelin antibody conjugated to the maytansinoid tubulin inhibitor DM4, was the first ADC clinically tested in MPM. Mesothelin is a cell surface antigen with unknown function that is expressed in normal mesothelial cells and overexpressed in most epithelial MPM tumors, but not in sarcomatoid MPM [36-38]. In preclinical research anetumab ravtansine was cytotoxic for MPM cell lines and showed antitumor activity in mouse models [39]. However, the primary end point, progression free survival, was not met in the phase II trial [40].

In **chapter 4**, we present the effects of 5T4 targeting ADCs. 5T4 is only expressed in tumor cells, making it an excellent candidate for this treatment strategy. We showed that most MPM tumors express 5T4, making it a suitable antigen for ADC targeted therapies in MPM. Subsequently, we showed that the ADC is internalized in MPM cells and enters the lysosomal compartment to release the associated toxin. Unexpectedly, the 5T4 ADCs were only able to kill high 5T4-expressing cells and not the low expressing cells.

To make this treatment strategy suitable for more patients, the minimal expression of 5T4 required to kill the cells (the threshold expression) should be lowered. This is possible by changing the linker and/ or drug of the ADC or by using antibodies with a higher affinity for the target. Each change, however could also lead to unwanted toxicities and should therefore be carefully tested. Another problem of ADC treatment in MPM is lysosomal sequestration of the ADC. Neutralizing the lysosomes by adding chloroquine to the treatment schedule could solve this problem, but this should be further tested in physiologically relevant pre-clinical models.

Before the 5T4 targeting ADCs could be tested in the clinic, they should be further optimized and tested in other relevant models such as mouse models. However, in general, ADC treatment is an elegant strategy by limiting the toxicity to the target cells, minimizing side effects. Because not all biopsies express 5T4 and many MPM tumors progress on treatment at some point, it is important to find more targets specific for MPM tumor cells. Biomarkers

studies could provide more and new options for the ADC treatment strategy.

## Other treatment modalities in MPM

Other treatment modalities with positive results on the prognosis of MPM, not studied in this thesis, are the anti-vascular agent bevacizumab and immunotherapy.

### *First-line treatment*

The addition of the anti-vascular agent bevacizumab to standard of care chemotherapy is so far the only progress that was recently established in the first-line treatment of patients with MPM. Bevacizumab is an antibody binding the vascular endothelial growth factor (VEGF). VEGF expression levels are high in most MPM biopsies and VEGF signaling plays a part in MPM cell physiopathology [41, 42]. Addition of bevacizumab to the first-line treatment gave a significant longer survival (18.8 months) compared to cisplatin and pemetrexed (16.1 months) [12]. Because inclusion criteria and study design could have influenced OS, the standard first-line treatment is not yet adjusted.

### *Immuno-oncology therapeutics*

Immunotherapy in MPM is mainly focused on immune checkpoint inhibitors against cytotoxic lymphocyte antigen 4 (CTLA-4), programmed cell death protein 1 (PD-1) and its ligand PD-L1 [43, 44]. Although two single-arm phase II trials with tremelimumab, a selective antibody against CTLA-4 [44, 45], showed promising results [46, 47], the large double-blind placebo-controlled phase IIb trial DETERMINE did not improve OS [45]. Pembrolizumab and nivolumab are molecular antibodies against PD-1 [48, 49] and avelumab and durvalumab block PD-L1 [49]. For both pembrolizumab and nivolumab, response percentages of around 25% are reported [50-53], while avelumab showed a response rate of 14.3% in PD-L1 positive patients [54] and a clinical trial with durvalumab is ongoing (NCT02899195). The promising early results with monotherapy blockers resulted in combining CTLA-4 blockers with PD-1/PD-L1 blockers to enhance T-cell activity in a complementary way. Clinical trials with durvalumab and tremelimumab (NCT02588131, NCT03075527, NCT02592551) or ipilimumab and nivolumab (NCT02716272, NCT02899299) are now recruiting patients.

Response rates in the first clinical trials show that immunotherapy in MPM is promising. However, not all patients will respond to immunotherapy. It is therefore important to find markers that could select patients that will benefit from this therapy. One of the markers that is tested is PD-L1, which is expressed in 20% to 70% of the MPM biopsies [55-59]. Overall, PD-L1 expression was not a good biomarker for PD-1 or PD-L1 blockers. For CTLA-4 blockers there are no predictive biomarkers available [20]. Whether tumor immune infiltrates, like lymphocytes or other tumor molecular features, could be predictive biomarkers should be

further investigated.

## **Gaps in MPM research**

Although our understanding of the molecular and biological behavior of MPM has increased, there are still knowledge gaps in MPM research. As mentioned above, novel biomarkers would strongly facilitate selecting patients for chemotherapy, immunotherapy or targeted treatments, but it can also play a role in finding new targets for ADC treatment.

The insight into MPM genetics provides many opportunities for drug development, however the molecular mechanism behind these genes and the interaction between the mechanisms are not fully understood yet. Insight in the molecular mechanism is very important as it will indicate targetable pathways for which candidate drugs could be explored.

Finally, a rather unexplored research area is heterogeneity in MPM. A better understanding of this topic will undoubtedly strongly improve our insights in how to treat this tumor.

## **Join forces**

To address the major challenge and knowledge gaps in MPM, and to implement this knowledge in the clinic, it is of vital importance to join forces.

### *Physicians and researchers.*

Many drugs evaluated in phase Ib/II clinical trials are tested without a good rational or decent preclinical research. History has proven that this approach has resulted in many failures. To increase the success rate of clinical trials, it is very important that physicians and researchers collaborate. Not only to translate preclinical results to clinical trials, but also to translate clinical problems to concrete research questions. Thereby, high-quality translational research is only possible when clinical trials are conducted in such a way that they facilitate research. With more clinical material available, more research can be performed. Chapter 2 is a strong example of close collaboration between doctors and researchers, which provided the very basis of true personalized therapy in MPM.

### *Researchers and researchers.*

When researchers from different fields work together, more therapies could be developed for patients with MPM. For instance, as described above, biomarker research can help developing new antibody drug conjugates. Furthermore, research on epigenetics in MPM revealed new targetable pathways. Fundamental research further exploring these pathways will give insights in candidate targets. New compounds focusing on these targets could then

be preclinically tested. The EZH2 inhibitor tazemetostat is a prime example, which illustrates that genomic studies in MPM and further exploration of downstream pathways can yield new treatment opportunities in MPM [60]. Undoubtedly, there are more opportunities to find new drugs or combinations of drugs.

*Physicians and physicians.*

The population of patients with MPM is small. To conduct large clinical trials, it is important that doctors from different centers collaborate. Furthermore, to be able to compare small phase I/II trials with each other, it is critical that trials are conducted in a uniform matter. That is only possible when doctors work together. When patient populations and sample collection are similar between trials, translational research from different trials can be interpreted in a better way. MPM research, and ultimately the patient, will benefit from this. Our understanding of MPM showed a great improvement, which resulted in promising new treatment strategies. However, there are still a lot of opportunities. By joining forces (even more) we will further improve the survival of patients with MPM.

## References

1. Suzuki, Y., *Pathology of human malignant mesothelioma--preliminary analysis of 1,517 mesothelioma cases*. Ind Health, 2001. **39**(2): p. 183-5.
2. van Zandwijk, N., et al., *Guidelines for the diagnosis and treatment of malignant pleural mesothelioma*. J Thorac Dis, 2013. **5**(6): p. E254-307.
3. Remon, J., et al., *Malignant mesothelioma: new insights into a rare disease*. Cancer Treat Rev, 2013. **39**(6): p. 584-91.
4. Martini, N., et al., *Pleural mesothelioma*. Ann Thorac Surg, 1987. **43**(1): p. 113-20.
5. Attanoos, R.L. and A.R. Gibbs, *Pathology of malignant mesothelioma*. Histopathology, 1997. **30**(5): p. 403-18.
6. Inai, K., *Pathology of mesothelioma*. Environ Health Prev Med, 2008. **13**(2): p. 60-4.
7. Brenner, J., et al., *Malignant mesothelioma of the pleura: review of 123 patients*. Cancer, 1982. **49**(11): p. 2431-5.
8. Wagner, J.C., C.A. Sleggs, and P. Marchand, *Diffuse pleural mesothelioma and asbestos exposure in the North Western Cape Province*. Br J Ind Med, 1960. **17**: p. 260-71.
9. Carbone, M., et al., *Malignant mesothelioma: facts, myths, and hypotheses*. J Cell Physiol, 2012. **227**(1): p. 44-58.
10. Baas, P., et al., *Malignant pleural mesothelioma: ESMO Clinical Practice Guidelines for diagnosis, treatment and follow-up*. Ann Oncol, 2015. **26** Suppl 5: p. v31-9.
11. Vogelzang, N.J., et al., *Phase III study of pemetrexed in combination with cisplatin versus cisplatin alone in patients with malignant pleural mesothelioma*. J Clin Oncol, 2003. **21**(14): p. 2636-44.
12. Zalcman, G., et al., *Bevacizumab for newly diagnosed pleural mesothelioma in the Mesothelioma Avastin Cisplatin Pemetrexed Study (MAPS): a randomised, controlled, open-label, phase 3 trial*. Lancet, 2016. **387**(10026): p. 1405-1414.
13. Kato, S., et al., *Genomic Landscape of Malignant Mesotheliomas*. Mol Cancer Ther, 2016. **15**(10): p. 2498-2507.
14. Guo, G., et al., *Whole-exome sequencing reveals frequent genetic alterations in BAP1, NF2, CDKN2A, and CUL1 in malignant pleural mesothelioma*. Cancer Res, 2015. **75**(2): p. 264-9.
15. Bott, M., et al., *The nuclear deubiquitinase BAP1 is commonly inactivated by somatic mutations and 3p21.1 losses in malignant pleural mesothelioma*. Nat Genet, 2011. **43**(7): p. 668-72.
16. Bueno, R., et al., *Comprehensive genomic analysis of malignant pleural mesothelioma identifies recurrent mutations, gene fusions and splicing alterations*. Nat Genet, 2016. **48**(4): p. 407-16.
17. Cheng, J.Q., et al., *p16 alterations and deletion mapping of 9p21-p22 in malignant mesothelioma*. Cancer Res, 1994. **54**(21): p. 5547-51.
18. Xio, S., et al., *Codeletion of p15 and p16 in primary malignant mesothelioma*. Oncogene, 1995. **11**(3): p. 511-5.
19. Fennell, D.A., et al., *Statistical validation of the EORTC prognostic model for malignant pleural mesothelioma based on three consecutive phase II trials*. J Clin Oncol, 2005. **23**(1): p. 184-9.
20. Yap, T.A., et al., *Novel insights into mesothelioma biology and implications for therapy*. Nat Rev Cancer, 2017. **17**(8): p. 475-488.
21. Comertpay, S., et al., *Evaluation of clonal origin of malignant mesothelioma*. J Transl Med, 2014. **12**: p. 301.
22. Schelch, K., et al., *Fibroblast growth factor receptor inhibition is active against mesothelioma and synergizes with radio- and chemotherapy*. Am J Respir Crit Care Med, 2014. **190**(7): p. 763-72.
23. Marek, L.A., et al., *Nonamplified FGFR1 is a growth driver in malignant pleural mesothelioma*. Mol Cancer Res, 2014. **12**(10): p. 1460-9.
24. Plones, T., et al., *Absence of amplification of the FGFR1-gene in human malignant mesothelioma of the pleura: a pilot study*. BMC Res Notes, 2014. **7**: p. 549.
25. Laurie, S.A., et al., *A phase II trial of dovitinib in previously-treated advanced pleural mesothelioma: The Ontario Clinical Oncology Group*. Lung Cancer, 2017. **104**: p. 65-69.
26. Nasu, M., et al., *High Incidence of Somatic BAP1 alterations in sporadic malignant mesothelioma*. J Thorac Oncol, 2015. **10**(4): p. 565-76.
27. Yoshikawa, Y., et al., *Frequent inactivation of the BAP1 gene in epithelioid-type malignant mesothelioma*. Cancer Sci, 2012. **103**(5): p. 868-74.
28. Lo Iacono, M., et al., *Targeted next-generation sequencing of cancer genes in advanced stage malignant*

- pleural mesothelioma: a retrospective study.* J Thorac Oncol, 2015. **10**(3): p. 492-9.
29. Shinozaki-Ushiku, A., et al., *Diagnostic utility of BAP1 and EZH2 expression in malignant mesothelioma.* Histopathology, 2016.
  30. Hida, T., et al., *BAP1 immunohistochemistry and p16 FISH results in combination provide higher confidence in malignant pleural mesothelioma diagnosis: ROC analysis of the two tests.* Pathol Int, 2016. **66**(10): p. 563-570.
  31. Righi, L., et al., *BRCA1-Associated Protein 1 (BAP1) Immunohistochemical Expression as a Diagnostic Tool in Malignant Pleural Mesothelioma Classification: A Large Retrospective Study.* J Thorac Oncol, 2016. **11**(11): p. 2006-2017.
  32. Yap, T.A., A. Omlin, and J.S. de Bono, *Development of therapeutic combinations targeting major cancer signaling pathways.* J Clin Oncol, 2013. **31**(12): p. 1592-605.
  33. Erickson, H.K., et al., *Antibody-maytansinoid conjugates are activated in targeted cancer cells by lysosomal degradation and linker-dependent intracellular processing.* Cancer Res, 2006. **66**(8): p. 4426-33.
  34. Damelin, M., et al., *Evolving Strategies for Target Selection for Antibody-Drug Conjugates.* Pharm Res, 2015. **32**(11): p. 3494-507.
  35. Lambert, J.M. and C.Q. Morris, *Antibody-Drug Conjugates (ADCs) for Personalized Treatment of Solid Tumors: A Review.* Adv Ther, 2017. **34**(5): p. 1015-1035.
  36. Hassan, R., T. Bera, and I. Pastan, *Mesothelin: a new target for immunotherapy.* Clin Cancer Res, 2004. **10**(12 Pt 1): p. 3937-42.
  37. Ordonez, N.G., *Value of mesothelin immunostaining in the diagnosis of mesothelioma.* Mod Pathol, 2003. **16**(3): p. 192-7.
  38. Chang, K., et al., *Monoclonal antibody K1 reacts with epithelial mesothelioma but not with lung adenocarcinoma.* Am J Surg Pathol, 1992. **16**(3): p. 259-68.
  39. Golfier, S., et al., *Anetumab ravtansine: a novel mesothelin-targeting antibody-drug conjugate cures tumors with heterogeneous target expression favored by bystander effect.* Mol Cancer Ther, 2014. **13**(6): p. 1537-48.
  40. Kindler, H.L., et al., *Randomized Phase II Study of Anetumab Ravtansine or Vinorelbine in Patients with Malignant Pleural Mesothelioma in 18th World Conference on Lung Cancer.* 2017: Yokohama, Japan.
  41. Ohta, Y., et al., *VEGF and VEGF type C play an important role in angiogenesis and lymphangiogenesis in human malignant mesothelioma tumours.* Br J Cancer, 1999. **81**(1): p. 54-61.
  42. Strizzi, L., et al., *Vascular endothelial growth factor is an autocrine growth factor in human malignant mesothelioma.* J Pathol, 2001. **193**(4): p. 468-75.
  43. Khan, S., et al., *Tremelimumab (anti-CTLA4) mediates immune responses mainly by direct activation of T effector cells rather than by affecting T regulatory cells.* Clin Immunol, 2011. **138**(1): p. 85-96.
  44. Pardoll, D.M., *The blockade of immune checkpoints in cancer immunotherapy.* Nat Rev Cancer, 2012. **12**(4): p. 252-64.
  45. Maio, M., et al., *Tremelimumab as second-line or third-line treatment in relapsed malignant mesothelioma (DETERMINE): a multicentre, international, randomised, double-blind, placebo-controlled phase 2b trial.* Lancet Oncol, 2017. **18**(9): p. 1261-1273.
  46. Calabro, L., et al., *Tremelimumab for patients with chemotherapy-resistant advanced malignant mesothelioma: an open-label, single-arm, phase 2 trial.* Lancet Oncol, 2013. **14**(11): p. 1104-11.
  47. Calabro, L., et al., *Efficacy and safety of an intensified schedule of tremelimumab for chemotherapy-resistant malignant mesothelioma: an open-label, single-arm, phase 2 study.* Lancet Respir Med, 2015. **3**(4): p. 301-9.
  48. Dozier, J., H. Zheng, and P.S. Adusumilli, *Immunotherapy for malignant pleural mesothelioma: current status and future directions.* Transl Lung Cancer Res, 2017. **6**(3): p. 315-324.
  49. Mancuso, M.R. and J.W. Neal, *Novel systemic therapy against malignant pleural mesothelioma.* Transl Lung Cancer Res, 2017. **6**(3): p. 295-314.
  50. Disselhorst, M.M.J., S.J.A. Burgers, and P. Baas, *Optimal Therapy of Advanced Stage Mesothelioma.* Curr Treat Options Oncol, 2017. **18**(8): p. 48.
  51. Quispel-Janssen, J., et al., *A phase II study of nivolumab in malignant pleural mesothelioma (NivoMes): with translational research (TR) biopsies (OA13.01).* J Thorac Oncol, 2017. **12**(S292-S293).
  52. Alley, E.W., et al., *Clinical safety and activity of pembrolizumab in patients with malignant pleural mesothelioma (KEYNOTE-028): preliminary results from a non-randomised, open-label, phase 1b trial.* Lancet Oncol, 2017. **18**(5): p. 623-630.
  53. Kindler, H.L., *Phase II trial of pembrolizumab in patients with malignant mesothelioma (MM): interim*

- analysis*. World Conference on Lung Cancer 2016. **OA 13.02**.
54. Hassan, R., et al., *Avelumab (MSB0010718C; anti-PD-L1) in patients with advanced unresectable mesothelioma from the JAVELIN solid tumor phase Ib trial: Safety, clinical activity, and PD-L1 expression*. J Clin Oncol, 2016. **34**(abstr 8503).
  55. Combaz-Lair, C., et al., *Immune biomarkers PD-1/PD-L1 and TLR3 in malignant pleural mesotheliomas*. Hum Pathol, 2016. **52**: p. 9-18.
  56. Mansfield, A.S., et al., *B7-H1 expression in malignant pleural mesothelioma is associated with sarcomatoid histology and poor prognosis*. J Thorac Oncol, 2014. **9**(7): p. 1036-40.
  57. Cedres, S., et al., *Analysis of expression of programmed cell death 1 ligand 1 (PD-L1) in malignant pleural mesothelioma (MPM)*. PLoS One, 2015. **10**(3): p. e0121071.
  58. Cedres, S., et al., *Analysis of expression of PTEN/PI3K pathway and programmed cell death ligand 1 (PD-L1) in malignant pleural mesothelioma (MPM)*. Lung Cancer, 2016. **96**: p. 1-6.
  59. Nguyen, B.H., et al., *PD-L1 expression associated with worse survival outcome in malignant pleural mesothelioma*. Asia Pac J Clin Oncol, 2018. **14**(1): p. 69-73.
  60. LaFave, L.M., et al., *Loss of BAP1 function leads to EZH2-dependent transformation*. 2015. **21**(11): p. 1344-9.





# Addendum





## English summary.

### What is this thesis about?

This thesis is about finding new treatment options for patients with malignant pleural mesothelioma (MPM). MPM is a tumor of the mesothelial cells lining the pleural cavity. It is also known as asbestos cancer due to its association with asbestos. Even though all handling of asbestos is strictly regulated since 2005, still 500-600 patients per year are diagnosed with MPM in the Netherlands. This is caused by a latency period of 20-50 years between asbestos exposure and development of the tumor. These numbers are not expected to decrease in the coming years. The prognosis for these patients is poor and without treatment most patients die within a year. This stretched the need for new treatment options for MPM.

### What is done?

**Chapter 1** gives an overview of which new treatments have been tested over the last couple of years. First-line chemotherapy consists of a platinum-based drug combined with pemetrexed. This combination gives a survival benefit of 16.1 months compared to patients that did not receive treatment. Around 40% of the patients respond to this combination. For patients that do not respond to first-line chemotherapy or become progressive after treatment, there is no standard second-line regimen. Many new treatments, like growth factor inhibitors, angiogenesis inhibitor, other targeted agents, oncolytic viral therapy and vaccines have been tested as second-line treatment. However, none of these therapies showed a significant survival benefit. That all these treatments fail in phase II clinical studies while active in preclinical studies shows the urgent need for better preclinical models that resemble the patients tumor, but are also easy to handle and fast in its readout. **Chapter 1** also describes the latest developments in preclinical models, like cell lines, primary tumor cultures and mouse models, and their own advantages and disadvantages.

### Personalized treatment

In **chapter 2** I present a personalized treatment strategy based on primary tumor cultures. A method for screening multiple chemotherapies on the patients' own tumor cells is developed, to generate chemical profiles and select the best therapeutic option. For ten patients treatment decision was based on these chemical profiles. There was a strong correlation between the *in vitro* results and the actual tumor response in these patients, which indicates this personalized treatment strategy is possible in patients with MPM. Further validation is currently ongoing in a phase II trial named the PROOF study.

Based on the chemical profiles of all tumor cultures, these tumor cultures could be divided in three groups. Tumor cultures that respond to almost all tested chemotherapies so called 'responders', tumor cultures that did not respond to chemotherapy, so called 'non-responders' and a group of tumor cultures that was sensitive to some of the chemotherapies, but not too all, the so called 'intermediate responders'. When comparing these groups genetically, a gene expression profile that distinguished the 'responders' from the 'non-responders' was identified. The 'intermediate responders', showed a different unique genetic profile, which did at some levels overlapped with the 'responders' or 'non-responders' group. With these gene expression profiles we were able to identify the fibroblast growth factor receptor (FGFR) as a new target for the treatment of MPM.

## FGFR

FGFR was not only found in the gene expression profiles of our primary tumor cultures. The screening of multiple new therapies on different MPM cells lines and primary tumor cultures, as described in **chapter 3**, also showed that a subset of the cultures were sensitive to FGFR inhibitors. A MPM mouse xenograft model confirmed the sensitivity to FGFR inhibitors. The cultures sensitive to FGFR inhibitors showed elevated levels of FGF9 mRNA. FGF9 is known to have a high affinity for FGFR3. All the sensitive cell lines were dependent on FGFR3 mediated signaling which was regulated by BRCA-associated protein 1 (BAP1). Therefore BAP1 protein loss, could serve as a biomarker to select patients for FGFR inhibitor treatment.

## Antibody drug conjugates

Another treatment strategy that is described in this thesis is antibody drug conjugates (ADCs). ADCs consist if a monoclonal antibody chemically conjugated to a potent cytotoxic drug. When the antibody binds the target antigen, the ADC will internalize into the cell and release the drug that will kill the tumor cell. When the target antigen is only expressed on tumor cells the drug will only kill the tumor cell and not affect the normal cells, giving fewer side effects. Expression on tumor cells and not on normal cells, internalization into the cell and releasing of the drug are all important factors in this therapy strategy.

**Chapter 4** shows that throphoblast glycoprotein, or 5T4, is a suitable target for ADC treatment in MPM. The antigen is expressed in most of the MPM tumors and not expressed in normal tissue. Upon binding the whole complex internalizes into the cell. Two of the three ADCs that were tested were able to kill the tumor cells that had a strong expression of 5T4. One ADC was not able to kill the tumor cells. We showed that the released drug was trapped in the lysosomal compartment of the cells. By changing the pH of the cells with cloroquine,

an anti-malaria drug, this ADC was also able to kill the tumor cells.

## **BAP1**

BAP1 is a molecular target that has been identified as a potential novel target in the treatment of MPM. BAP1 is a tumor suppressor gene regulating target genes in transcription, cell cycle control, DNA damage repair and cellular differentiation. Somatic mutations in BAP1 are seen in 47-67% of the patients with MPM. **Chapter 5** describes how therapeutic agents could reverse phenotypic effects of BAP1 protein loss. However since the exact molecular mechanism of BAP1 function is not yet fully clarified, further research may reveal even more therapeutic options. Thereby, BAP1 has many interaction partners as well as downstream substrates, which makes it wise to test combinations of therapeutic agents that can reverse the phenotypic effect of BAP1 protein loss.



## Nederlandse samenvatting.

### Waar gaat dit proefschrift over?

Dit proefschrift gaat over het vinden van nieuwe behandel mogelijkheden voor patiënten met maligne pleuraal mesotheliom (MPM). MPM is een tumor van de mesotheliale cellen die het borstvlies bekleden. De tumorsoort is ook bekend als asbestkanker door de associatie met asbest. Ondanks dat het handelen van asbest in Europa strikt gereguleerd is sinds 2005, worden er in Nederland nog elk jaar rond de 500-600 patiënten gediagnosticeerd met MPM. Dit komt doordat de ziekte een latentie tijd van 20-50 jaar tussen asbestexpositie en het ontwikkelen van de tumor kent. De verwachting is dat deze aantallen de komende jaren niet zullen dalen. De prognose voor patiënten met MPM is slecht en zonder therapie zullen de meeste mensen binnen een jaar overlijden. Dit geeft aan hoe belangrijk het is dat er nieuwe behandel mogelijkheden komen voor deze patiënten.

### Wat is er gedaan?

**Hoofdstuk 1** geeft een overzicht van alle nieuwe behandelingen die getest zijn de afgelopen jaren. De eerstelijns chemotherapie bestaat uit een platinum medicijn in combinatie met pemetrexed. Deze chemotherapie combinatie geeft een overlevingsvoordeel van 16,1 maanden vergeleken met patiënten die geen behandeling ondergaan. Rond de 40% van de patiënten reageert op deze chemotherapie combinatie. Voor de patiënten die niet reageren op de eerstelijns chemotherapie of waarvan de tumor recidiveert (weer gaat groeien) na behandeling is er geen standaard tweedelijns behandeling. Er zijn heel veel nieuwe behandelingen getest, zoals medicijnen die groeifactoren in de tumor remmen of angiogenese remmers. Maar ook andere medicijnen met een target, of oncolytische virus therapie en vaccinaties zijn getest als tweedelijns behandeling. Geen van deze therapieën liet een significant overlevingsvoordeel zien. Dat al deze handelingen falen in fase II klinische studies, terwijl ze actief waren in preklinische studies laat zien hoe belangrijk het is dat er betere preklinische modellen komen die overeenkomen met de tumor van de patiënten. Deze modellen moeten echter ook makkelijk in gebruik zijn en snel een uitslag kunnen geven. **Hoofdstuk 1** beschrijft de laatste ontwikkelingen in preklinische modellen zoals cellijnen, primaire tumorkweken en muismodellen, met daarbij hun eigen voordelen en nadelen.

### Persoonlijke behandeling

In **hoofdstuk 2** presenteer ik een persoonlijke behandel strategie gebaseerd op primaire tumor kweken. Een methode waarbij meerdere chemotherapieën getest kunnen worden op de eigen cellen van de patiënt is ontwikkeld. Hiermee genereerden we chemische profielen

en konden we de beste therapeutische optie selecteren. Voor tien patiënten werd de behandeling gekozen gebaseerd op zijn/haar chemische profiel. De tumor response van de patiënt kwam overeen met het effect gezien in de *in vitro* resultaten. Dit betekent dat deze persoonlijke behandel strategie mogelijk te gebruiken is in patiënten met MPM. Verdere validatie van deze methode is momenteel gaande in een fase II klinische studie genaamd PROOF.

Gebaseerd op de chemische profielen van alle kweken konden de kweken ingedeeld worden in drie groepen. Tumorkweken die reageren op bijna alle chemotherapieën of zogenoemde 'reageerders'. Tumorkweken die niet reageerden op de chemotherapieën ofwel zogenoemde 'niet-reageerders' en een groep tumorkweken die op sommige geteste chemotherapieën wel reageerden, maar op andere weer niet, zogenoemde 'intermediate reageerders'. Wanneer deze groepen genetisch met elkaar vergeleken werden, kon een genetische expressie profiel geïdentificeerd worden die de 'reageerders' en 'niet-reageerders' van elkaar kan onderscheiden. De 'intermediate-reageerders' lieten weer een ander uniek genetische profiel zien. Met dit gen expressie profiel waren we in staat een nieuw target voor de behandeling van MPM te identificeren, namelijk de fibroblast groei factor receptor (FGFR).

## FGFR

Het gen expressie profiel van de primaire kweken was niet het enige bewijs dat FGFR een nieuw behandel target kan zijn. Het screenen van meerdere nieuwe behandelingen op verschillende MPM cellijnen en primaire tumor kweken, zoals beschreven in **hoofdstuk 3**, liet ook zien dat een gedeelte van de kweken gevoelig is voor FGFR inhibitie. Een MPM muis model bevestigde de gevoeligheid voor medicijnen die FGFR blokken. De kweken die gevoelig waren voor deze FGFR medicijnen lieten een verhoogd level van FGF9 mRNA zien. Van FGF9 is bekend dat deze een sterke affiniteit voor FGFR3 heeft. Het bleek dat alle gevoelige cellijnen afhankelijk waren van FGFR3 signalen welke gereguleerd werden door BRCA geassocieerde eiwit 1 (BAP1). Daarom kan BAP1 eiwit verlies werken als een biomarker om patiënten te selecteren die gevoelig zijn voor medicijnen die FGFR blokken.

## Antilichaam drug conjugaties

Een andere behandel strategie beschreven in dit proefschrift zijn antilichaam drug conjugaties (ADCs). ADCs bestaan uit een monoklonaal antilichaam chemisch geconjugerd aan een toxische drug. Wanneer het antilichaam bindt met zijn target antigen zal de ADC internaliseren in de cel en de drug vrij laten zodat deze de tumorcel kan doden. Wanneer het target antigen alleen tot expressie komt in de tumorcel zal de drug alleen de tumorcel doden

en geen effect hebben op de normale cellen. Dit geeft minder ongewenste bijwerkingen. Expressie op de tumorcellen en niet op normale cellen, internalisatie van de ADC in de cel en het vrijlaten van de drug zijn allemaal belangrijke componenten voor deze therapie strategie.

**Hoofdstuk 4** laat zien dat het trofoblast glycoproteïne, ook wel 5T4 genoemd, een geschikt target is voor ADC behandeling in MPM. Het antigen komt tot expressie in de meeste MPM tumoren en niet in normaal weefsel. Wanneer het target gebonden wordt internaliseert het gehele ADC complex de cel in. Twee van de drie ADCs die getest zijn konden de tumorcellen die een hoge expressie van 5T4 hadden doden. Eén ADC was niet in staat om de tumorcellen te doden. Het bleek dat de vrijgelaten drug niet uit het lysosomale compartiment van de cel kon diffunderen. Door de pH van de cellen te veranderen met chloroquine, een anti-malaria medicijn, was ook deze ADC in staat de tumorcellen te doden.

## **BAP1**

BAP1 is een moleculair target dat geïdentificeerd is als een potentieel nieuw target in de behandeling van MPM. BAP1 is een tumor suppressor gen die genen reguleert in transcriptie, celcyclus controle, DNA breuken herstel en cellulaire differentiatie. Somatische mutaties in BAP1 komen voor in 47-67% van de patiënten met MPM. **Hoofdstuk 5** beschrijft hoe therapeutische middelen het fenotypische effect van BAP1 eiwit verlies ongedaan kunnen maken. Het exacte moleculaire mechanisme van BAP1 is nog niet compleet duidelijk dus verder onderzoek kan nog meer therapeutische opties onthullen. Daarnaast heeft BAP1 veel interactiepartners en eiwitten die onder invloed staan van BAP1. Daarom is het goed om combinaties van verschillende therapeutische middelen te testen.

## **Curriculum Vitae**

Laurel Schunselaar was born on the 17<sup>th</sup> of August, 1987, in Enschede. After receiving her VWO diploma at the Bonhoeffer College van der Waalslaan in Enschede, she started her study Technical Medicine at the University of Twente in 2005. After obtaining her bachelor degree in 2008, she continued with her masters. During this master she followed four clinical research internships in which both research and clinical activities were the focus. She started at the Dutch Burn Centre in Beverwijk, after which she moved to Utrecht for the second and third internship at the department of trauma surgery and the department of orthopedics in the University Medical Center. During her internship at the Antoni van Leeuwenhoek in Amsterdam she became acquainted with screening chemotherapy on mesothelioma cells. For her master thesis project she stayed at the Antoni van Leeuwenhoek – Netherlands Cancer Institute and worked for one year on the development of short term primary tumor cultures of mesothelioma cells for screening and development of new therapeutic compounds. At the end of 2012 she obtained her master degree in Technical Medicine and started as a PhD student in the Antoni van Leeuwenhoek - Netherlands Cancer Institute. In the group of Prof. Dr Jacques Neeffjes and later Prof. Dr. Zwart, but always in close collaboration with the thoracic oncology group of Prof. Dr. Paul Baas, she worked on new treatment options for patients with mesothelioma. The results of this research are described in this thesis. Nowadays Laurel is working at the hematology department of the LUMC, where she is coordinating a clinical trial testing aclarubicin in AML patients.

## List of publications

**Schunselaar, LM.** Monkhorst, K. Wijdeven, R. Peters, D. Zwart, W. Neefjes, J. Baas, P. *Throphoblast Glycoprotein is Associated with Favorable Outcome for Mesothelioma and a Target for Antibody Drug Conjugates.* J. Thorac Oncol. 2018 Oct. **13**(10): p.1577-1587

Quispel-Janssen, J. van der Noort, V. de Vries, JF. Zimmerman, M. Lalezari F. Thunissen, E. Monkhorst, K. Schouten, R. **Schunselaar, L.** Disselhorst, M. Klomp, H. Hartemink, K. Burgers, S. Buikhuisen, W. Baas, P. *Programmed Death 1 Blockade With Nivolumab in Patients With Recurrent Malignant Pleural Mesothelioma.* J. Thorac Oncol. 2018 Oct. **13**(10): p. 1569-1576

**Schunselaar, LM.\*** Quispel-Janssen, JMMF.\* Kim, Y. Alifrangis, C. Zwart, W. Baas, P. Neefjes, J. *Chemical profiling of primary mesothelioma cultures defines subtypes with different expression profiles and clinical responses.* Clin Cancer Res. 2018 Apr. **24**(7): p. 1761-1770.

Quispel-Janssen JM,\* Badhai J,\* **Schunselaar L,\*** Price S, Brammeld J, Iorio F, Kolluri K, Garnett M, Berns A, Baas P, McDermott U, Neefjes J, Alifrangis C. *Comprehensive pharmacogenomic profiling of malignant pleural mesothelioma identifies a subgroup sensitive to FGFR inhibition.* Clin Cancer Res. 2018 Jan. **24**(1): p. 84-94.

**Schunselaar LM,** Zwart W, Baas P. *Targeting BAP1: a new paradigm for mesothelioma.* Lung Cancer. 2017 Jul. **109**: p. 145-146.

**Schunselaar LM,** Quispel-Janssen JM, Neefjes JJ, Baas P. *A catalogue of treatment and technologies for malignant pleural mesothelioma.* Expert Rev Anticancer Ther, 2016. **16**(4): p. 455-63.



## **Dankwoord**

Het laatste onderdeel van mijn thesis wil ik graag gebruiken om mijn dank uit te spreken naar alle mensen die geholpen hebben dit boekje tot stand te brengen. Allereerst mijn promotoren en co-promotor, Sjaak, Paul en Wilbert, hartelijk dank voor jullie steun en begeleiding. Daarnaast mijn promotiecommissie, hartelijk dank voor het lezen van mijn proefschrift, Rob Hoeben, Huib Ovaa, Mario van der Stelt, Bob van der Water, Piet Postmus, Frank Baas, Dean Fennel, Marie Jose Goumans, Ilana Berlin en Sjaak Burgers. En natuurlijk mijn OIO commissie leden Reuven en Sjaak. Dank voor alle zetten in de juiste richting.

Aangezien onderzoek in je eentje een stuk saaier is wil ik graag al mijn collega's van het voormalige B6 cell biology II, het voormalige C2 molecular pathology, het huidige H5 oncogenomics en de thorax oncologie bedanken.

Als laatste wil ik graag mijn vrienden, schoonfamilie, ouders, zusje en broertje bedanken. Of het nu goed ging of iets minder bij jullie kon ik altijd mijn hart luchten. En natuurlijk, mijn grote liefde, Dennis zonder jou was dit alles niet gelukt.